AN ABSTRACT OF THE THESIS OF

Harold Gregory Smith for the degree of Doctor of Philosophy

in Geography presented on _____

Title: Growth Modeling for Conifer Regeneration in the Northeastern Sierra Nevada of California

Abstract approved: _____
(type name of prof.)

Knowledge of the timber production potential of a wildland area plays an important role in its wise management. For the past several years, resource managers of the United States Forest Service (USFS) at the Plumas National Forest have been concerned with the establishment of a procedure to evaluate timber production potential of the northeastern Sierra Nevada. A lack of critical detailed data on topography, soil type, soil plant available water, solar insolation and potential evapotranspiration has limited the success of silviculturalists in defining timber production potential and selecting forest regeneration sites in the area. Airborne and spaceborne remotely sensed data combined with ground acquired data can provide the type of information required for the assessment of timber production potential of such a wildland area.

This study uses remotely sensed data as a part of a scheme for the development of a data base and model to aid forest managers in evaluating areas in terms of timber production potential.

©Copyright by Harold Gregory Smith

All Rights Reserved

Growth Modeling for Conifer Regeneration in the Northwestern Sierra Nevada of California

by

Harold Gregory Smith

A THESIS

Submitted to

Oregon State University

In partial fulfillment of
the requirements for the
degree of

Doctor of Philosophy

Completed

Commencement June 1982

APPROVED:

_____

Professor of Geography in Charge of Major

_____

Chairperson of Geography

_____

Dean of Graduate School

Date thesis is presented _____

Typed by Judy M. Auzenne for Harold Gregory Smith

ACKNOWLEDGEMENTS

My deepest gratitude is extended to the late Dr. James F. Lahey who served as a source of inspiration and guidance throughout this study and my college career.

I would like to thank the resource managers of the USFS at the Plumas National Forest for their cooperation in the collection and laboratory analysis of the field data. I also thank Dr. Robert N. Colwell, Mr. Stephen D. DeGloria, Mr. Agnis Kaugars, Mr. Kevin Dummer, Mr. Anthony Travlos, Ms. Catherine Brown, Mr. Derrick Taylor and Mr. Stephen Harui of the Remote Sensing Research Program at the University of California, Berkeley, for their invaluable asistance in the processing of much of the digital data used in this study. I thank Mr. George Vasick of Hewlett-Packard, Inc. for computer programming assistance early in the study and Dr. Siamak Khorram for making much of this study possible.

Finally, I thank Dr. Anthony Lewis , Dr. Thomas Maresh, Dr. David Thomas and Dr. Jon Kimerling for stepping in to offer reassurance and guide this study to its completion.

This study was funded through NASA Grant NGL 05-003-404, NASA Office of University Affairs and NASA Contract NAS 9-15800.

To my mother, father and brothers Gary and Doug.

TABLE OF CONTENTS

LIST OF FIGURES

LIST OF FIGURES - CONCLUDED

GROWTH MODELING FOR CONIFER REGENERATION IN THE NORTHEASTERN SIERRA NEVADA OF CALIFORNIA

Introduction

The concept of multiple use in public forest lands has increased the need for efficient management. The demand for wood products must be balanced with other uses such as mining, grazing, recreation and asthetics. A primal requirement for any type of management is access to information. Information that is accessible, current, and relevant is very important in allowing flexibility in management decisions. In order to organize and process quantities of information quickly, computerization is necessary. With computerization comes the ability to construct a multipurpose data base system. An environmental data base that combines many different types of areal and point data becomes a powerful tool by which objective management may be carried out. Computerization also lends an element of dynamicism to the data base in that updating and editing data is accomplished with relative ease. A computerized data base, as a single entity, becomes accessible to many people such as managers and scientists who can each contribute knowledge to substantiate management decisions.

The concept of a computer data base for the management of forest lands is particularly appealing. Large tracts of land are often involved, many types of information are used and change is continual over both the short and long term. Because many forest lands are often in remote areas, information about them is often incomplete or altogether lacking. The availability of remotely sensed data can help fill this information gap for many forest lands. Remotely sensed digital data provide computer compatible spectral data, often in pixel based form, adaptable to image based geographic information systems.

To date little work has been devoted to the development of a comprehensive computer data base for forested lands. However, current and future management decision requirements indicate the need for the development of a data base that will incorporate areal ground data and take advantage of widely available remotely sensed digital data.

Modeling, an integral aspect of management decision making, is greatly facilitated by the existence of a data base. Physical and biological modeling can provide insights into forest characteristics and interactions that are used to enhance management decisions. A model that could evaluate forest land capability for timber growth would be particularly helpful to a manager concerned with timber production and forest regeneration.

Forest regeneration is a high priority concern in the Sierra Nevada of California. Current decisions regarding regeneration whether right or wrong, optimal or suboptimal will affect the future economy and ecology of a forest. Closely associated with forest regeneration is land capability for regeneration. If land capability cannot be satisfactorily determined the probability of regeneration success is an unknown, whereas if land capability can be adequately judged the probability of regeneration success could be "determined" (i.e. the risks are at least partially known).

The success of forest regeneration efforts by United States Forest Service (USFS) silviculturists has been severely limited along the eastern escarpment of the Sierra Nevada. The problem centers around pressures on managers to increase future timber production and a general lack of comprehensive information about the area. Detailed topographic information, solar radiant loading, potential evapotranspiration and soil plant available water as general descriptors of the environment need to be evaluated in determining land capabilities for timber regeneration. The development of a computer data base that would incorporate all of the above information and provide for a capability to statistically model phenomena based on these variables would be of great help in regeneration decisions.

In March of 1978 a meeting between personnel of the USFS, Plumas County Planning Department and reserchers from the Remote Sensing Research Program of the University of California, Berkeley at the Plumas National Forest Supervisor's office in Quincy, California set the stage for land capability modeling research.

The study area, approximately 40,470 hectares (100,000 acres) encompassing the Frenchman Reservoir Basin is located within the uppermost portion of the Middle Fork of the Feather River along the northeastern

edge of the Sierra Nevada in the southeastern portion of Plumas County. (Figure 1). The area, identified by the USFS in need of study in terms of forest regeneration methods, had been the subject of long term study by the University of California's Remote Sensing Research Program.

As a result, a good data base in terms of aerial photography, maps, imagery and digital products, was available. The study area, situated on the eastern edge of the Sierra Nevada, is marginal in terms of timber production potential. The area also represents a region where land exchange between Plumas County and the USFS is anticipated.

Figure 1.- Location of Study Area

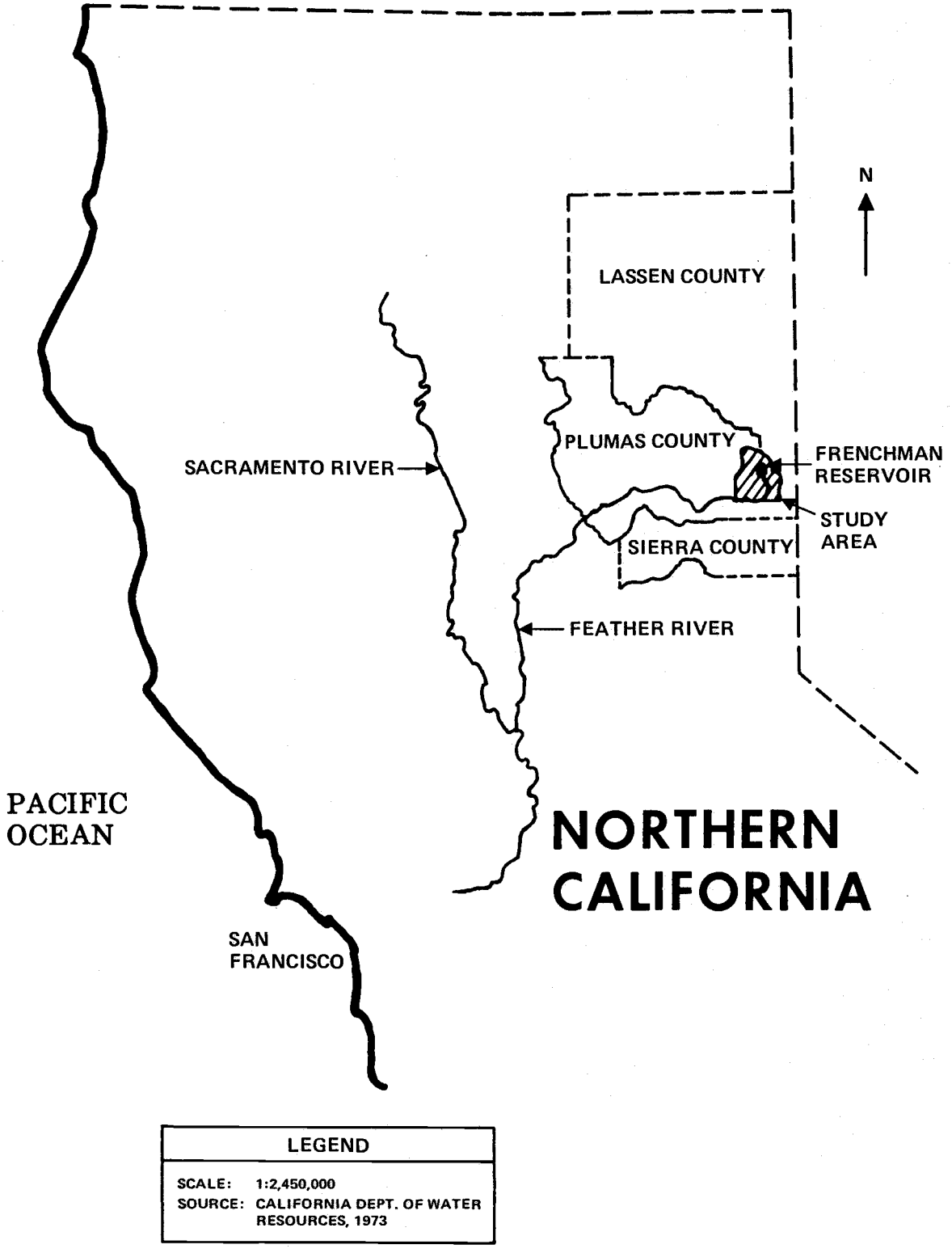

Physical and Economic Description of the Study Area

Climate

The generally high elevation of the study area (1525m - 2704m+ or 5000 - 9000ft above sea level) and the mountainous character of the area around it result in a continental temperature regime with temperature extremes ranging from above 38°C (100°F) to minima below -18°C (0°F).

The daily range of temperature varies about 16°C (28°F) during the winter to 25°C (45°F) or more during the summer. This range, along with the absolute values provides for a variety of distinct seasons. In January, the mean minimum temperature is below freezing (0°C) with extreme low readings of less than 0°C. Maximum temperatures are 0 to 10°C, so heating requirements are high. The mean maximum temperature in July in the lower portions of the study area (approximately 1525m above sea level) is in the high 20's to low 30's °C, whereas minimum temperatures average 0 to 10°C. Frost can be expected every month of the year (California Department of Water Resources 1973).

The annual crop growing season in the study area is very short. The median date of the last spring frost occurs late in June, and the first fall freeze occurs in July. Seasonal totals of precipitation range from 76 to 90 cm (30 to 35 inches) in the western portion of the study area to less than 38 cm (15 inches) in the eastern part. Maximum precipitation occurs in winter with much of the moisture at higher elevations falling in the form of snow. Precipitation totals during July, August and September are usually less than 2.54 cm (1 inch) per month.

Humidities are low during the summer, but remain high throughout the winter period, with intermediate values in the spring and fall.

On average, winds are light and variable over much of the study area. Exposed locations frequently experience strong winds during the winter months. The direction of the winds normally depends on the orientation of valleys and canyons in the immediate area. Historically wind directions have been predominantly from the southwest.

Sunshine is abundant throughout the year, with the study area receiving about 3200 hours of sunshine annually. In relation to the maximum possible sunshine during the four seasons, the area receives approximately 90 percent during the summer, 70 percent during spring and

fall, and only about 60 percent during the winter (California Department of Water Resources, 1973).

Geology

The study area is situated in a complexely faulted region of the Sierra Nevada; this can be interpreted from the rocks in and near the study area. The oldest rocks record periods of ocean deposition, ancient volcanism, crustal warping, granitic intrusion, mountain building, and erosion of mountains nearly to sea level.

At the beginning of the Tertiary Period (approximately 70 million years ago), the area was uplifted, streams were resultantly rejuvenated, and coarse gold-bearing gravels were depositied in stream valleys. Tertiary drainage systems, with few exceptions, were very similar to the present systems. The main exception was an ancestral river system called the Jura which originated in Nevada County north of Lake Tahoe and flowed northwesterly across the Sierra Valley - Mohawk Valley area to a point west of Susanville, California where it turned eastward toward Nevada (Figure 1). The bed of the Jura River is now exposed near the crest of the ridge (reverse topography) above Genesee, California.

Periods of intermittent volcanism began early in the Tertiary and extended through the Pliocene epoch. Volcanism was vigorous, with extensive flows of basalt and masses of andesite mudflow breccia. There were also periods of explosive volcanic activity during which deposits of rhyolite tuff were formed. At other times, andesite and rhyolite plugs and sills were injected into the rock. This complex now forms the many and varied Tertiary volcanic rocks found through the area.

After the emplacement of the Tertiary volcanic rocks, the area was subjected to extensive faulting associated with the uplift of the Sierra Nevada. It was during this period that the major valley of the study area (Sierra) was formed. Subsequently, the valleys became the location of lakes that received sediments from the surrounding areas. These sediments now constitute the lake and near shore deposits in the valleys.

During the Pleistocene epoch, glaciers mantled the upper portions of the Sierra Nevada and lakes occupied many of the areas that are valleys today. Glaciers formed the lateral and terminal moraines now found near the southern portion of the study area (California Department of Water Resources, 1963).

The potential for seismic activity affecting the region around the study area is considered high (California Department of Water Resources, 1973). The University of California seismograph network has located the epicenters of 29 earthquakes of Richter magnitude 4 and greater within 40 km of the study area since 1932. The most recent significant shock recorded in the area was the "Truckee" earthquake of September 12, 1966 with a magnitude of 5.8.

The structural relationships and tectonic history of the study area are quite similar to those found in the Mt. Whitney-Owens Valley area near the southern end of the Sierra Nevada.

Soils

There are 37 soil mapping associations in the study area (Table 1). The soils of each are of about the same type of profile. Except for differences in surface texture all members of a series have major horizons or layers that are similar in thickness, arrangement and physical character (USDA, 1975).

Vegetation

The vegetation cover of the study area can be classified into the general categories of cultivated land, rangeland and timber land. Along the study area southern boundary agricultural lands grade very gradually into timber land. The remainder of the study area, generally of an upland character, is almost exclusively timber land. The most important commercial species are: white fir (Abies concolor), Red fir (Abies magnifica), Jeffrey pine (Pinus jeffreyi), and Ponderosa pine (Pine ponderosa). Other commercial species that occur in lesser amounts are, Lodgepole pine (Pinus contorta), Western white pine (Pinus monticola), Sugar pine (Pinus lambertiana), Incense cedar (Libocedrus decurrens), Douglas fir (Pseudotsuga menziesii), and Mountain hemlock (Tsuga mertensiana). Non-commercial species that are important to wildlife and watershed include, Cottonwood (Populus trichocarpa), Aspen (Populus tremuloides), Black oak (Quercus kelloggii), and Western juniper (Juniperus occidentalis).

Water Resources

In 1936, the California Department of Water Resources prepared a report (California Department of Water Resources, 1937) which was the

TABLE 1.- Study Area Soil Mapping Associations

Soil series	Position	Vegetation	Parent Material	Drainage	Effective Depth
Aldax	Hilly upland	Sparse grass, mountain mahogany	Hard basic rock	Well	20.3 to 35.6 cm. (8 to 14 in.)
Badenaugh	Fan terraces	Grass, sage	Cobbly lake sediments	Well	76.2 to 127.0 cm. (30 to 50 in.)
Balman	Basin	Sage-grass and halophytes	Stratified sand loams or loams, deep to fine textured lake sediments	Moderately well	152.4 cm. + (60 in. +)
Beckwourth	Low terrace, flood plain	Sage-grass	Loamy coarse sand and sand, fine textured sediments	Somewhat poorly	152.4 cm. + (60 in. +)
Bellavista	Basin	Sage-grass and halophytes	Lime cemented pan over stratified course sediments	Moderately well	91.4 to 152 cm. (36 to 60 in.)
Bidwell	Steam terrances	Sage-grass	Stratified, sands, gravels, loamy sands, and coarse sandy loams	Moderately well	91.4 to 152.4 cm. (36 to 60 in.)
Bieber	Terrace	Sage-grass	Lime and silica pan over weakly consolidated stratified sediments	Well	15.2 to 38.1 cm (6 to 15 in.)

TABLE 1.- Continued

Soil series	Position	Vegetation	Parent Material	Drainage	Effective Depth
Bonta	Mountainous uplands	Jeffrey Pine, white fir	Weathered to hard granitics	Well	76.2 to 152.4 cm. (30 to 60 in.)
Buntingville	Basin	Meadow-grass	Recent alluvium	Somewhat poorly	61 to 152.4 cm. (24 to 60 in.)
Calpine	Low terrace	Sage, bitter-brush grass	Granitic alluvium	Well to moderately well	122 to 152.4 cm. (48 to 60 in. +)
Childs	Fans	Grass, lodge-pole and Jeffrey pine	Basic alluvium	Well	101.6 to 152.4 cm. (40 to 60 in. +)
Coolbirth	Steam, terrances and alluvial fans	Sage-grass	Sandy loam to coarse gravelly sand, massive, slightly acid to neutral	Moderately well	114.3 to 152.4 cm. (45 to 60 in.)
Correco	Terraces and fans	Sparse grass, sage, bitter-brush, rabbit-brush	Soft lake sediments	Well	61 to 152.4 cm. (24 to 60 in.)
Delleker	Hilly uplands	Sage, bitter-brush, jeffrey pine	Waterlain ashy alluvium and igneous rock	Well	101.6 to 152.4 cm. (40 to 60 in.)

TABLE 1.- Continued

Soil series	Position	Vegetation	Parent Material	Drainage	Effective Depth
Lovejoy	Low terrances	Meadow grass	Mixed water-laid sediments, cemented by lime-silica	Well to moderatly well	20.3 to 50.8 cm. (8 to 20 in.)
Martineck	Low terrances	Sage, bitterbrush, perennial grass	Lake sediments	Well	30.5 to 45.7 cm. (12 to 18 in.)
Meiss	Volcanic uplands	Grass, forbs	Hard to slightly weathered volcanic rock	Excessive	25.4 to 51 cm. (10 to 20 in.)
Millich	Hilly uplands	Sage, bitterbrush, Mt. Mahogany, Manzanita, Jeffrey pine	Hard volcanic	Well	7.6 to 45.7 cm. (3 to 18 in.)
Mottsville	Terrace	Sage-grass	Granitic alluvium (loamy sand)	Somewhat excessive	152.4 cm. + (60 in. +)
Nanny	Fans	Lodgepole pine, Jeffrey pine, grass, bitter-brush	Alluvium and lake sediments	Moderately well	101.6 to 152.4 cm. (40 to 60 in.)

TABLE 1.- Continued

Soil series	Position	Vegetation	Parent Material	Drainage	Effective Depth
Newlands	Upland	Sage-grass	Meta-basic rock	Well	76.2 to 127 cm. (30 to 50 in.)
Ormsby	Terrace, or flood plain	Sage-grass	Loamy coarse sands and sands, fine textured sediments	Somewhat poorly	152.4 cm. + (60 in. +)
Pasquetti	Basin	Sedge-grass	Ashy and fine textured lake sediments, sand and gravels	Poor	152.4 cm. + (60 in. +)
Portola	Mountainous uplands	Mixed conifers, sage, Manzanita	Softly consolidated pyroclastic rock	Well	76.2 to 127 cm. (30 to 50 in.)
Quincy	Terrace	Sage-grass	Sand	Excessive	152.4 cm. + (60 in. +)
Sattley	Mountainous uplands	Jeffrey pine, white fir, Manzanita	Hard volcanics	Well	76.2 to 152.4 cm. (30 to 60 in.)
Smithneck	Flood plain, Stream terrace	Sedge-grass, some sage	Stratified coarse textured basic alluvium	Somewhat poorly or Moderately well	152.4 cm. + (60 in. +)
Toiyabe	Mountainous uplands	Jeffrey pine, ponderosa pine, Manzanita	Weathered granitic rock	Well	30.5 to 61 cm. (12 to 24 in.)

TABLE 1.- Concluded

Soil series	Position	Vegetation	Parent Material	Drainage	Effective Depth
Trojan	Mountainous uplands	Pines, mixed conifer, oak	Weathered volcanic rock	Well	76.2 to 152.4 cm. (30 to 60 in.)
Trosi	Terrace benches	Big sagebrush, low sagebrush	Stony, stratified pleistocene lake sediment	Well	53.3 to 101.6 cm. (21 to 40 in.)

Source: USDA, 1975

basis for incorporation of all surface waters into the public domain in Sierra Valley. Watermasters of the Department have been distributing the waters since incorporation. Subsequently, the department investigated ground water basins, land and water use and the potential for water development within the Upper Feather River Basin, and as a result the Frenchman Dam was constructed in 1961 (Figure 1).

In 1971, the department published the "Lake Davis Water Investigation" which described the present water quality conditions in the Lake Davis Basin. The report was a basis for Plumas County regulations regarding septic tanks - leaching systems within the basin (California Department of Water Resources, 1971).

Economy

Principal economic activities in the study area include agriculture, forestry, and recreation.

Agriculture is the most important economic activity within the study area (Table 2). The percentage of the population employed in this section of the economy does not reflect its magnitude as is the case in the U.S. in general (Table 3). The total agricultural area has not changed for many years although some consolidation of farms has taken place.

Recreationalists account for a considerable portion of the taxable sales in the study area. The average daily per capital expenditure by recreationalists is over $5.00 with the total amount being in excess of 2 million dollars (California Department of Water Resources 1973). This does not include the tax income from recreational lands that have increased in value and in turn have created higher assessed values. The recreation industry should continue to play a vital role in future economic growth.

Mineral deposits of commercially exploitable quantities have not been found in the study area, although extensive gold and copper deposits are located in adjacent areas. In 1956, 25 tons of 3 percent copper ore was sold from the Climax Claim near Crystal Peak. Other minerals found in the area include molybdenum and minor secondary uranium enriched with copper (California Department of Water Resources, 1973).

The forest products industry contributes a major portion of the gross income in the study area (Table 2). During 1978 in the adjacent five county area considered to be within hauling radius of the study

TABLE 2.- Summary of Study Area Socio-Economic Data

Principal Economic Activities (1971)	Amount (thousands of dollars)
Agriculture, Livestock	2,278
Gross value of crops	1,130
Timber production	
Private	72
Public	0
Public Finance (1970-71)	
Assessed Valuation	3,622
Property tax levies	180
Expenditures	345

From: California Department of Water Resources, 1978

TABLE 3.- Plumas County Employment by Major Categories, 1960, 1970, and 1980

	1960			1970			1980		
	Number employed	% empl. of tot. emplymt.	% empl. of tot. pop.	Number employed	% empl. of tot. emplymt.	% empl. of tot. pop.	Number employed	% empl. of tot. emplymt.	% empl. of tot. pop.
Agriculture, forestry and fisheries	332	7.8	2.9	284	6.8	2.4	354	7.0	2.1
Mining and construction	211	5.0	1.8	220	5.3	1.9	217	4.3	1.3
Manufacturing	1,027	24.1	8.8	741	17.7	6.3	642	12.7	3.8
Service	2,689	63.1	23.1	2,932	70.2	25.0	3,841	76.0	22.9
Total employment	4,259	100.0	36.6	4,177	100.0	35.6	5,054	100.0	30.1
Total population	11,620			11,707			16,800		

Sources: U.S. Bureau of the Census, U.S. Census of Population.

area, timber production had a value of 15 million dollars. Within the five county area, there is an estimated 1.3 million hectares of forest land containing some 37.5 billion board feet of timber (California Department of Water Resources, 1973). Of this amount about 67 percent is publicly owned. There remains a potential for further development of this industry to further enhance the economy. To realize this the resource must be managed in the most efficient manner possible requiring current, accurate and relevant information. It is by means of a computerized data base that such information may be assembled used and updated. Models based on information in the data base can provide different representations thereby aiding management decisions. Related to timber production, modeling for an index of land capability would be valuable. A parcel of land could be evaluated in terms of capability for timber production, greatly facilitating decisions regarding cutting cycles, regeneration and the bringing of new lands into production.

CHAPTER 2. THE MODELING APPROACH

A logical method of deriving an index for land capability as related to timber production would be to evaluate tree growth. Rather than measuring the rate of tree growth for every tree in an area of interest an effective means of evaluation would be to model tree growth potential.

Although tree growth modeling has been the subject of much research in the past century, typical efforts have been very limited in scope. Yang et al. (1978) derived a growth function that was flexible enough to accomodate most biological growth behavior, but was only applicable to single trees. Ek and Monserud (1979) described and compared a distance dependent individual tree based model (FOREST) and a diameter class growth model (SHAF) for describing changes in stand density and structure. Both performed well when tested in a Michigan northern hardwood stand, but FOREST was extremely expensive to operate and SHAF was less sensitive to environmental changes than was desirable for forest management. A novel approach by Hatch et al. (1975) created a mathematical index representing relative growth potential of an individual tree. The index measures the relative competitiveness of an individual tree rather than the relative competitive pressure being exerted on an individual tree by surrounding trees. The model that generated this growth potential index was one of the first to incorporate characteristics of the tree as well as aspects of the ambient physical environment. Implementation of the model was extremely expensive and only appropriate for individual trees or small groups. Curtis et al. (1974) sought to develop regression models relating height and site index. Curtis' models provided estimates of site index for stands of known present age and height and of expected heights at different ages for stands of specified site index. They were valid conceptually but required as input information that most managers would like to have as model output and therefore have not been used operationally by forest managers.

Beck (1971) derived an exponential growth model to fit sets of height-growth data. His goal was to study patterns of height growth of dominant and codominant trees as related to topographic features. The study was well designed in that the data were easily gathered (tree height measurement and slope, aspect, and elevation measurements) and the

results provided some insight into general environmental effects on tree growth and competition. Finally, Faye and MacDonald (1977) examined and modeled patterns of annual height growth in conifers as compared to changing environmental conditions. Distinct patterns were observed for sets of general environmental conditions which demonstrated that site potential or land capability for timber production could be modeled, albeit only on an individual tree basis.

Present and future forest management needs require the ability to evaluate tree growth or land capability for timber production on extensive and often remote areas. Most current model technology, based on a single tree, is too expensive or impractical to implement over large areas where data are limited. With the introduction of digital terrain data and modeling techniques along with the launch of Landsat and other environmental satellites, the ability to collect and manipulate environmental data for large areas is possible. It is with these data that this study will seek to develop a tree growth model whose output can be interpreted as an index of land capability for timber production.

Modeling begins with three basic steps in any scientific study; identification, approximation and idealization. In any modeling exercise the objective is to define a problem as precisely as possible by attempting to identify and select those variables to be considered as basic in a study, eliminating unnecessary information and simplifying the retained concepts, variables, and data. At this point the context of modeling is still in terms of real, as opposed to abstract concepts and is referred to as the construction of a real model (Dym and Ivey, 1980). The modeling process involves two worlds, one conceptual and the other external. The external world is usually referred to as reality, where various phenomena of natural or human origin can be observed and noted. The conceptual work is the world of the intellect. This is the world within the mind that everyone lives with, talks about and contemplates when trying to understand what goes on in the external world.

The conceptual world can be divided up into three stages; observation, models, and prediction. The observation portion relates to perceiving the real world and interpreting what is going on in the real world. Observations may be through direct use of the human senses or through indirect use of measurement equipment. This portion of the

scientific method is devoted to data collection that provides information about the perceived world. The retrieval of information is most effective if the objectives of the model are understood. The model can then be used as a guide to inform the observer as to what can be expected and what should be collected or observed.

The second major component of the scientific method in the development of the conceptual world is the development of models to analyze a situation. This component is usually much less well defined and frequently involves a high degree of creativity. The real world is examined in an attempt to identify the operative processes at work, the goal being the expression of the entire situation in symbolic terms. The real world then is represented by a statistical or mathematical model in which the real functions and processes are replaced by symbols and mathematic operations. Much of the value of any study hinges on this step because an inappropriate identification between the real world and the statistical or mathematical world is unlikely to lead to useful results. Because a dozen different people are likely to come up with a dozen different definitions, there is usually no single best model for describing a situation. If the wrong things are emphasized in this process, the model will be inappropriate. If too much is taken into consideration, the resulting model will be hopelessly complex and will probably require incredible amounts of data. A proper selection of what is to be explained or predicted is essential since only those things that can be explained should be modeled (Bender, 1978). The resulting model may be used to aid in understanding the observations that were made. This understanding comes about by using the model as a guide for observations, as a predictor for future observation and as a test of the validity and consistency of the observations. A model is then important in informing observers as well as in making predictions. In other words, the modeling process is intricately entwined with the observation and prediction processes. The observations are a guide to the model, and the model is a guide to the observations.

The final stage in a pure scientific method is that of prediction, and as was stated earlier, prediction is intricately tied to the observation and modeling processes and in fact is informed by both. This also implies that the pure prediction process is modified into the design

process for building a new model (Figure 2). In the pure scientific method the role of a model is unambiguous; a model provides the basis for informed prediction, and the predictions are followed by observation to test the validity of the model. If observations of

Figure 2.- The Generalized Modeling Process

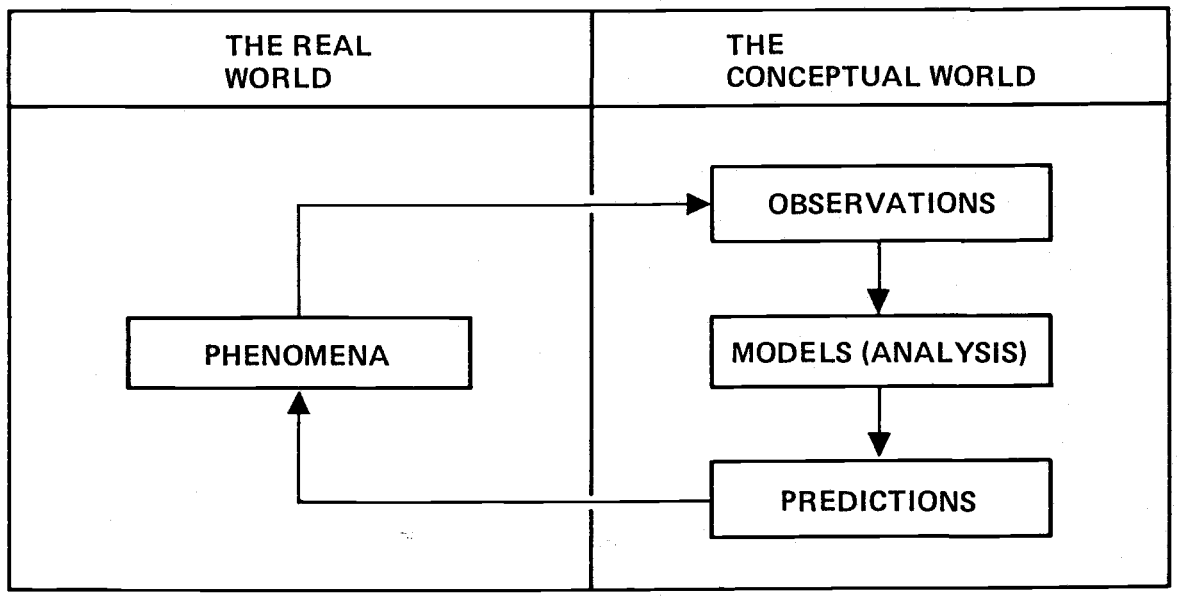

Modified from: Dym and Ivey, 1980

subsequent phenomena agree with the predictions based on the model, the model can be considered verified. Commonly this agreement is not observed, at least on the initial attempt. A much more typical situation is that the set of conclusions from the model contains some that seem to agree and some that seem to disagree with the outcome of the validation experiments. In such a case every step of the modeling process needs to be examined. Several questions need to be considered. Was there a significant omission in the step from the real world to the real model? Does the model reflect all the important aspects of the real model, and does it avoid introducing extraneous behavior not observed in the real world? Is the mathematical work free from error? Usually the modeling process proceeds through several iterations, each a refinement of the preceding until an acceptable one is found. Pictorially, the process can be characterized in the following way:

Figure 3.- Schematic of the Modeling Process

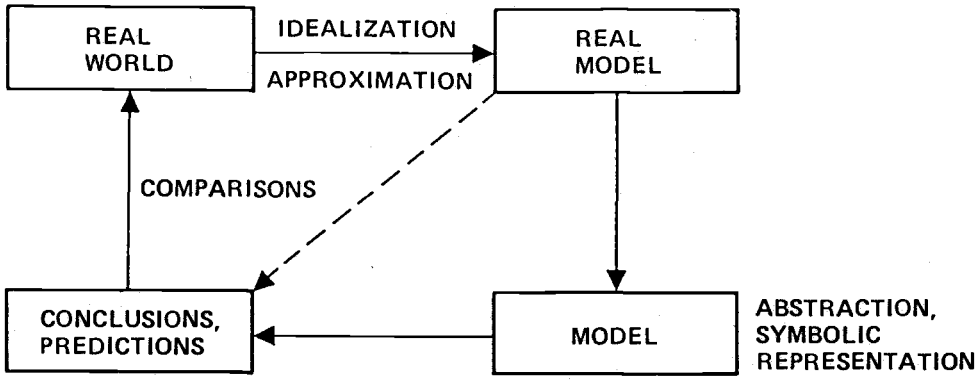

Source: Maki and Thompson, 1973

The solid lines indicate the process of building, developing and testing a model. The dashed line is used to indicate an abbreviated version of the process which is often used in practice. The shortened version is common in the biological and social sciences where quantification of concepts is difficult. The steps in this process may be extremely complex and there may be complicated interactions between them. It should be noted that a distinction between real models and mathematical or statistical models is somewhat artificial. It is a convenient way to represent a basic part of the process, but in many cases it is very difficult to decide where the real model ends and the statistical or mathematical model begins. In general most researchers do not make such a distinction. As a result, in practice it is usually the case that predictions and conclusions are based on a hyprid type of model, part real and part statistical or mathematical, with no clear distinction between the two. There is some danger in this. While it may be appropriate to work with the real model in some cases and the statistical or mathematical model in others, it is important to maintain perspective in terms of the setting in which the model is used. At best it can be confusing when the real model and the statistical or mathematical model are not differentiated. At worst this lack of discrimination can lead directly to incorrect conclusions. Essential aspects of a problem may be lost in the transition from the real world to the statistical or mathematical model. In cases like these, conclusions based on the derived model may not be conclusions about the real world or the real model. Therefore there are cases where it is crucial to distinguish the model to which a conclusions refers.

In the process of building a statistical or mathematical model numbers are constantly manipulated. The numbers often come from experimental observations that are always somewhat inaccurate or in error. Error is the difference between a measured value and the true or exact value. The amount of error introduced depends upon the sensitivity and accuracy of the measuring device and the ability and skill of the observer. No matter how skilled the observer, no matter how precise the instrumentation may be, error is always present. For this reason, every analysis of experimental results should account for the errors involved. There are two basic types of errors, systematic and random. When an observed value deviates from the true value in a consistent way, the error is systematic. Random errors are produced when repeated observations of a quantity are made. They arise because most experimental situations have a large number of unpredictable and unknown sources of inaccuracy. Random error varies in magnitude, with both positive and negative values occurring in a random sequence. The distribution of truly random errors follows statistical laws.

It should be pointed out that errors and mistakes are not the same thing. Errors are defined above, and mistakes are human induced in accuracies made by the experimentor and can include such things as incorrectly reading instruments, erroneously recording numbers or making arithmetic errors in calculating results. These types of inaccurancies can of course be largely avoided by working and meticulously.

With reference to errors and accuracy, the evaluation of a model can include a number of aspects; an organizing function, a heuristic function, a predictive function and a measuring function. A model may be evaluated with respect to each of these functions. Is the model able to order and relate disjointed data and show similarities or connections between them which had previously remained unperceived? A model provides a frame of reference for consideration of a problem. This is often an advantage even if the preliminary model does not lead to successful prediction. A model may suggest informational gaps which are not immediately apparent and consequently suggest fruitful lines for action. When a model is tested the character of the failure may sometimes provide a clue to the deficiencies of the model. Some of the greatest scientific advantages have been produced by failure of a model. Does the model

provide predictions that are sufficient qualitatively and quantitatively? If the model provides prediction that cannot be evaluated, can it serve as a heuristic device leading to the possible discovery of new facts and new methods? Is the model an improbable one, i.e. is it original? And finally, what is the degree of reliance that may be placed on the model's ability to represent some approximation of physical reality? Model making brings into the open the problem of abstraction. Some degree of abstraction is necessary for decision making.

A model maker must decide which real world attributes will be incorporated into the model. By making the process of abstraction deliberate, the use of a model may bring such questions to light. Moreover, it may suggest preliminary experiments to determine which characteristics are relevant to the particular problem under consideration.

The process of modeling carries with it some disadvantages. A model is subject to the usual dangers inherent in abstraction, i.e. a model may require gross oversimplifications. There is no guarantee that an investment of time and effort in constructing a model will pay dividends in the form of satisfactory prediction. There is also the danger of confusing a model with reality. This is a problem that many scientists face when dealing with a modeling problem for extended periods.

When entering into the actual mechanics of model building, one of the first things that should be determined about the situation is whether it is most appropriately modeled in deterministic or stochastic terms. A model is described as deterministic if it predicts the exact behavior of a phenomenum given the required information. Conversely, a model is stochastic if it incorporates probabilistic behavior. For this type of model the predictions are such that no matter how much is known about a phenomenon, it is impossible to determine the exact nature of the system. This type of model can appear very appropriate in the light of experimental results. Many of the most useful models, especially in the life and social sciences are of this type. This is understandable since the real world shows strong evidence of being a stochastic system. (Kenney et al., 1957).

Regardless of whether a deterministic or stochastic model is to be derived, an excellent way to begin a data analysis is to examine bivariate plots (graphs) of all variables against one another. Graphs are

useful in examining relationships because people can take in an entire picture rather quickly and then deduce consequences by using their geometric intuition. It then logically follows that graphs should be useful in conveying information. A mind acting as a analog computer can rapidly locate certain patterns in visually presented data. One of the easiest to spot is a straight line. For this reason a variety of forms of graph paper (rectangular, polar, log-log, normal probability, etc.) are utilized so that plotted data will appear linear if the anticipated relationship exists.

Graphs are probably most useful in conveying qualitative relationships or approximate data which involve only a few variables. If the analysis and model building procedure is to examine several variables, other techniques need to be utilized that may provide insight into interactions and relationships in a more sophisticated manner.

Regression and correlation are very popular tools for the exploratory analysis of many variable data. The methods are excellent when little is known about the data and the phenomenon that is to be modeled. The methods can provide relationships that can become focal points for further study. Also, both statistics approximate human judgment and are tied to deductive reasoning. However, the limitations of these methods are frequently minimized in discussions of applied statistics. In reality many researchers use regression and correlation sparingly. In part this is because of a discontent with the legitimate use of these statistics. The v^2+2v-1 statistics (where v is the number of predictor variables) consisting of means, variances, covariances, intercorrelations and regression weights alone and the fact that they are evaluated both individually and together makes interpretation extremely difficult. For practical reasons only many researchers are forced to avoid these statistics. Since the correlation coefficient is mathematically related to the regression coefficient, the limitations of one are the limitations of the other. Chance alone can influence the value of a correlation coefficient. This is an overriding problem in any statistical analysis. Even a sample that satisfies the assumption of being randomly sampled from a multivariate normal population can represent an extreme of that population. In terms of correlation coefficients, the set may contain misleadingly high or low values. Extending this is the option that given many

measurements, high nonsense correlations are likely. Correlations of two variables with a third measured or unmeasured variable can modify correlations between the original two.

For examining variation and relationships between variables from a population, principal components analysis (PCA) is probably more appropriate. This is because of the general validity of the method and the more comprehensive results that are produced. The most extensive regression and correlation analysis for the purpose of examining variation does not match the potential outcome of a principal component analysis of the same data.

The mathematics of PCA are extremely important in the evaluation of principal components. For most purposes the assumption that each data vector (set of measurements for each object in the sample) is composed of random variables is sufficient for meaningful conclusions. In other words, each variable assumes values of a specific set with a specific relative frequency or probability. If the variables are continuous this leads to a multivariate distribution, conservatively a multivariate normal distribution for variables, whether they are discrete or continuous.

The interpretation of components as related to the above properties according to Pimentel (1979) consider that:

(1) The component scores of a set are uncorrelated with one another so each component can be interpreted individually.

(2) The components are ordered in terms of the magnitude of their variances, the i^{th} component having the i^{th} largest variation. In conjunction with the former property, successive decreasing variation can be expected.

(3) Components partition the variance into p additive fractions (p is the number of variables) that sum to the total variance, i.e. the i^{th} component accounts for an additive portion of the variation of the original variables.

(4) The first component is the linear combination which best discriminates (produces the maximum distance) between individuals of a sample. This can be applied to graphing component scores (including their ordination) and to examining eigenvector coefficients to disclose the interplay of variables involved.

(5) The first through r^{th} components define a subspace that provides the best r-space representation of the data. The best r-space is important in terms of extending and summarizing discrimination among individuals, by ordination; unravelling the participation of variables in discrimination; and using a few components to summarize information provided by the data.

The nature of the interplay of the variables is discerned by "reading" each eigenvector in a physical sense. Positive values for coefficients are interpreted as increases in magnitude of the corresponding variables and negative coefficients are interpreted as decreases.

The collective signs of coefficients of components are important when all signs are the same, the implication is that all variables are increasing together. This type of component is referred to as a general component. When the signs are mixed the eignevector is called a bipolar component.

PCA is a very powerful tool; howeve, it is far from being an objective method that leads to direct conclusions. The reasons for this can be expressed in terms of the mathematical model, the data, and decisions by the investigator.

Each component of a set can be considered as an independent response to a single influence and the set of coefficients as indicative of the interplay of variables in the response. Unfortunately, this does not translate into a one to one correspondence between each component and each feature. Two or more features can be intertwined in a single component.

Principal component analysis can be considered arbitrary owing to decisions regarding which variables were studied, their transformation vector choice, objectivity, sample size, and many group comparisons.

The aim of PCA can be to obtain a set of eigenvectors that describes independent influences in an overall phenomenon. To fulfill this, the inclusion of meaningless variables that can wrap the vectors into uninterpretable dimensions must be avoided. Random sampling and a linear relationship among variables need approximation if component models are to have meaning. The problem of which vectors to interpret and which to ignore as random variation is a problem. As an example a significant eigenvalue may pertain to nothing more than significant experimental

error. Conversly, a lack of significance might ignore an extremely important relationship.

Any PCA is subject to the criticism of lacking objectively since there are relatively few tests of specific null hypotheses. Significance tests are not applied to individual component coefficients so the sample used must be sufficiently large to provide some reliability in the coefficients. A minimum might include as few as 30 observations although larger samples are definietly preferred. Regardless, the number of observations should exceed the number of measurements so that all dimensions are defined.

In summary, careful thought needs to be devoted to the conceptual structure and mathematical/statistical technique used in building a model. Awareness and itemization of limitations and advantages of each component of the model building procedure are important in the final evaluation of the model. Important too in the construction of a model is access to and processing of the required data and information. The next chapter will address the preparation of a unique comprehensive data base for tree growth/land capability for timber production modeling.

CHAPTER 3. DATA SET PREPARATION

The gathering, integration and manipulation of many large data sets as the input phase of the modeling process requires careful thought and highly specialized computing hardware and software.

Computing hardware at the Remote Sensing Research Program (RSRP), University of California, where this study was conducted was acquired and configured to enable scientists to perform data analyses utilizing the widest possible array of image and non-image information sources. In the construction of the system an emphasis was placed on the efficient combination and coordination of information that would provide the most cost effective and accurate results within the limits of modern technology.

There are three independent hardware systems at the RSRP (Figures 4a-c). Two of these systems are used primarily for the preprocessing of raw data and the evaluation of results. System one includes high speed storage and display devices that are used for interactive display of digital data, bulk storage and software development. More specifically, this first system consists of a Data General NOVA 840 minicomputer and a number of I/O devices. The computer has the capability of writing images on four "frame memories". Each "frame memory" consists of 340 x 240 pixels which can be set to any of 256 intensity levels and displayed on a 19 inch color television monitor. A single frame (band) can be displayed in black-and-white and three frames can be combined to produce a color image. The information in each "frame memory" can be changed rapidly based on various functions, allowing for a flexible interactive display. Features in the display capability include zooming and scrolling, along with a cursor for obtaining coordinate information.

The second system is made up of slower devices and is used for digitizing and non-interactive display. Included within this system is a standard Data General NOVA minicomputer with 16K words of memory and a memory cycle time of 2.6 microseconds. The overall task of this machine is to gather data from and control a number of slow I/O devices leaving the first system free to do larger computations and run the faster devices. The slow I/O devices include a scanning microdensitometer that can scan and digitize photographic transparencies up to 15.24 cm

Figure 4a.- Hardware System One

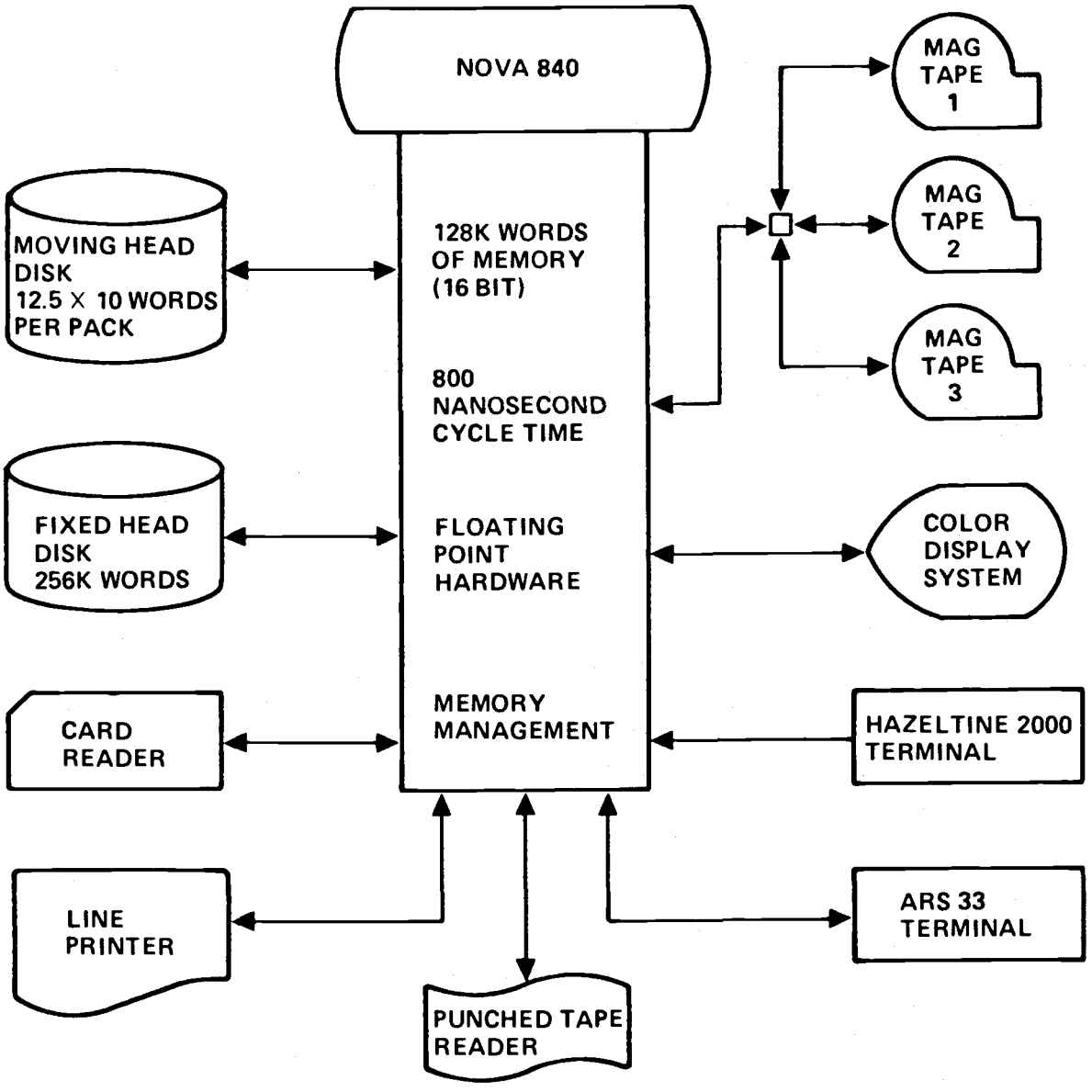

Figure 4b.- Hardware System Two

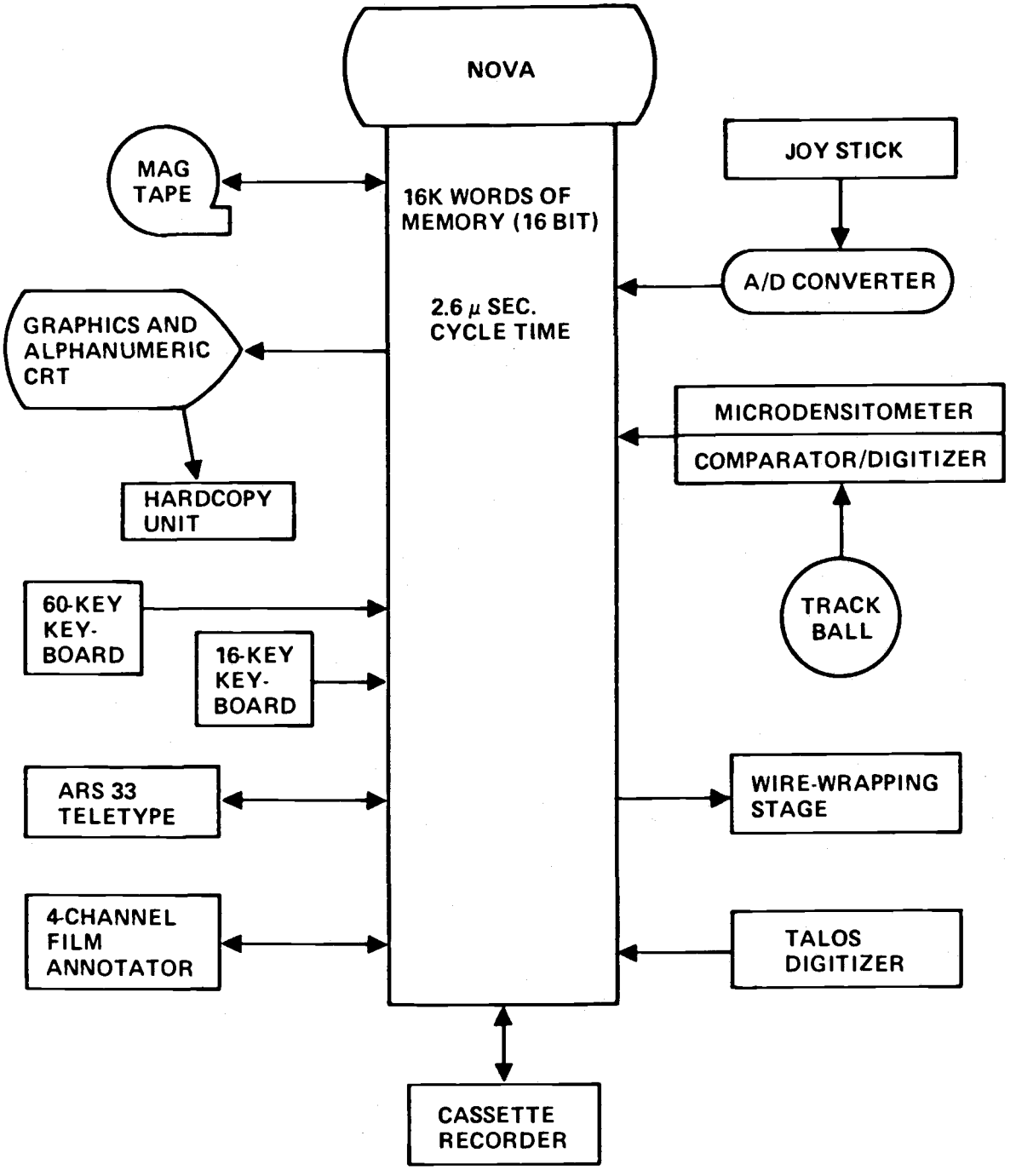

Figure 4c.- Hardware System Three

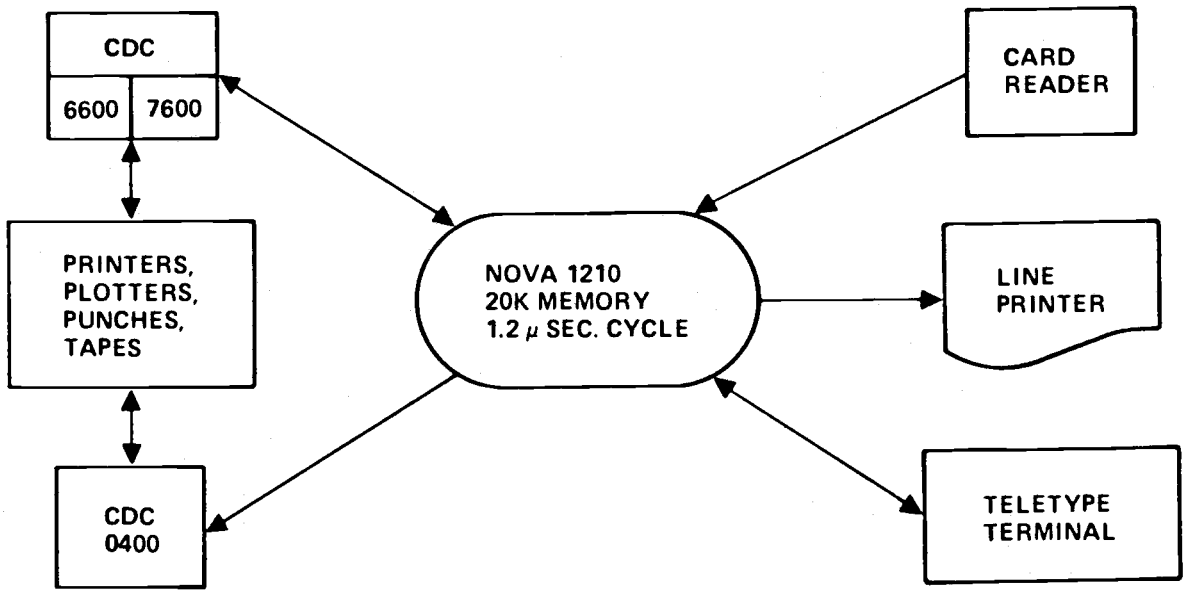

(6 inches) square with a geometric resolution of 0.0127 cm (0.005 inches) and a density range of 4096 grey levels. Under normal control the devices may also be used to create digitized coordinate maps, although a newer device, a table coordinate digitizer with a 76.2 cm x 101.6 cm (30 inch x 40 inch) tablet and geometric resolution of 0.00254 cm (0.001 inches), is better suited for this type of work. This system also includes a black-and-white graphics CRT that allows graphic and alpha-numeric displays to be drawn on a high resolution screen that may be transferred to a hard copy device. Finally, the system possesses a 4-channel film annotator that is used to make photographic imagery of very high resolution from data provided by either system one or two. This device is capable of providing four images of 70mm size in less than one half hour and can produce 35mm through 22.8cm x 22.8cm (9 inch x 9 inch) positives or negatives at a resolution of 500 lines per inch.

The third system functions as a remote batch terminal linking the RSRP to several large main frame computing systems at the University of California, Berkeley and at the U.S. Department of Energy Lawrence Berkeley Laboratory. This system is primarily used for programs that require the large capacity and high speed of large system computers. The system is controlled by a Data General NOVA 1210 linked via conventional telephone lines to the three large computers at the University of California, Berkeley and the Lawrence Berkeley Laboratory. I/O devices included in system three are a 450 card per minute reader, a 1000 line per minute line printer and a teletype used as an interactive communication device.

Software at the RSRP can be loosely grouped into three categories: Image interpretation statistical analysis; and operating systems.

Programs in the image interpretation category can be further grouped into the following subcategories: Data preparation and display programs; multi-feature classification and; programs for the presentation and analysis of results. As this grouping implies, the discriminant analysis (sorting of the multi-feature data into selected classes) is the central function of the image interpretation software. Data preparation is the acquisition and organization of multi-feature data for submission to the classifier. Presentation and analysis of results is the post processing of the classifier's output. For these reasons, most of the programs in

this section will be described in terms of their relation to CALSCAN, the primary multi-feature discriminant analysis classifier at the RSRP. CALSCAN is the RSRP adaptation of the discriminant analysis program, LARSYSAA, developed at the Laboratory for Applications of Remote Sensing at Purdue University.

Types of data that can be used in the data preparation and display software include multispectral digital data from Landsat or any other satellite, conventional photographic imagery, textural data generated from multispectral data, or non-spectral features such as topography, rainfall, soil types, and stratification boundaries. These data may be gathered from a wide variety of sources and have a wide variety of formats. The programs described below have been written to acquire, reformat, and combine the data into the CALSCAN multi-feature data format.

Software Description

A. Landsat Multispectral Data

(1) Landsat MSS Reformatter

The MSS reformatter rewrites an entire Landsat scene tape into the RSRP internal format which is compatible with the CALSCAN input format.

(2) Raw Landsat Display

A reformatted Landsat tape or test tape can be displayed on the color television monitor, either one band at a time or as a combination of three of the four bands in false color. This process can be used to verify a test tape or to locate areas to be used to train or test the classifier.

(3) Landigor

A reformatted or test Landsat tape can be reproduced on the four channel film annotator (IGOR), one MSS band per channel. The resulting film is a permanent image of the initial data, before the classification process. The film may be used to locate test or training areas, either separately or combined in a color image.

B. Photographic Data

(1) SCAN/MOVE

To use a photographic image as input, the image must be converted to a suitable digital format. This is done by the scanning microdensitometer (scanner) under the control of SCAN/MOVE.

The scanner processes transparencies, either negatives or positives. The image is placed on the scanning stage and the size and resolution of the area to be scanned are specified. The scanner then takes a density reading for each point at the spacing requested up to 79 per cm (200 per inch). This information is written onto a magnetic tape, and is the digital version of the image in one

band. A color image may be digitized by using filters in the scanner and doing several scans of the same area, each scan representing a different spectral band.

(2) SCAN DISPLAY

This program is used to display the products of SCAN/MOVE to aid in training and test area extraction. One scan can be written to each of the four "frame memories" of the color display system, then viewed singly or in any combination of three.

(3) RESCAN

Scans produced by SCAN/MOVE are not in a format acceptable to CALSCAN and must be rewritten. Up to 15 images of scanned digital one band spectral data from one area may be rewritten into the CALSCAN format by the use of RESCAN. The program accepts as inputs the scanned images from SCAN/MOVE and punched control cards describing the data, and produces a scaled and interleaved version of the data on magnetic tape.

C. Textural Data

(1) TEXTURE

Program Texture quantifies the texture of scanned photographs, (Landsat data) and calculates sets of means and standard deviations of the inputs of density readings of reflectance. The means and standard deviations are written onto magnetic tape in a format acceptable to ADDFEAT (described later) for combination with spectral data in the CALSCAN format. The size of the standard deviations is sensitive to the size of features in a given area, their spacing, and the contrast between them. The means measure differences in density or reflectance so that two areas of different average density but identical standard deviations can be distinguished from one another.

D. Non-spectral Data

There are many non-spectral features which can be of use at some point in many remote sensing data analyses. Some of these features are valuable inputs to the discriminant function used by CALSCAN in the point-by-point classification of multi-feature digital imagery (e.g. soil types, elevation, slope and aspect). Others, such as economic considerations may be used to control the action of CALSCAN in other areas (e.g., direct it to ignore points within one area, classify points within a second area into agricultural classes, and classify points within a third area into timber classes). Finally, many non-spectral features are of use in post processing as elements of a data bank. A user may specify them as parameters for a resource inventory, answering questions like, "How much timber of types A, B and C is growing on private lands in Benton county where the slope is less than 20 percent and the elevation is between 500 and 1500 feet above mean sea level?"

Non-spectral features are processed in a manner similar to photographic transparencies. First, the raw data are converted to a digital representation, then the digital data are converted to the format required by the program to which the features are to be input.

(1) DIGICAL and NINEBY (Coordinate digitizing routines)

These routines are used to convert linear information on maps, photos and other images into coordinate information suitable for computer input. The coordinate information can be geometrically transformed to overlay spectral data by a polynominal generated least squares fit for a set of control points. The routines convert any closed line on an image to a list of X-Y coordinates representing that line. Information such as topographic elevation linear political or geographic boundaries, field outlines and agricultural or wildland strata can be successfully digitized in this manner.

The digitizing process represents the original line by a series of straight line segments and records the coordinates of the end points. In this way the coordinate information is an approximation of a curved line on an image. Once digitized, information may be displayed graphically on the black-and-white CRT and the area enclosed by each closed line can be computed

(2) ADDTOPO

Elevation data are available in several formats: on USGS maps which can be digitized, punched cards from various souces and digital tapes. The program ADDTOPO accepts as inputs elevation data on cards or magnetic tape. Spectral data in CALSCAN format, and punched control cards and produces on magnetic tape a combined version of the data in CALSCAN format. The program will generate slope and aspect values from the elevation data and add these as two additional features.

(3) ADDFEAT

A wide variety of non-spectral features can be digitized by the coordinate digitizing routines. The program ADDFEAT accepts as inputs data on magnetic tape describing such features plus multi-feature data in the CALSCAN format, plus punched cards, and produce on magnetic tape a final multi-feature CALSCAN-compatible version of all the data. The features produced by the program TEXTURE are also processed by ADDEFEAT.

(4) MASK function of MAPIT

As previously discussed, some features can be useful for pre-sorting of data into general classes, each of which is treated by CALSCAN in a different manner. Such features are digitized by DIGICAL, as described earlier, but are not combined with the spectral data since they are not used in the discriminant function in CALSCAN. Instead, these features are processed by the MASK function of the program

MAPIT (MAPIT is described in the upcoming section on presentation and analysis of results). The result is a special tape called the mask tape or stratification mask which is provided to CALSCAN in addition to the standard multi-feature data tape.

Several programs have been developed at the RSRP to assist in multi-feature data analysis. Traditionally these programs can be placed in one of three groups that make up the classification process; training; feature selection; or classification.

Under the training group the RSRP utilizes two major algorithms. The first, CALSCAN, is a so-called supervised classifier in the sense that it requires information about what classes exist in the data. This information is provided in the form of training cells. Certain areas are designated that are known to contain only one class of interest. One or more areas are chosen for each class in the data. On the basis of this information the program generates a statistical model for each class. The classification is performed by placing each pixel into it's most likely statistical class. Some data are not well suited for processing through the use of predetermined class statistics. Typically, wildland and forest areas are of this sort, i.e. the selection of training cells is difficult and tedious. ISOCLAS, an algorithm developed by Lockheed Corporation for NASA at the Johnson Space Center in Houston, Texas was adapted at RSRP for assistance with this problem. The user of the program designates an area upon which the program is to work, and the number of classes presumed to exist in that area. By the process of clustering, ISOCLAS sorts the data into classes, using the number set by the user as a maximum. The user must then determine to what real (ground truth) class each program generated class belongs. This method of classification is generally much more expensive than supervised classification in terms of computer time but involves considerably less work for the user.

An organized method for storing and manipulating multiple sets of digital data is important for any remote sensing research effort. The data bank storage and retrieval system MAPIT at RSRP has a structure and capabilities such that a researcher may create and analyze maps or images

and store, retrieve, and display them as in a pure data storage system. The MAPIT system is heavily oriented toward the efficient use of user time involved in data preparation and machine interaction.

MAPIT is a system of programs used on the large main frame computing system at the Lawrence Berkeley Laboratory. It may be operated in two modes, interactive and batch oriented around "profiles" (also referred to as feature maps).

A profile conceptually represents a relationship between a point and some attribute or condition of that point. The point is described by an x, y coordinate pair; the attributes belonging to that point are usually referred to as its z values. This generalized definition of a profile applies to maps, photos, CALSCAN results, Landsat data or any structure relating an areal unit to some attribute. The attribute or feature referred to here could be anything from soil types to population. In the case of images the attribute is the density value of its picture elements. Often many different attributes must be considered for the analysis of an area, as in, land suitability for conifer growth modeling. One of MAPIT's assests is it's ability to handle any number of profiles for an area. A resulting attribute map of an area could be defined as the set of all profiles for the area as illustrated in Figure 5 (RSRP, 1974). As was previously mentioned, general environmental descriptor variables (spectral, topographic, climatic), available in digital form may be used to construct a computer data base for use in modeling research.

As the first data feature or profile to be included in the conifer growth model build set, Landsat spectral data will be used to simulate earth surface albedo. The albedo information then is to be used as an input to an algorithm that will estimate net incident solar radiation and potential evapotranspiration which in turn will be used as factors in modeling conifer growth as an indicator of land capability for timber production.

The Landsat program imcorporates three satellites, one of which is still active at this writing. The craft were designed as research and development tools to demonstrate the feasibility of systematic remote sensing from Earth orbit for resource and environmental monitoring. Landsat 1, originally designated Earth Resources Technology Satellite

Figure 5.- Data Bank Configuration

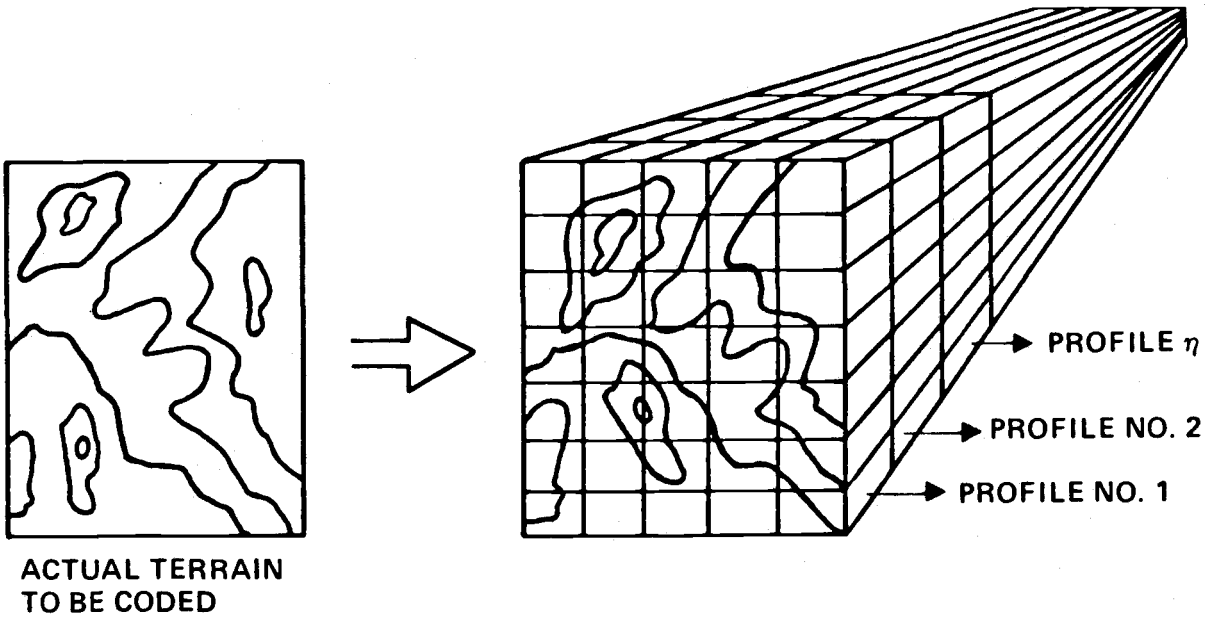

Shown above is the conceptual approach to storing and retrieving information about an area of interest. The data bank is a three-dimensional array of data points with X and Y coordinates representing ground location points. The Z coordinates are profiles of discrete information in the data bank, such as data about topography, soils, solar radiation or even evapotranspiration potential. The amount of profile information which can be stacked on the X and Y coordinates is virtually unlimited.

(ERTS) was launched in July 1972, Landsat 2 in January 1975 and Landsat 3 in March 1978. The latter satellite, Landsat 3 is functional while Landsats 1 and 2 are no longer operational. Each satellite orbits at an altitude of approximately 900 km (570 miles) in near polar orbits that are sun synchronous. The satellites cross the Equator on the day side of earth 14 times daily at approximately 9:30 am local time. Each successive orbit shifts westward about 1785 miles (2875 km) at the equator. On the following day the next 14 orbits parallel those of the previous day, but each one is offset westward by about 99 miles (159 km). Images obtained for any two adjacent orbits and collected on successive days exhibit about 15 percent sidelap at the Equator, increasing to about 85 percent near the poles. The same point in any region overpassed by a Landsat is imaged every 18 days. The orbit of Landsats 2 and 3 were complementary in a manner that allowed each point imaged to be examined once every 9 days.

Two imaging sensor systems operate on each of the Landsat. The first is known as the RBV (return beam vidicon), a television camera system that was shut down early in the operation of Landsat 1 and used little on Landsats 2 and 3. On Landsats 1 and 2 the RBV was a three band sensor spanning the visible and near infrared wavelengths of the electromagnetic spectrum, while on Landsat 3 the RBV was single band panchromatic. The second sensor which is identical on all three Landsats is called the multispectral scanner (MSS) produces a continuous image strip built up from successive scan lines extended perpendicular to the forward direction of the satellite orbital motion. Electromagnetic energy from the ground is transferred by an oscillating mirror in the MSS to a recording system after passing through filters that select different wavelength intervals to sample. Four wavelength channels are processed according to the following arrangement:

TABLE 4.- Landsat MSS Wave Band Description

Band Number*	Wavelength Interval (μm)	Spectral Region
4	0.5 - 0.6	Green
5	0.6 - 0.7	Red
6	0.7 - 0.8	Near IR
7	0.8 - 1.1	Near IR

*Numbered in this manner to avoid confusion with the three RBV bands of Landsats 1 and 2 (USDI, 1976).

A primary use of the multispectral capability of the MSS stems from a basic property of materials. Because different classes of features found on the Earth's surface reflect and emit differing amounts of electromagnetic energy in different wavelength intervals, they may be identified to a degree by their own characteristic spectral signatures. It was this fundamental relationship that was exploited in this study. Before this relationship could be utilized, the data, in this case an appropriate Landsat scene needed to be ordered and readied for use.

Because of project time constraints it was decided to inventory and choose a scene or scenes from data that had been archived at the EROS Data Center (i.e. already processed by the Goddard Space Flight Center). The study area is remote and decidely little change has taken place that would require the most recent Landsat coverage available. With many years of data to choose from, the likelihood of purchasing a scene of excellent radiometric quality was good. The search for a suitable Landsat data set was initiated by sending a request to the EROS Data Center for a computer search of their archived data. The list was screened for possibilities. To insure a proper scene selection, microfilm of the perspective Landsat scenes were screened at the USGS Western Mapping Center in Menlo Park, California. The most recent high quality scene that would emphasize the study area and its coniferous forests was dated August 14, 1977. The data for this scene were reformatted so that they would become compatible with the in-house computing system. The study area was found to cross the boundary between two quadrants of the scene. This required that a test data set be created by isolating the study

area, splicing the two quadrants together and writing the data to tape. The data were then ready for use in modeling surface albedo. To facilitate the task of albedo modeling ancillary information in the form of maps and aerial photography (medium scale 1:80,000 CIR and Natural Color) were assembled.

Through the use of Landsat imagery and aerial photography training sites were selected throughout the study area. These sites encompassed the spectral variation that was likely to occur throughout the study area. This task usually requires extensive knowledge of the area. The selected training areas were located on the Landsat digital data and the aerial photography. The location of these sites on the Landsat digital data was easily accomplished through an interactive display of the data. The x and y coordinates of the training site block corners were then found by displaying the Landsat image and determining the training site location from its general position on the aerial photography. The exact position on the training sites were defined by the Landsat image of the training sites. The area could then be plotted with greater flexibility on the aerial photography. This was due to the display restrictions usually associated with the Landsat digital data. Figure 6 shows the spatial distribution of Landsat training sites throughout the study area.

Once the position of the training sites on the Landsat digital data had been determined, a computer compatible tape containing each training site was generated. The tape was input to the unsupervised classification algorithm ISOCLAS to cluster the Landsat data of each training site into like groups. The end product was a list of image classes defined by their spectral mean, standard deviation and convariance. Table 5 shows these statistics for training block one. In order to attempt specific vegetation/terrain classes to each cluster, a technique known as 7 to 5 ratioing (a vegetation index) was used to aid in spectrally organizing the data. Table 6 depicts the 7 to MSS band 5 ratio information for training block one. To help in the organization of the data for display purposes, unique colors were given to each cluster beginning with lavender and red for high 7 to 5 ratio clusters, through brown, orange, yellow and green, and finally to blue for the lowest 7 to 5 ratio clusters. Figure 7 shows how training block one appeared.

Figure 6.- Study Area Training Site Location

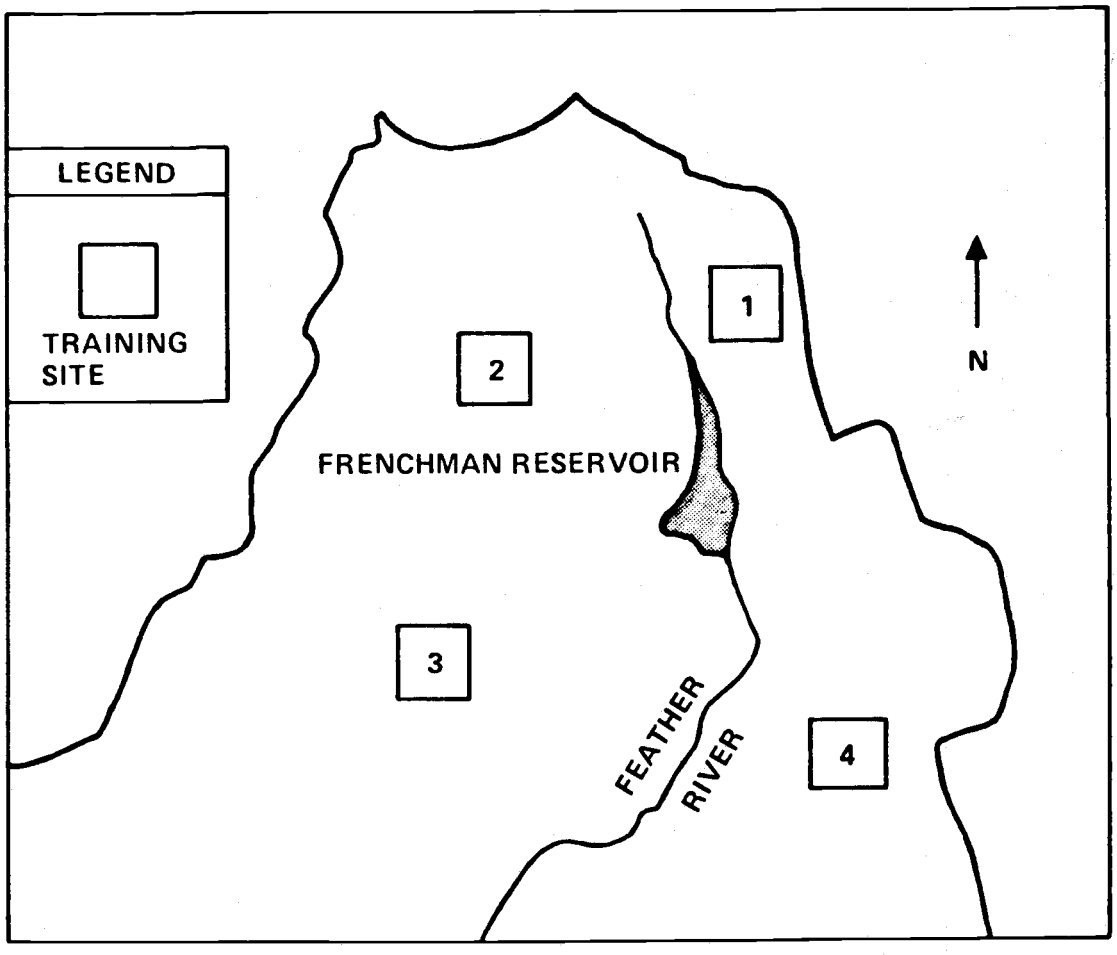

TABLE 5.- Statistics for Training Site One

Cluster	MSS Band 4		MSS Band 5		MSS Band 6		MSS Band 7	
	Mean	STD	Mean	STD	Mean	STD	Mean	STD
1	21.27	1.20	28.81	2.26	33.79	2.19	17.34	1.44
2	30.37	1.25	31.68	1.75	35.95	1.62	18.19	1.13
3	24.27	2.16	23.90	1.63	29.89	1.81	15.99	1.37
4	23.73	1.35	35.57	2.08	38.70	2.64	19.62	2.49
5	18.97	2.05	15.66	2.17	31.83	2.05	19.21	1.47
6	28.34	1.05	27.98	1.65	31.99	1.64	16.44	1.29
7	17.53	1.75	14.49	1.72	26.28	1.95	15.42	1.52
8	32.29	1.26	35.19	1.86	39.28	1.48	19.77	1.18
9	22.33	2.17	20.98	2.33	36.80	2.61	21.57	1.77
10	21.79	1.68	19.34	1.74	27.33	2.00	15.17	1.68
11	36.61	5.78	41.69	5.81	43.66	4.19	21.67	2.35
12	26.99	2.26	27.06	2.15	39.09	2.29	21.82	1.79
13	37.52	1.51	43.76	1.88	47.78	1.49	23.98	1.20
14	39.94	3.99	50.24	2.93	54.98	3.75	27.24	1.99
15	27.13	4.10	46.83	8.59	46.85	7.28	24.80	5.27
16	33.49	1.30	27.30	2.18	43.16	1.51	22.03	1.52
17	26.57	1.72	38.72	3.05	43.94	1.98	22.75	1.76
18	19.71	36.89	35.86	35.33	0.00	0.00	0.00	0.00
19	.02	.15	4.49	15.00	0.00	0.00	2.84	11.05

TABLE 6.- Landsat MSS Band 7 to Band 5 Ratio Data for Training Site One

Band 7/Band 5 Ratio*	Numerical Order	Cluster	Color Assignment Group
2.4534	1	5	
2.1284	2	7	Lavenders & Reds
2.0276	3	9	
1.6127	4	12	
1.5688	5	10	
1.3381	6	3	Browns & Oranges
1.2037	7	1	
1.1812	8	16	
1.1751	9	17	
1.1751	10	6	Yellows
1.1484	11	2	
1.1236	12	8	
1.1032	13	4	Greens
1.0960	14	13	
1.0844	15	14	
1.0592	16	15	Blues
1.0396	17	11	
------	18	--	Black
------	19	--	

*The actual equation for the Band 7/Band 5 ratio is:

2 x (Band 7 mean scene brightness value of cluster n) ÷ (Band 5 mean of scene brightness value of cluster n) where n goes from 1 to 17 inclusively.

Figure 7.- Landsat MSS Band 7 to Band 5 Ratio Display of ISOCLAS Training Site One

Using aerial photography and the 7 to 5 ratio image product image analysts grouped and separated the different clusters into meaningful vegetation/ terrain classes. Table 7 shows the result of this process.

The cluster means, standard deviation, and covariances for the set of classes discussed above were used to drive the final supervised classification (by CALSCAN) of the entire study area.

With the ground cover completely analyzed, it was a matter of assigning published albedo indices to each vegetation/terrain class to form the albedo data set. The albedo indices were derived from a variety of sources illustrated in Table 8.

The albedo data set was then the first profile of information to be entered into the study area data base. For consistency in reference, all subsequent data profiles were registered and resampled to the Landsat coordinate system of the original August 14, 1977 Landsat scene.

In the compilation of a comprehensive data base for a wildland area the inclusion of topographic information is essential. Topographic data are available in both digital and map form. For the purposes of this study, digital topographic data are preferred. Such data are inexpensive, derived from map based information, and completely computer compatible.

The digital terrain data are available in blocks one degree latitude by one degree longitude, as produced by the Defense Mapping Agency Topographic Center (DMATC) through the digitization of 1:250,000 series USGS topographic maps. Each one degree block, labeled either east or west, corresponds to one half of a 1:250,000 scale map sheet. The digitization procedure produces a grid of elevation values for every 0.004 cm (0.01 inches) on the map, which corresponds to approximately 208 feet (63m) on the ground (USDI, 1970).

Initially, it was necessary to locate and plot the study area boundary on two adjoining 1:250,000 scale maps. Upon the completion of this task, it was apparent which one degree blocks had to be ordered to completely cover the study area. The data were then ordered (2 blocks - the eastern sections of the Susanville, California and Chico, California 1:250,000 scale topographic maps) in an 800 bpi 9 track format so as to be compatible with the RSRP in-house computing system.

TABLE 7.- Landsat MSS Band 7 to Band 5 Ratio Cluster Labels

Vegetation/Terrain Class	Cluster	Band 7/Band 5 Ratio
High density eastside conifer	5	2.4534
	7	2.1284
Low density castside conifer	9	2.0276
Brush/Chaparral	10	1.5688
Sagebrush/Bare Soil	12	1.6127
	2	1.1484
	4	1.1032
	8	1.1236
	16	1.1812
Sagebrush	1	1.2037
	3	1.3381
	6	1.1751
Bare Soil	11	1.0396
	13	1.0960
	14	1.0844
	15	1.0592

TABLE 8.- Earth Surface Albedo Indices

Stand	Albedo (Percent)
Fresh snow cover	75-95
Dense cloud cover	60-95
Old snow cover	40-70
Clean firn snow	50-65
Ice, sparse snow cover	69
Clean glacier ice	20-50
Light sand dunes, surf	30-46
Sand soil	15-40
Meadow and fields	12-30
Meadow, low grass	15-25
Field, plowed, dry	20-25
Densely built-up area	15-25
Woods	5-20
Dark cultivated soil	7-10
Douglas-fir	13-14
Pine	14
Conifers	10-15
Deciduous forest, fall	15
Deciduous forest, summer	10
Coniferous forest, summer	8
Coniferous forest, winter	3
Meadow dry grass	10
Field Crops, ripe	15
Spruce	8-9
Earth roads	3
Black top roads	8
" " "	9

From: Geiger, 1975.

After the data had been received, it was necessary to reformat them so that they would be compatible with data types used by the RSRP system.

In dealing with more than one block of data, the first major concern was to merge the data into one continuous block. After the data blocks were displayed side by side on the interactive display system it was discovered that they could not be simply joined together to produce one continuous data plane. Lines of data were missing that would be necessary to produce a planimetrically accurate singular data block. Through several shifts in the relative position of each block on the display in conjunction with a close evaluation of the 1:250,000 scale base maps, an optimum separation was determined. To fill the gap produced by the separation of the blocks, a linear interpolation was performed that would provide new data based on the existing data trends within each of the original blocks.

Because the data were originally digitized line by line from north to south from the 1:250,000 scale topographic sheets, the data appear to be rotated 90° counter-clockwise. This causes north to be shifted to the left, south to the right and correspondingly, east to the top and west to the bottom of the color display. It was then necessary to reorient the data so that each line was east-west trending and transform the data to the Landsat coordinate system.

To exclude non-essential data from the final data profile, the study area boundary was digitized and overlain onto the single elevation data block. The result was a map of the study area with an elevation value for each data cell, or Landsat pixel in this case (Figure 8). This became the second profile in the study area data base.

To expand the topographic information base, the elevation data were used as input to algorithms designed to model slope and aspect. The slope determination routine considers the elevation gradient between data cells that surround the cell for which the slope is being calculated (Figure 9). Based on these elevation differences, a sloping plane is described whose normal vector is calculated and used as a measure of slope. The azimuthal orientation of this normal vector describes aspect.

Figure 8.- Study Area Digital Elevation Image

COLOR	ELEVATION (METERS ABOVE MEAN SEA LEVEL)
BLUE	1463-1585 (4800-5200 FT.)
SKY BLUE	1586-1708 (5201-5600 FT.)
BLUE GREEN	1709-1801 (5601-5900 FT.)
DARK GREEN	1802-1832 (5901-6000 FT.)
GREEN	1833-1864 (6001-6100 FT.)
LIGHT GREEN	1865-1895 (6101-6200 FT.)
YELLOW GREEN	1896-1957 (6201-6400 FT.)
YELLOW	1958-2019 (6401-6600 FT.)
YELLOW ORANGE	2020-2051 (6601-6700 FT.)
ORANGE	2052-2082 (6701-6800 FT.)
LIGHT RED	2083-2114 (6801-6900 FT.)
RED	2115-2145 (6901-7000 FT.)
MAGENTA	2146-2268 (7001-7400 FT.)
BROWN	2269-2391 (7401-7800 FT.)
GRAY	2392-2453 (7801-8000 FT.)
WHITE	2454-2515 (8001-8200 FT.)

Figure 9.- Slope Algorithm Calculation Notation

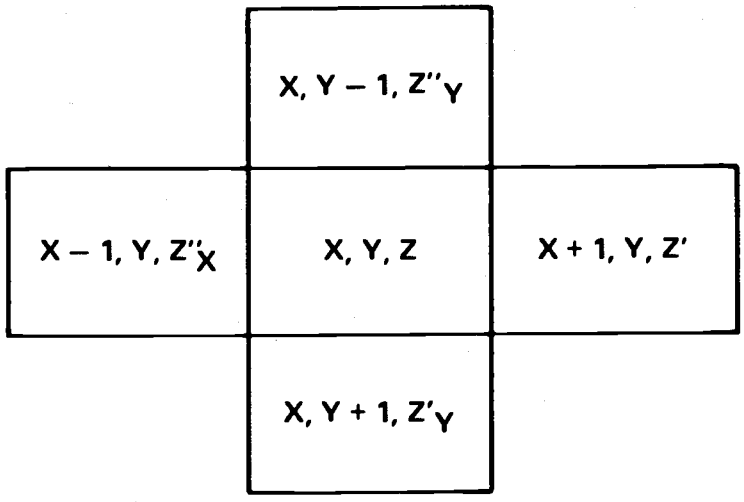

Using the vector's cross-product formula, the normal vector is

$$\vec{n} = 1,0,\frac{Z''_x - Z'_x}{2} \times 0,1,\frac{Z''_y - Z'_y}{2}.$$

Once the normal vector is $\vec{n}$ is computed the slope is calculatable since it is the angle between the normal vector and the vertical vector (0,0,1) subtracted from $\pi/2$ in radians. Therefore

$$\theta = \arccos \frac{n_z}{||\vec{n}||} \text{ and slope} = \pi/2 - \theta \text{ where}$$

n_x, n_y, and n_x are the coordinates of the normal vector and

$$||\vec{n}|| = n_x^2 + n_y^2 + n_z^2$$

then slope is converted to percent.

The aspect is determined from the x, y projection of the normal vector. The number of degrees from true North will determine the aspect,

$$\emptyset = \arctan \frac{n_y}{n_x}, \text{ where}$$

$\emptyset$ is the angle from the x-axis in radians. This is then converted to degrees and added to 90 to give the aspect in degrees from the true North direction (Khorram and Smith, 1977).

Therefore, slope and aspect formed the third and fourth data profiles in the study area data set.

Since the major goal of this study is to model conifer growth and infer land capability for timber production, potential evapotranspiration and net solar radiation are important factors to consider. Surface temperature is a critical input to models that approximate net incoming solar radiation and potential evapotranspiration. Thermal data for the conifer growing season (April-June in the study area) was necessary to model these conditions and stresses. No ground point data for temperature were available, so meteorological satellite data were chosen as the most reliable, consistently good quality data source. Specifically data from the NOAA-5 satellite were utilized.

The NOAA-5 satellite is an environmental satellite in a sun synchronous near polar orbit. At the time of this study NOAA-5 was the latest in a series of satellites launched by NASA and administered by NOAA after becoming operational. The satellite has an orbital inclination of 102°, an altitude of 1450 km and a period of 115 minutes. Its daytime pass covers the earth in a general northeast to southwest direction, crossing the equator at an angle of 78° at approximately 9:00 am local solar time.

NOAA-5 is equipped with two separate west to east scanning Very High Resolution Radiometers (VHRR). The VHRR is a two channel scanning radiometer covering the visible (0.6 - 0.7μm) and the thermal infrared (10.5 - 12.5μm) portions of the electromagnetic spectrum. Each VHRR instrument views the earth by means of a rotating mirror. The mirror is aligned to provide cross-track scanning of the earth. As a result of the design of the scanning system, the normal operating mode of the satellite calls for direct transmission of the visible and infrared data from both radiometers continuously on a real time basis. The data are transmitted in analog form from the satellite, and received and digitized at three NOAA ground stations. The nominal spatial resolution of the data is 0.9km at the satellite subpoint for both visible and infrared sensors.

Digital data are available from both the ascending and descending nodes (day and night passes respectively) of NOAA-5. All data available for the study period April to June 1978 were ordered and screened for cloud cover and bad data. After the screening process just five full days (day and night passes) of data remained.

Fortunately these dates (May 8, 1, 27 and June 17, 22) were reasonably spread over the most important months of conifer growth. The day-night pairs were used to estimate mean daily temperature by averaging day and night temperature. The five data sets were geoometrically corrected and resampled to the Landsat coordinate system and entered as the next series of profiles of the study area data set.

The amount of energy available to sustain photosynthesis and associated transpiration activity by coniferous vegetation in the study area is important in determining the potential amount of growth. The primary source of this energy is the sun, in the form of emitted radiation. The portion of solar radiation that actually reaches the earth's surface is dependent upon the transparency of the atmosphere. In the absence of cloud cover the amount is quite consistent. The atmospheric transmission coefficient varies from about 80 percent at the time of winter solstice to about 85 percent at the time of summer solstice (California Department of Water Resources, 1974). Atmospheric transmission coefficients are based on the total insolation received at the earth's surface including both direct and diffuse radiation. By far the largest variations in the amount of transmitted solar radiation are caused by clouds. The transmitted radiation varies with the type, height, density, and amount of clouds.

Since clouds are such a powerful controlling factor in radiative heat exchange, other minor factors such as humidity of the air are often ignored.

Similar to cloud effects, ground cover conditions such as the presence of a forest canopy exert a powerful controlling influence on net all wave radiation exchange. The forest canopy has a different effect than that of clouds, particulary with respect to shortwave radiation. Clouds are highly reflective, while a forest canopy absorbs much of the radiation. Consequently, the forest canopy tends to be warmed and in turn gives up a portion of its absorbed energy for evapotranspiration.

Total incoming radiation (D and I) is defined as the direct (D) and diffuse or indirect (I) shortwave radiation reaching the earth's surface through the atmosphere. Some of the incident radiation is reflected back to the atmosphere (R), and the remainder is absorbed by objects on the earth's surface. Part of the absorbed radiation is dissipated into the

atmosphere from the ground (G) as longwave radiation. In turn, a portion of the dissipated longwave radiation is absorbed by the clouds and atmospheric aerosols, and a portion of it is returned to the ground (A). The returned longwave radiation from the atmosphere to the ground (A) is called atmospheric radiation. The difference between upgoing (G) and atmospheric (A) longwave radiation may be defined as net longwave radiation.

Net radiation (Q_n), as is shown in the following equation, is the sum of the net shortwave radiation (D+I-R) and net longwave radiation (-G+A).

$$Q_n = (D+I-R) + (A-G)$$

The method used for estimating net radiation in this study employs a series of mathematical models and uses appropriate techniques for providing the required input information to the models. The categories of input include physiographic data (slope, elevation, aspect), albedo, climatic data and some meteorological constants.

The net all wave radiation model is described as:

$$Q_n = (1-\alpha)Q_S - Q_{nL}$$

where α is albedo, Q_S is the total flux of shortwave radiation from the sun and sky and Q_{nL} is the net upward flux of longwave radiation.

The net longwave component is computed as follows:

$$Q^*_{nL} = Q_{Ld} - Q_{Lu}$$

$$Q_{Ld} = 0.971 \times 10^{-10} T_K^4 - 0.245 \text{ (cal cm}^{-2}\text{min}^{-1}\text{)}$$

$$Q_{Lu} = 0.813 \times 10^{-10} T_K^4 \text{ (cal cm}^{-2}\text{min}^{-1}\text{)}$$

where Q^*_{nL} is the net flux of longwave radiation in cloudless conditions, Q_{Ld} is the downward flux of longwave radiation from the formula of Christiansen, (1966), T_k is the ambient temperature in degrees Kelvin and Q_{Lu} is the upward flux of longwave radiation from a surface with unit emissivity (Linacre, 1968).

Q_{nL} is then defined as:

$$Q^{*}_{nL}\ b+(1-b)\frac{n}{n}$$

where there are n hours of actual sunshine in a daylength of N hours. The term b has been taken by previous investigators to be either 0.10 (Penman, 1948), or 0.30 (Frank and Lee, 1966). A value of 0.20 has been adopted in the present study as a compromise (Linacre 1968).

The resulting equation is:

$$Q_{nL} = (-0.24 + 0.158 \times 10^{-10} T_k^4)(0.2 - 0.8\frac{n}{n})\ \text{cal cm}^{-2}\text{min}^{-1}$$

The value of Q_S is estimated by Linacre (1967) by means of the modified Angstrom equation:

$$Q_S = Q_A\ c+d\frac{n}{n}$$

where Q_A is the value of Q_S above the atmosphere, c and d are empirically derived constants related to atmospheric turbidity and n and N are as previously defined. The value for n is measured whereas values of N depend on the latitude and time of year and are available in standard meteorological tables. Table 9 shows values for c and d. The value of Q_A for a day or less (considering slope and aspect) are estimated by the following equation (Frank and Lee, 1966):

$$A_A = \frac{I_o}{e^2}(t_2-t_1)\sin\theta'\sin(\delta+\frac{12}{\pi})\cos\theta'\cos\delta(\sin wt_2'-\sin wt_1')$$

where

I_o = solar constant

e = ratio of earth-sun distance at a particular time to its mean

t_1 = number of hours before solar noon (negative)

t_2 = number of hours after solar noon (positive)

δ = solar declination

w = angular velocity of the earth's rotation

$\frac{12}{\pi} = \frac{1}{w}$ in radians

$\theta' = \arcsin(\sin k \cos h \cos\theta + \cos k \sin\theta)$

TABLE 9.- Published Values of Factors c and d for Modeling Solar Insolation

Source	Location	Latitude	c	d	c + d
Black et al. (1954)	Stockholm, Fairbanks	59°N, 65°N	0.22	0.52	0.74
Penman (1948)	Rothamsted, U.K.	52°N	0.18	0.55	0.73
Black et al. (1954)	Kew, U.K.	51°N	0.19	0.57	0.76
Tanner and Pelton (1960)	Wisconsin	43°N	0.18	0.55	0.73
Black et al. (1954)	Dry Creek	35°S	0.30	0.50	0.80
Black et al. (1954)	Batavia	6°S	0.29	0.29	0.58
Black et al. (1954)	General	-	0.23	0.48	0.71
Turc (1961)	General	-	0.18	0.62	0.80

where θ = latitude

k = slope in degrees

h = aspect in degrees from north

$wt' = wt + x$

where

$$\alpha = \arctan\left(\frac{\sin h \sin k}{\cos h \cos \theta - \cos h \sin k \sin \theta}\right)$$

Combining the equations for net shortwave and net longwave radiation, the net radiation on the earth's surface is estimated by the following equation:

$$Q_n = (1-\alpha)Q_s(-0.245+0.158\times10^{-10}T_k^4)(0.2+0.8\frac{n}{n})$$

Using this model, calculations of net solar radiation for each of five dates for which temperature information was available, were made. The five new profiles of information about the study area were then added to the study area data base.

Evaporation, and in particular potential evapotranspiration, is largely dependent on net solar radiation, and in large part is an indicator of moisture stress on a living plant (such as a conifer). The degree of moisture stress during the primary growing season of a conifer will in large part determine the rate and amount of growth that will take place. This is particularly true in the study area where the most significant limiting factor during the growing season is moisture availability.

Evapotranspiration may be defined as the transfer of water vapor from a nonvegetated surface on the earth into the atmosphere. Evapotranspiration is the combined evaporation from all surfaces and the transpiration of plants. Except for the omission of a negligible amount of water used in the metabolic activities, evapotranspiration is the same as the "consumptive use" of plants. The fact that the rate of evapotranspiration from a partially wet surface is greatly affected by the nature of the ground leads to the concept of potential evapotranspiration. Tanner and Pelton, (1960) define potential evapotranspiration as the amount of water transpired in unit time by a short green crop,

completely shading the ground, of uniform height and never short of water. Pruitt (1964) designated the term "potential maximum evapotranspiration" to describe the situation where advected energy is present. This removes any confusion on Penman's definition.

Many methods have been used to estimate evapotranspiration. Water balance, energy balance, aerodynamic, combination and empirical methods are numerous and all make assumptions with respect to at least one input variable.

Water balance methods are used for both terrestrial and water surface evaporation measurement. They are based on a hydrological equation which is usually considered on a large scale or catchment basin basis. With these methods water gain (precipitation, stream input) balances water loss (stream flow, evapotranspiration, water in solid form, subsurface storage), so if one knows the ways in which water is lost, evapotranspiration can then be measured or estimated.

Energy balance methods utilize the concept of energy conservation between air, soil and vegetation. Energy used for evapotranspiration, and consequently the amount of evapotranspiration can be estimated.

Aerodynamic methods assume set relationships between the flux of momentum, heat and water vapor in the atmosphere to estimate evapotranspiration. These assumptions are almost never valid, so these methods are rarely used.

Combination methods usually combine energy balance and aerodynamic methods. Limitations of applicability to general situations and lack of adequate input data have made these methods less desirable than their potential indicates.

Empirical methods are based on empirically derived model coefficients. Estimation of evapotranspiration based on empirical equations may be realistic only for localities and time periods for which the coefficients used in the equations were derived. Conversely, several general methods for estimating evaporation or evapotranspiration have been developed that required only minor modification to be applicable to local situations where an appropriate weather record exists.

The Jensen and Haise (1963) method is emphically based and shows good evidence of being generally applicable. Desirable attributes of their model include:

(1) Use of solar radiation, a variable highly correlated to evapotranspiration, as a primary variable (which is included in the study area data base);

(2) The first law of thermodynamics, which has been repeatedly shown to be a reliable and conservative method of determining evapotranspiration for both short and long periods;

(3) Being based partially on energy balance and therefore is semi-physically realistic (i.e. semi-empirical), a characteristic that may maximize reliability over time;

(4) Input variable data that may be derived from satellite information and;

(5) A calculation of potential evapotranspiration which may be input to more sophisticated models.

The Jensen-Haise model uses total shortwave radiation (R_s), expressed in inches of evaporation equivalent, as the climatic factor, and a dimensionless vegetation coefficient (ET/R_s) to reflect general vegetation type as well as climatic factors not accounted for by solar radiation. So the model is expressed as:

$$ET_p = (0.014T - 0.37)R_s$$

where ET_p is potential evapotranspiration in inches of water, T is mean daily temperature in degrees farenheit and R_s is total solar radiation in inches of evaporation equivalent. The linear temperature correction factor was derived by plotting ET/R_s versus T for selected vegetation types in which evaporating and transpiring surfaces were not limiting the vaporization of the water.

The Jensen-Haise equation was run on the five temperature and solar radiation data profiles in the study area data set forming five new data profiles in the study area data set forming five new data profiles describing potential evapotranspiration on each of the dates.

Water and its availability are extremely important in the development and survival of any plant. A measure of soil moisture available to a conifer (or any other tree) during its growth should provide

information in the evaluation of a growth rate for the tree. Before such plant available water data could be derived for the study area an inventory and map of the area distribution of soil types was required.

At the initiation of this study, official soils data were generally lacking. Several sources needed to be exploited in the creation of a study area soil type map.

Partial maps from the California Department of Water Resources, the Soil Conservation Service and results of a reconnaisance soil survey (described in the following chapter) were combined to create a composite soil map of the study area. Based on information available in the Soil Conservation Service Soil Survey for the region along with laboratory data (to be described in the following chapter) a plant available water value was derived for each soil type present on the study area map. The map was subsequently digitized by a coordinate digitizer to place the data into the study area data base. The soils data were the last to be entered into the study area data base.

A comprehensive, registered study area data base which contained components pertaining to albedo, topographic data (slope, elevation, aspect), solar radiation, potential evapotranspiration and soils data was created. Subsequent modeling involving any subset or all of these variables allows a model to be extended over the entire study area.

To build a model based on these data that would evaluate conifer growth as an indicator of land capability for timber production involves ground sampling to evaluate real conditions of growth and area characteristics. Chapter four will discuss the initial model building sampling effort.

CHAPTER 4. INITIAL SAMPLING EFFORT

During August and September of 1978 a ground sampling strategy was devised and instituted to obtain data that would be used in the construction of the conifer growth model.

The sampling effort involved cooperators from a number of groups and agencies. Expertise from the U.S. Forest Service (professional and summer intern people), the Youth Conservation Corps (YCC) and the author as a representative of Oregon State University and the University of California were involved in data gathering.

Important in deciding what type of observations to make at each sample site was a consideration of the balance between volume and appropriateness of data, together with time and manpower constraints. Aspects of a site that served to indicate conifer growth conditions were particularly important. These, of course, included soil and topographic characteristics of the area. Observations of secondary importance included vegetation composition and surface geology. Also included was a measure of conifer growth for each site. It was important to select trees that truly exhibited the growth potential of the site. For this reason one dominant tree and two co-dominant trees were selected for height and age measurement (Figure 10).

The most labor intensive activity in the sampling methodology was the construction of soil pits from which soil character observations were made and samples taken. Based on time and manpower limitations this task served to limit the number of sites that could be visited. It was decided that the largest group of cooperators with the least amount of technical skills would be utilized for this activity. This meant that the YCC people would be used in soil pit construction. The YCC group (approximtely 30 boys and girls) became available on loan from a larger project in the Sierra Nevada for a period of two weeks early in the summer (June and July). To effectively utilize this work force, U.S. Forest Service personnel close to the study area were used as supervisors in overseeing the work and determining sample site location. The principal overseer was the Plumas National Forest Watershed Branch Manager Mr. Jim McLaughlin who had an integral part in the conception and design of this study. It was entirely upon his knowledge of the study area and

Figure 10.- Sample Site Data Gathering Schematic

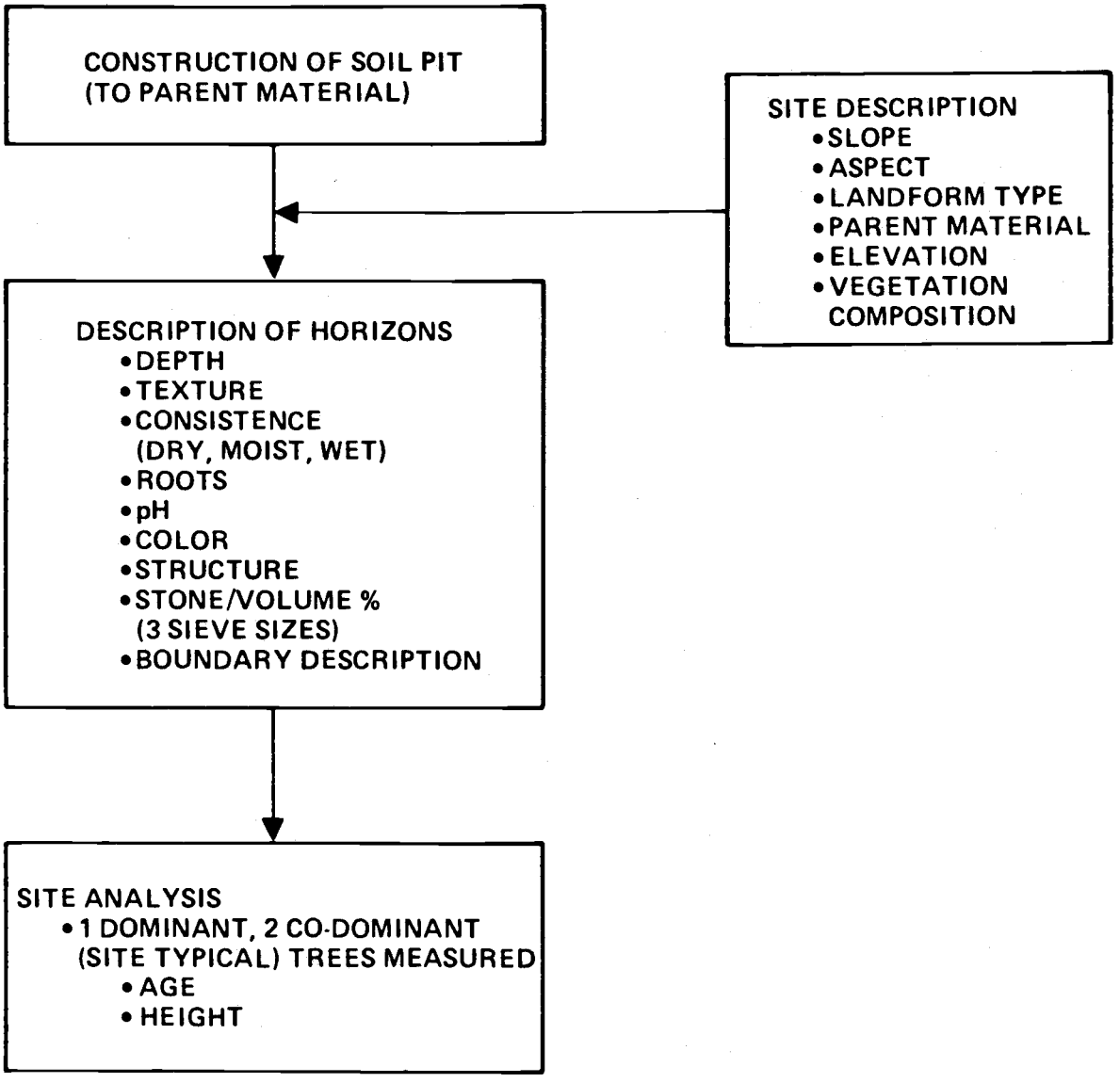

experiment goals that the sample site locations were based. A total of 35 sample sites spread over the entire study area were visited. Each site located in the field represented primarily north or south aspects and volcanic or granite parent material soils. In this way it was felt that two of the most obvious and overriding environmental factors influencing conifer grwoth would be sufficiently represented.

The obvious subjectivity in sample site location will be evident when the final model is evaluated in the next chapter. The development of a rigorous sampling methodology would have been more appropriate, but costs and more importantly, time was not available for such an undertaking.

Later in the summer (August and September) observations were taken and tallied for each sample site. Appendix I shows an example of the type of data gathered by site and used in the construction of the conifer growth model.

As each sample site was visited, its location was indicated on aerial photography. These locations were later plotted on a 1:62,500 scale USGS topographic map where UTM coordinates were derived for each site (Figure 11). A relationship was then developed that allowed for the transformation of UTM coordinates to study area data base Landsat coordinates. In this way the study area data base could be accessed to retrieve information about each sample site. Because of some uncertainty in the location of the sample sites (i.e. imprecision in the UTM-Landsat transformation) in the study area data base, a 3 x 3 block of pixels were averaged to represent any site location (Table 10).

With the study area ground and computer data bases completed the statistical analysis and model building could begin.

Figure 11.- Study Area Sample site location

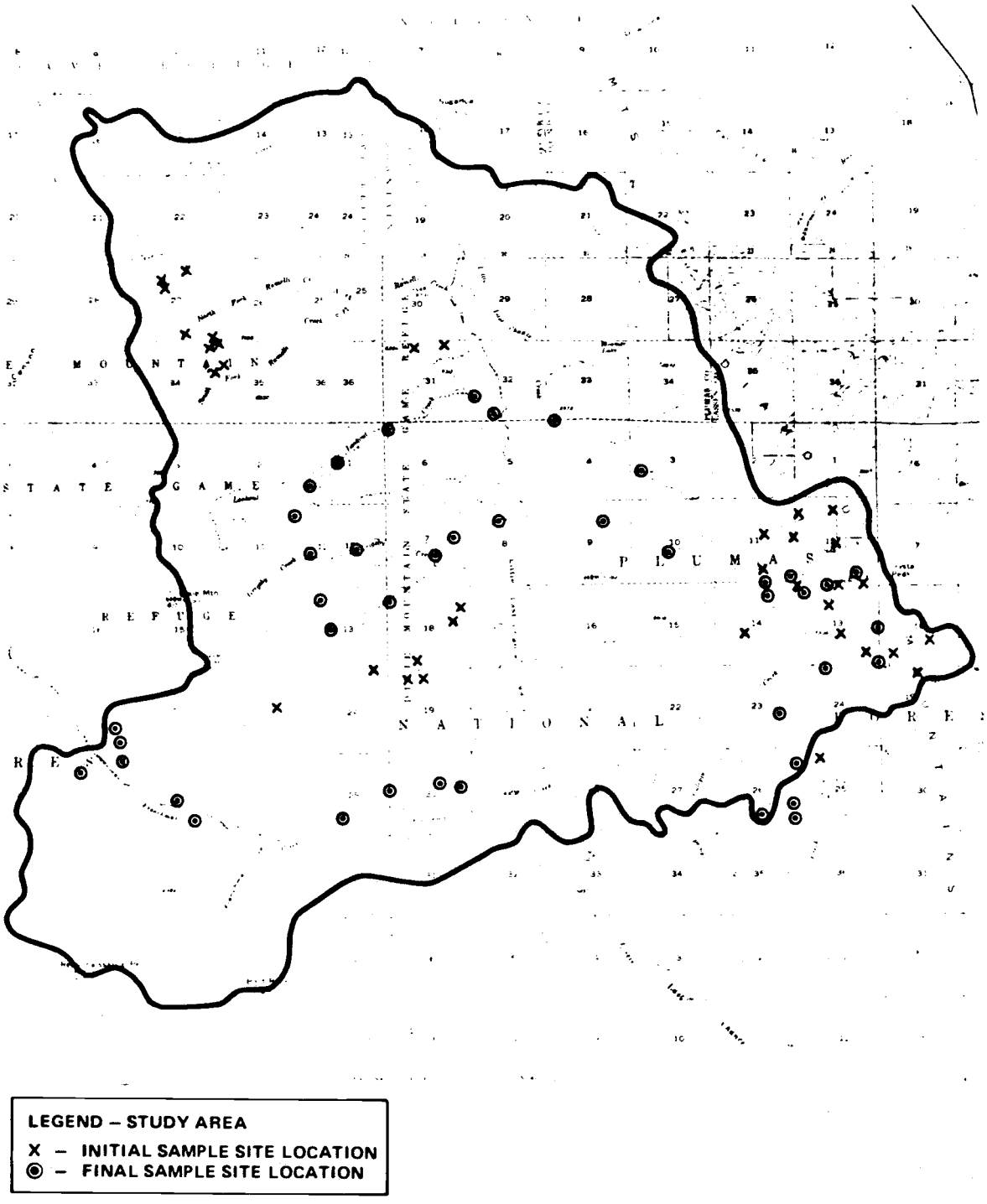

TABLE 10.- 3x3 Cell Data for Initial Study Area Sample Sites

Site Number and Landsat Coord. (x,y)	Solar Rad. (1y/dy)	Pot Evapotran. (in x 100)	Elevation (ft/100)	Slope (%)	Aspect (°)
	100	93	61	10	46
	98	89	60	13	47
1	95	83	60	15	48
(609,152)	101	76	61	9	44
	99	93	61	9	44
	95	84	61	11	47
	102	99	61	8	40
	102	100	61	9	40
	102	104	61	12	29
	MEAN = 99	MEAN = 93	MEAN = 61	MEAN = 11	MEAN = 43
	97	82	65	11	49
	93	79	64	11	49
2	99	88	64	9	48
(605,148)	97	81	64	10	50
	97	81	64	10	50
	103	91	64	8	49
	97	79	64	9	51
	97	79	63	20	51
	104	93	63	30	49
	MEAN = 98	MEAN = 84	MEAN = 64	MEAN = 13	MEAN = 50
	76	54	62	0	46
	70	0	62	0	57
3	105	99	61	6	39
(605,153)	106	99	61	0	0
	106	99	61	1	0
	104	99	61	1	38
	95	88	61	0	0
	85	3	61	0	57
	85	2	61	0	57
	MEAN = 92	MEAN = 60	MEAN = 61	MEAN = 1	MEAN = 33

TABLE 10.- Continued

Site Number and Landsat Coord. (x,y)	Solar Rad. (ly/dy)	Pot Evapotran. (in x 100)	Elevation (ft/100)	Slope (%)	Aspect (°)
	97	82	65	13	49
	93	65	65	11	52
4	94	68	65	10	52
(599,151)	90	53	64	11	53
	93	60	64	11	53
	97	77	64	10	51
	93	61	64	11	53
	93	61	63	28	53
	97	77	63	336	51
	MEAN = 94	MEAN = 67	MEAN = 64	MEAN = 16	MEAN = 52
	109	109	60	10	36
	109	106	59	8	34
	106	107	59	8	33
	108	112	60	13	29
5	104	108	60	10	31
(615,133)	104	108	59	8	31
	105	110	61	14	29
	108	112	60	12	31
	104	108	60	12	31
	MEAN = 106	MEAN = 109	MEAN = 60	MEAN = 11	MEAN = 32
	93	46	62	0	30
	109	111	61	0	30
	101	109	61	15	31
6	111	107	62	2	0
(614,137)	111	107	61	1	0
	100	104	61	33	39
	111	107	62	3	35
	111	107	61	3	37
	72	38	61	25	48
	MEAN = 102	MEAN = 93	MEAN = 61	MEAN = 9	MEAN = 27

TABLE 10.- Continued

Site Number and Landsat Coord. (x,y)	Solar Rad. (1y/dy)	Pot Evapotran. (in x 100)	Elevation (ft/100)	Slope (%)	Aspect (°)
	99	86	71	13	39
	98	84	70	13	43
7	102	85	70	11	44
(499,81)	97	80	70	14	44
	96	77	70	14	45
	97	79	70	14	46
	94	77	71	15	45
	94	77	70	15	45
	94	75	69	7	46
	MEAN = 97	MEAN = 80	MEAN = 70	MEAN = 13	MEAN = 44
	103	87	68	0	37
	104	86	67	4	42
8	102	88	67	7	39
(508,80)	105	87	67	1	0
	103	87	67	3	38
	103	89	67	6	39
	104	85	67	7	45
	103	87	67	3	39
	103	89	67	2	37
	MEAN = 103	MEAN = 87	MEAN = 67	MEAN = 4	MEAN = 35
	103	89	67	2	37
	103	90	67	5	37
9	103	91	67	5	34
(510,82)	106	89	67	7	38
	103	89	67	4	35
	103	91	67	5	31
	102	88	68	17	29
	104	89	69	19	30
	103	90	68	28	28
	MEAN = 103	MEAN = 90	MEAN = 67	MEAN = 10	MEAN = 33

TABLE 10.- Continued

Site Number and Landsat Coord. (x,y)	Solar Rad. (ly/dy)	Pot Evapotran. (in x 100)	Elevation (ft/100)	Slope (%)	Aspect (°)
	96	54	68	12	20
	106	89	67	7	38
10	103	89	67	4	35
(509,83)	98	85	68	15	27
	102	88	68	17	29
	104	87	69	19	30
	98	81	69	11	26
	97	62	69	7	27
	89	68	69	9	25
	MEAN = 99	MEAN = 81	MEAN = 69	MEAN = 11	MEAN = 29
	100	93	61	10	46
	98	89	60	13	47
11	95	83	60	15	48
(609,152)	101	76	61	9	44
	99	93	61	9	44
	95	84	61	11	47
	102	99	61	8	40
	102	100	61	9	40
	102	104	61	12	29
	MEAN = 99	MEAN = 93	MEAN = 61	MEAN = 11	MEAN = 43
	97	82	65	11	49
	93	79	64	11	49
12	99	88	64	9	48
(605,148)	97	81	64	10	50
	97	81	64	10	50
	103	91	64	8	49
	97	79	64	9	51
	97	79	63	20	51
	104	93	63	30	49
	MEAN = 98	MEAN = 84	MEAN = 64	MEAN = 13	MEAN = 50

TABLE 10.- Continued

Site Number and Landsat Coord. (x,y)	Solar Rad. (ly/dy)	Pot Evapotran. (in x 100)	Elevation (ft/100)	Slope (%)	Aspect (°)
	76	54	62	0	46
	70	0	62	0	57
13	105	99	61	6	39
(605,153)	106	99	61	0	0
	106	99	61	1	0
	104	99	61	1	38
	95	88	61	0	0
	85	3	61	0	57
	85	2	61	0	57
	MEAN = 92	MEAN = 60	MEAN = 61	MEAN = 1	MEAN = 33
	97	82	65	13	49
	93	65	65	11	52
14	94	68	65	10	52
(599,151)	90	53	64	11	53
	93	60	64	11	53
	97	77	64	10	51
	93	61	64	11	53
	93	61	63	28	53
	97	77	63	36	51
	MEAN = 94	MEAN = 67	MEAN = 64	MEAN = 16	MEAN = 52
	109	109	60	10	36
	104	106	59	8	34
	106	107	59	8	33
	108	112	60	13	29
15	104	108	60	10	31
(615,133)	104	108	59	8	31
	105	110	61	14	29
	108	112	60	12	31
	104	108	60	12	31
	MEAN = 106	MEAN = 109	MEAN = 60	MEAN = 11	MEAN = 32

TABLE 10.- Continued

Site Number and Landsat Coord. (x,y)	Solar Rad. (1y/dy)	Pot Evapotran. (in x 100)	Elevation (ft/100)	Slope (%)	Aspect (°)
	100	85	68	7	25
	98	80	69	9	24
16	103	92	68	11	27
(487,70)	96	63	68	8	22
	97	71	69	9	23
	103	88	69	9	26
	87	25	69	8	20
	82	1	69	8	21
	82	1	69	9	21
	MEAN = 94	MEAN = 56	MEAN = 69	MEAN = 9	MEAN = 23
	96	63	69	8	22
	97	71	69	9	23
17	103	88	69	9	26
(487,71)	87	25	69	8	20
	82	1	69	8	21
	83	1	69	9	21
	98	73	69	6	23
	90	43	69	13	19
	92	52	70	11	18
	MEAN = 92	MEAN = 46	MEAN = 69	MEAN = 9	MEAN = 21
	92	76	69	3	68
	100	81	69	8	68
18	100	80	70	15	70
(745,122)	103	79	69	1	70
	100	79	69	5	69
	94	76	70	11	67
	104	82	69	2	62
	101	80	69	4	3
	98	79	70	9	70
	MEAN = 99	MEAN = 79	MEAN = 69	MEAN = 6	MEAN = 61

TABLE 10.- Continued

Site Number and Landsat Coord. (x,y)	Solar Rad. (1y/dy)	Pot Evapotran. (in x 100)	Elevation (ft/100)	Slope (%)	Aspect (°)
	193	81	71	2	50
	99	81	71	2	58
19	103	82	71	2	68
(738,115)	103	81	71	11	48
	103	83	71	6	63
	93	73	71	3	63
	90	50	71	19	53
	100	77	71	12	59
	97	79	71	8	62
	MEAN = 99	MEAN = 76	MEAN = 71	MEAN = 7	MEAN = 58
	101	79	73	12	65
	78	0	73	10	57
	80	0	73	8	57
	85	47	72	11	58
20	90	61	73	10	59
(740,110)	97	69	73	10	59
	94	62	72	10	59
	92	67	72	12	60
	92	67	72	10	60
	MEAN = 90	MEAN = 50	MEAN = 73	MEAN = 10	MEAN = 59
	102	83	74	8	70
	103	83	75	8	72
21	101	83	75	8	1
(748,108)	100	83	74	7	70
	100	81	74	8	70
	100	81	75	8	70
	101	81	74	10	68
	100	86	74	9	70
	100	80	75	8	70
	MEAN = 101	MEAN = 82	MEAN = 74	MEAN = 8	MEAN = 62

TABLE 10.- Continued

Site Number and Landsat Coord. (x,y)	Solar Rad. (ly/dy)	Pot Evapotran. (in x 100)	Elevation (ft/100)	Slope (%)	Aspect (°)
	106	82	69	3	7
	107	83	69	1	7
22	108	83	69	0	9
(713,110)	99	54	69	0	20
	108	86	69	0	23
	108	85	69	0	0
	108	85	69	0	0
	108	85	60	0	0
	108	85	69	1	0
	MEAN = 107	MEAN = 81	MEAN = 69	MEAN = 1	MEAN = 7
	106	88	69	0	0
	109	87	69	6	0
23	102	82	69	15	46
(713,126)	109	87	69	2	0
	106	87	69	11	43
	97	72	69	17	47
	108	77	69	4	39
	102	67	69	4	43
	96	82	69	14	44
	MEAN = 104	MEAN = 81	MEAN = 69	MEAN = 8	MEAN = 29
	101	82	73	8	64
	103	78	73	7	49
24	99	75	73	7	49
(764,124)	101	81	72	9	63
	88	65	72	7	59
	96	64	72	7	53
	99	80	72	9	62
	98	72	72	7	59
	84	48	72	7	54
	MEAN = 97	MEAN = 72	MEAN = 72	MEAN = 8	MEAN = 57

TABLE 10.- Continued

Site Number and Landsat Coord. (x,y)	Solar Rad. (ly/dy)	Pot Evapotran. (in x 100)	Elevation (ft/100)	Slope (%)	Aspect (°)
	111	102	73	23	32
	115	48	73	23	26
	113	96	72	14	26
	106	101	73	4	32
25	106	100	73	21	32
(775,119)	116	107	72	21	33
	103	85	73	15	39
	104	81	72	26	45
	109	98	72	7	39
	MEAN = 109	MEAN = 96	MEAN = 73	MEAN = 17	MEAN = 34
	104	86	66	4	67
	102	85	67	6	5
26	100	85	66	12	70
(493,65)	103	87	66	3	64
	103	87	66	5	68
	99	83	66	5	71
	104	86	66	7	68
	102	85	66	7	71
	106	89	66	7	71
	MEAN = 103	MEAN = 80	MEAN = 66	MEAN = 6	MEAN = 62
	106	99	59	1	0
	106	97	59	1	48
27	106	98	59	1	46
(571,191)	106	98	59	1	45
	106	98	59	1	44
	106	97	59	1	45
	106	100	59	0	43
	106	100	59	1	43
	106	100	59	1	43
	MEAN = 106	MEAN = 99	MEAN = 59	MEAN = 1	MEAN = 40

TABLE 10.- Continued

Site Number and Landsat Coord. (x,y)	Solar Rad. (ly/dy)	Pot Evapotran. (in x 100)	Elevation (ft/100)	Slope (%)	Aspect (°)
	100	86	69	8	42
	99	87	69	8	39
28	100	89	69	8	37
(513,89)	101	86	69	5	41
	101	87	69	8	41
	103	89	69	8	39
	103	86	69	5	40
	101	88	69	7	38
	101	89	69	8	37
	MEAN = 101	MEAN = 87	MEAN = 69	MEAN = 7	MEAN = 39
	88	72	69	13	45
	96	85	68	15	41
29	100	88	67	8	39
(514,87)	98	87	69	11	39
	96	86	68	10	40
	102	90	68	10	33
	99	87	69	8	39
	100	89	69	8	37
	100	89	68	9	37
	MEAN = 98	MEAN = 86	MEAN = 68	MEAN = 10	MEAN = 39
	99	105	61	8	33
	001	105	61	16	34
	105	104	60	13	33
	93	93	61	5	34
30	98	104	61	13	35
(586,71)	101	104	61	11	34
	94	92	61	5	39
	90	94	61	10	36
	91	93	61	9	37
	MEAN = 97	MEAN = 99	MEAN = 61	MEAN = 10	MEAN = 35

TABLE 10.- Continued

Site Number and Landsat Coord. (x,y)	Solar Rad. (ly/dy)	Pot Evapotran. (in x 100)	Elevation (ft/100)	Slope (%)	Aspect (°)
	89	73	71	12	45
	100	79	70	10	48
31	98	75	70	9	49
(750,152)	84	27	70	13	55
	96	70	70	9	50
	98	75	70	9	49
	74	22	70	7	55
	89	39	69	11	55
	89	78	69	14	55
	MEAN = 91	MEAN = 55	MEAN = 70	MEAN = 10	MEAN = 51
	108	82	71	0	0
	108	84	71	0	0
32	106	86	71	0	0
(774,128)	108	85	71	0	0
	108	85	71	8	0
	106	83	72	15	0
	108	85	71	0	0
	99	78	71	8	3
	92	70	72	16	9
	MEAN = 105	MEAN = 79	MEAN = 71	MEAN = 5	MEAN = 1
	103	78	71	0	0
	103	78	71	0	0
33	105	78	71	3	0
(735,100)	103	78	71	0	0
	103	77	71	0	0
	103	79	71	0	0
	103	70	71	3	0
	92	79	71	0	0
	100	78	71	0	0
	MEAN = 102	MEAN = 77	MEAN = 71	MEAN = 1	MEAN = 0

TABLE 10.- Concluded

Site Number and Landsat Coord. (x,y)	Solar Rad. (ly/dy)	Pot Evapotran. (in x 100)	Elevation (ft/100)	Slope (%)	Aspect (°)
	124	96	71	1	47
	123	95	71	1	53
34	124	96	71	1	0
(720,95)	124	97	71	4	45
	124	97	71	3	45
	123	95	71	2	53
	122	96	71	7	46
	122	94	71	6	50
	121	92	71	5	64
	MEAN = 123	MEAN = 95	MEAN = 71	MEAN = 3	MEAN = 44
	96	79	69	7	65
	85	70	70	18	65
	87	71	71	14	67
35	90	73	70	0	62
(755,125)	92	75	69	11	66
	95	76	70	15	69
	103	80	69	0	0
	98	77	69	0	67
	94	74	69	0	70
	MEAN = 93	MEAN = 75	MEAN = 76	MEAN = 8	MEAN = 59

CHAPTER 5. STATISTICAL ANALYSIS

Before beginning the actual model building process, it is important to understand the structure of the data set that will be used.

Appropriateness and redundancy in the data need to be evaluated before variables are put together in the form of a model.

At the outset of this study a set of variables, which make up the study area data base, was deemed general environmental indicators and hence useful in conifer growth modeling. In this way all variables in the data set were defined as appropriate. The evaluation of redundancy is not as simple. Subset(s) of the variable data set may be related to such a degree as to be considered synonymous. To insure an efficient and meaningful final model this type of data duplication (or redundancy) should be removed. If the assumption of linearity of the data is accepted, a correlation analysis is most appropriate for this task.

An examination of the correlation structure of the data set can provide insight into relationships between variables and give clues about the behavior of the phenomenon of conifer growth. Relationships and trends derived from the correlation analysis can provide focal points for furthering the analysis. Correlation studies are particularly appealing because they approximate human judgement and are allied to Aristotelian logic.

By sample site, the potential independent variables in the data set include net solar radiation and potential evapotranspiration, both of which were averaged over the conifer growing season (April and May). In addition, elevation, slope, aspect (partioned into two components, sin (aspect) and cos (aspect) to preserve the periodicity of aspect angle) and soil plant available water are included in the set of independent variables.

The dependent or conifer growth response variable is the average age to height ratio measurement for each of three dominant - codominant conifers at each sample site. All site data are shown in Table 11. The Pearson product moment correlation matrix is shown in Table 12.

A careful examination of the matrix shows only one significantly high correlation. The correlation between net solar radiation and potential evapotranspiration, R = .7149, is significant in an

TABLE 11.- Study Area Sample Site Measured Variables

Site Numbers	Net Solar Radiation (ly/dy)	Potential Evapotranspiration (in. H_2O/dy)	Elevation (ft.)	Slope (%)	Aspect (°)	Plant Available Water (in.)	Growth (ft./yr.)
1	460.98	.420	6550	30	360	6.74	.7440
2	456.32	.379	6500	42	130	6.58	.6364
3	428.39	.271	6550	27	350	6.73	.7123
4	437.70	.303	6450	29	150	5.25	.6554
5	493.57	.492	6250	50	130	6.02	.7028
6	474.95	.420	6300	38	108	6.09	.6794
7	451.67	.361	7000	35	330	6.86	.5619
8	479.61	.393	7000	36	78	5.94	.6006
9	479.61	.406	6950	21	130	6.21	.2956
10	460.98	.366	6950	23	147	6.23	.4715
11	437.70	.253	7100	30	128	6.02	.7952
12	428.39	.208	7100	33	130	8.52	.8657
13	460.98	.357	7000	29	200	3.50	.3031
14	460.98	.343	7050	32	213	1.71	.2594
15	419.07	.226	7220	46	330	3.90	.3957
16	470.29	.370	7560	40	320	4.10	.5591
17	498.23	.366	6950	24	170	5.52	.5157
18	484.26	.366	6840	35	183	4.46	.5771
19	451.67	.325	7160	30	190	1.74	.6307
20	507.54	.434	7260	33	179	1.60	.6288
21	479.61	.388	6880	34	20	7.79	.7102
22	493.57	.447	6700	35	180	5.04	.5354
23	470.29	.393	6900	32	140	9.02	.4406
24	-	-	-	-	-	-	-
25	451.67	.447	6300	21	180	7.88	.3100
26	423.73	.248	6800	36	340	4.27	.4639
27	488.92	.357	7400	50	360	2.76	.4611
28	474.95	.348	7500	40	350	5.18	.4245
29	572.73	.429	7100	40	188	3.70	.2723

TABLE 11.- Concluded

Site Numbers	Net Solar Radiation (ly/dy)	Potential Evapotranspiration (in. H_2O/dy)	Elevation (ft.)	Slope (%)	Aspect (°)	Plant Available Water (in.)	Growth (ft./yr.)
30	433.04	.339	7000	25	190	6.60	.3321
31	479.61	.370	7300	30	320	6.55	.4113
32	456.32	.316	7100	48	336	4.48	.2357
33	456.32	.316	7000	35	350	3.49	.3942
34	488.92	.447	6300	13	200	4.89	.2428
35	474.95	.375	7000	40	360	3.58	.4387

TABLE 12.- Potential Independent Variable Correlation Matrix

SOR = net solar radiation
ET = potential evapotranspiration
ELEV = elevation
SLOP = slope
SASP = sine of aspect
CASP = cosine of aspect
PAW = plant available water

	SOR	ET	ELEV	SLOP	SASP	CASP	PAW
SOR	1.000						
ET	0.7149	1.000					
ELEV	0.0742	-0.3673	1.000				
SLOP	0.1157	-0.0869	0.2846	1.000			
SASP	-0.0317	-0.0495	0.1520	0.0915	1.000		
CASP	0.2437	0.0425	-0.0259	-0.1977	-0.0116	1.000	
PAW	-0.2309	0.0415	-0.3857	-0.2598	-0.0166	-0.1593	1.000

unsurprising way. The Jensen-Haise method for calculating potential evapotranspiration utilizes as its primary variable net solar radiation. This would seem to dismiss any possibility that this is only a spurious or nonsense correlation. The remaining variables in the data set seem to be correlated only in a weak sense.

Variability in the data set is nonuniform, in part because of the small sample size (Figures 12 through 17). To stabilize the variance, thereby allowing for a better model building data set, a logarithm transformation of the data was performed (Table 13). The transform also employed a shift of each variable so that any fit curve would pass through the origin. The fit, as evaluated by the magnitude of R^2 would tend to be better than if no shift had been performed. The method is summarized below.

Figure 12.- Plot of Net Solar Radiation vs. Growth

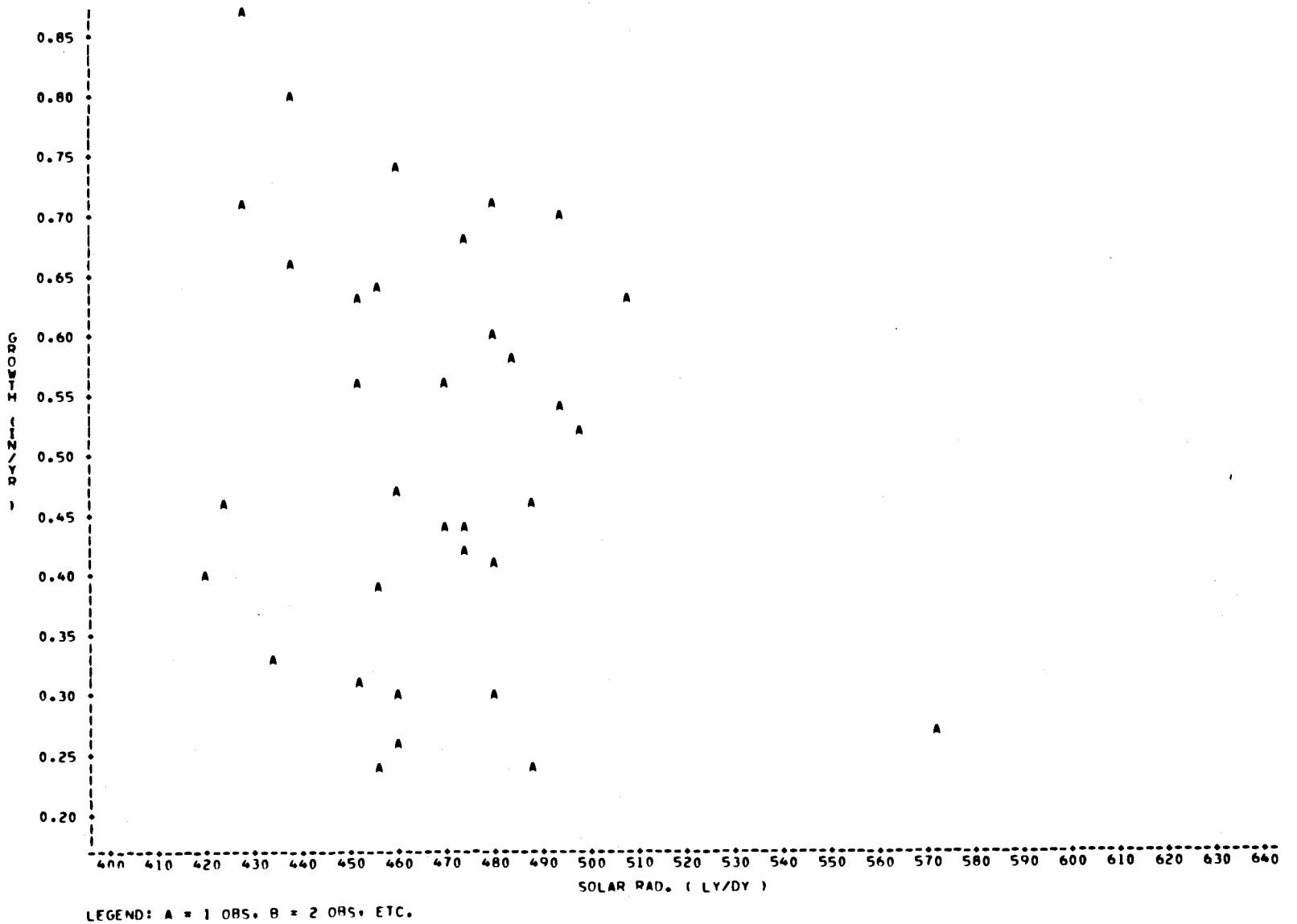

Figure 13.- Plot of Potential Evapotranspiration vs. Growth

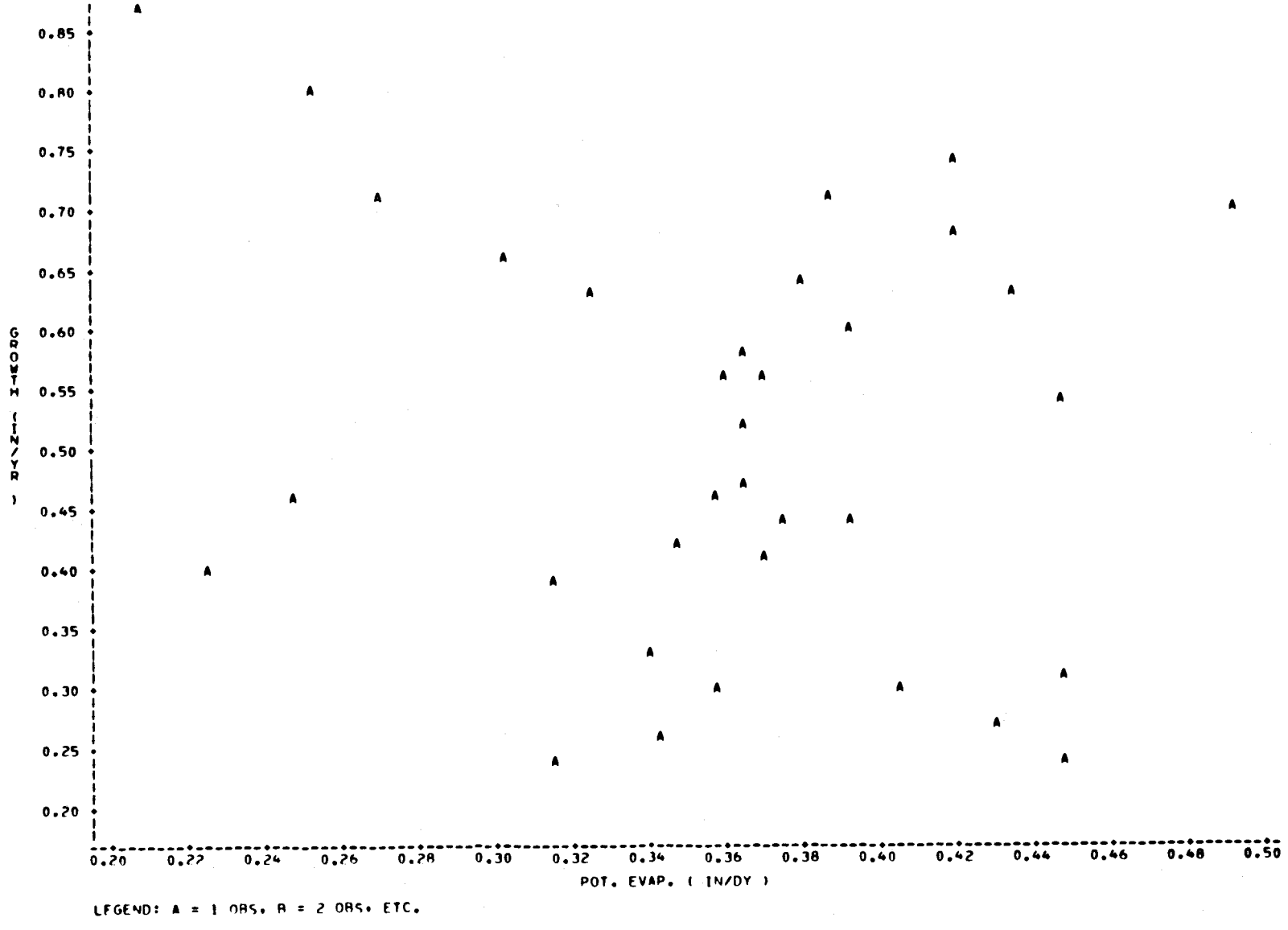

Figure 14.- Plot of Elevation vs. Growth

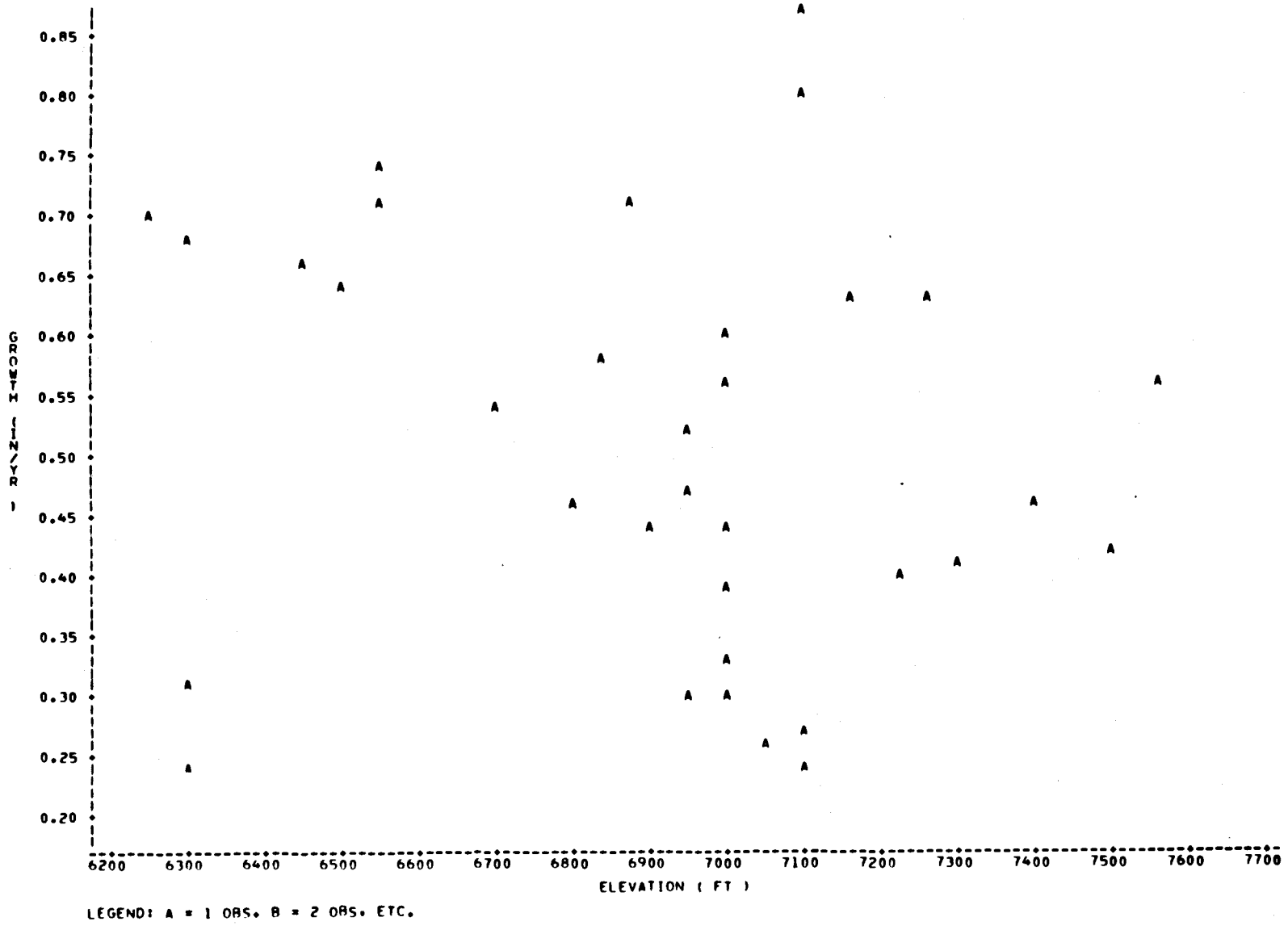

Figure 15.- Plot of Slope vs. Growth

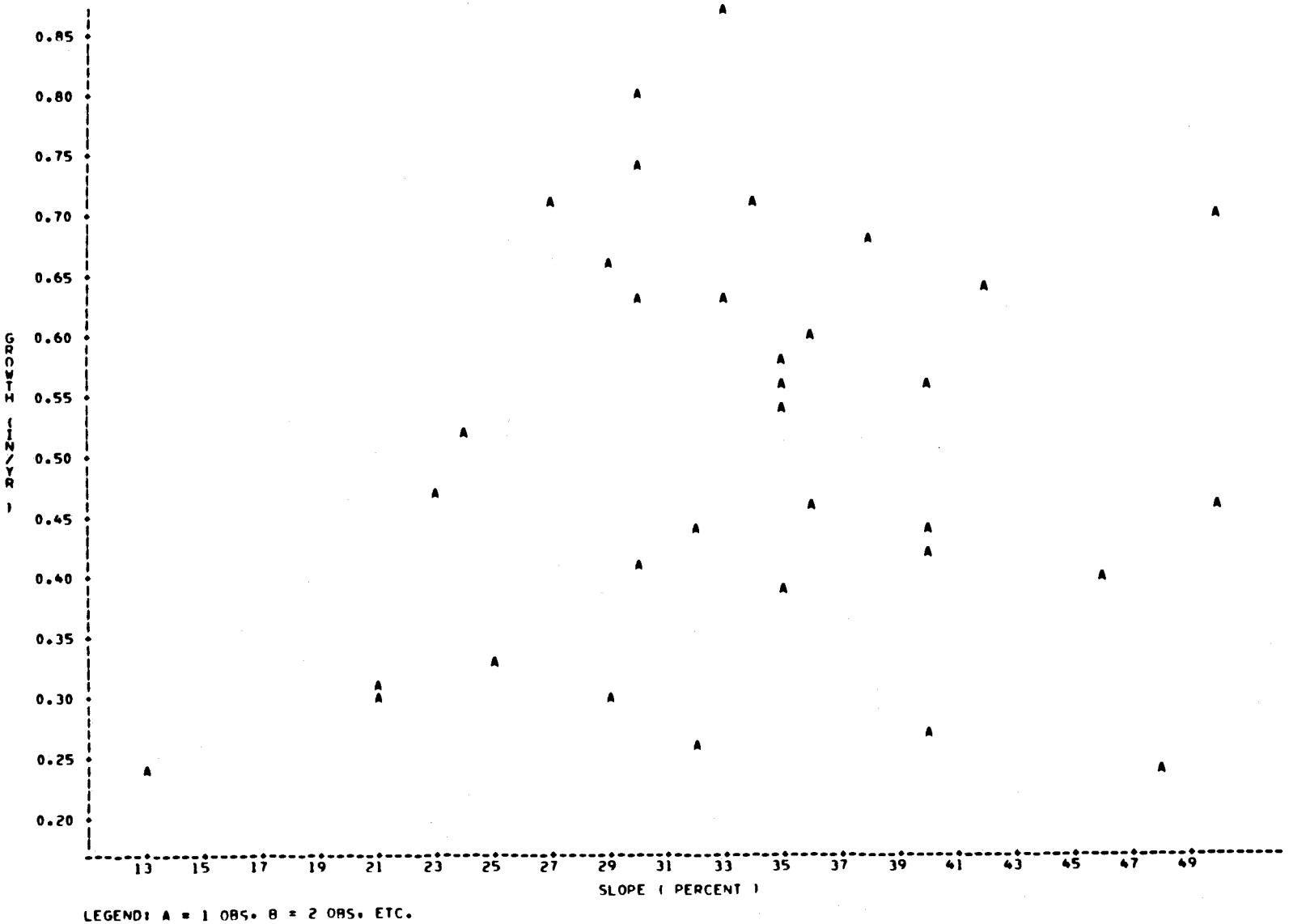

Figure 16.- Plot of Aspect vs. Growth

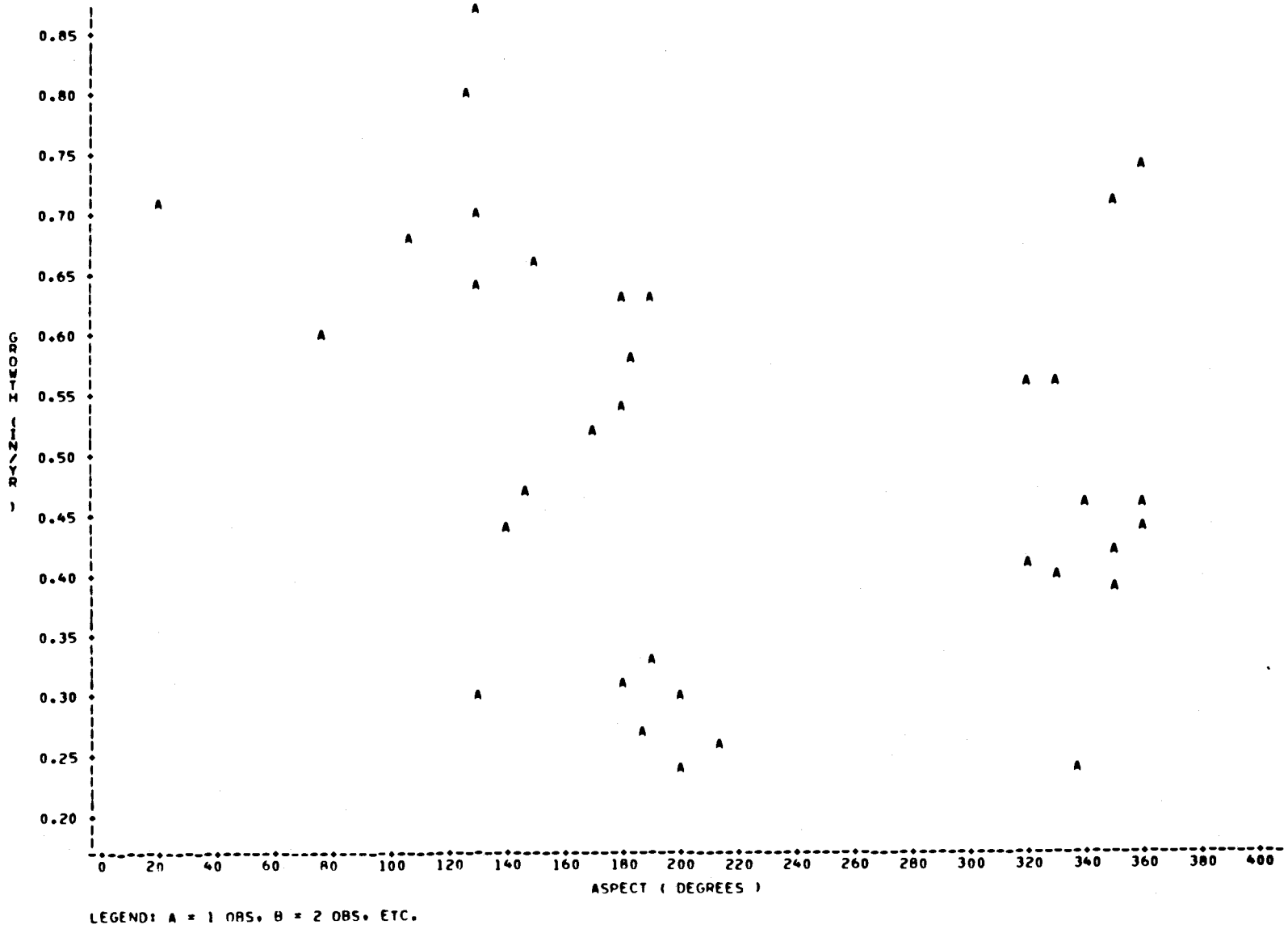

Figure 17.- Plot of Plant Available Water vs. Growth

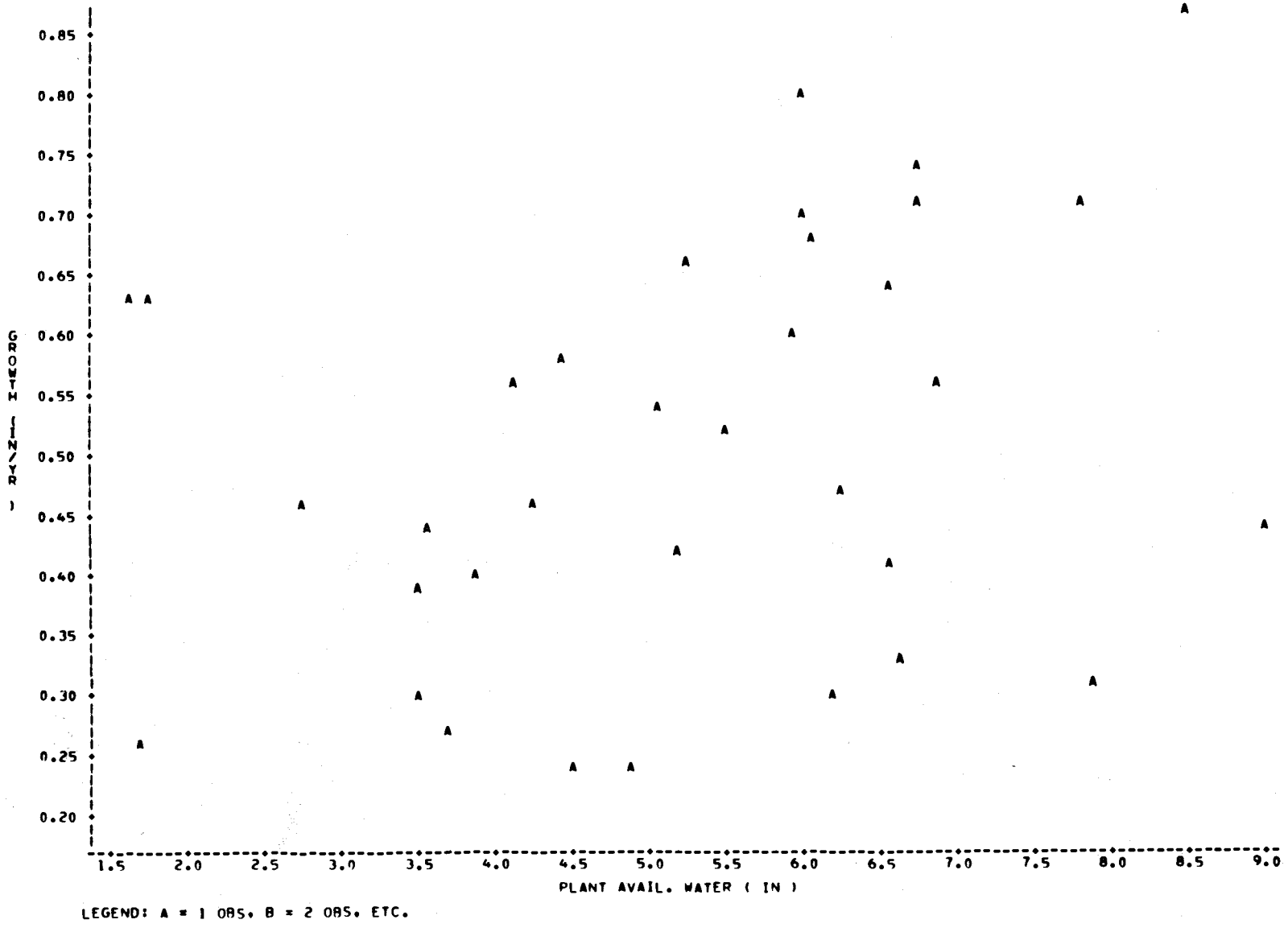

TABLE 13.- Transformed Study Area Sample Site Variables

Number	Potential Evapotranspiration	Elevation	Slope	Sine of Aspect	Cosine of Aspect	Plant Available Water	Growth
1	-2.263	6.310	2.890	-.900	-2.448	.583	-6.77
2	-2.765	6.397	1.792	.159	.442	.490	-.915
3	-3.101	6.310	3.045	-1.458	-2.639	.578	-.741
4	-4.343	6.477	2.944	-.098	.567	-1.197	-.868
5	-1.737	6.745	.693	.159	.442	.070	-.761
6	-2.263	6.685	2.303	.306	.201	.133	-.813
7	-3.101	4.605	2.565	-2.372	-3.046	.648	-1.121
8	-2.564	4.605	2.485	.326	-.349	-.008	-1.008
9	-2.408	5.011	3.296	.159	.442	.233	-2.817
10	-2.996	5.011	3.219	-.049	.561	.248	-1.445
11	-2.765	-9.210	2.890	.178	.425	.070	-.581
12	-2.226	-9.210	2.708	.159	.442	1.273	-.462
13	-3.194	4.605	2.944	-2.737	.617	.370	-2.699
14	-3.612	3.912	2.773	-1.979	.561	1.175	-3.747
15	-2.408	4.787	.693	-2.372	-3.046	.047	-1.833
16	-2.919	6.131	2.079	-1.443	-1.914	-.165	-1.129
17	-2.996	5.011	3.178	-.543	.641	-.559	-1.273
18	-2.996	5.561	2.565	-1.036	.648	-.717	-1.075
19	-4.711	4.094	2.890	-1.458	.641	1.166	-.929
20	-2.137	5.075	2.708	-.859	.649	1.208	-.934
21	-2.631	5.394	2.639	-.289	-3.632	1.045	-.746
22	-2.033	5.991	2.565	-.900	.349	-2.386	-1.205
23	-2.564	5.298	2.773	.049	.519	1.404	-1.568
24	-	-	-	-	-	-	-
25	-2.033	6.685	3.296	-.900	.649	1.076	-2.601
26	-2.688	5.704	2.485	-2.737	-3.632	-.389	-1.478
27	-3.194	5.704	.693	-.900	-2.448	.783	-1.490
28	-3.442	5.991	2.079	-1.458	-2.639	-1.461	-1.668
29	-2.180	-9.210	2.079	-1.318	.644	.222	-3.310

TABLE 13.- Concluded

Number	Potential Evapotranspiration	Elevation	Slope	Sine of Aspect	Cosine of Aspect	Plant Available Water	Growth
30	-3.772	4.605	3.135	-1.458	.641	.502	-2.340
31	-2.919	5.298	2.890	-1.443	-1.914	.471	-1.740
32	-18.421	-9.210	-13.816	-8.242	-7.696	-.759	-9.210
33	-18.421	4.605	2.565	-1.099	-2.639	.377	-1.843
34	-2.033	6.685	3.555	-2.737	.617	-2.847	-4.962
35	-2.830	4.605	2.079	-.900	-2.448	.313	-1.595

Data Transformation

Assumptions:

1. The desired function is of the form:

$$Y = f(x_1, x_2, \cdots, x_n) = a|x_1-b_1|^{c_1}|x_2-b_2|^{c_2}\cdots|x_n-b_n|^{c_n} + y_o$$

where a and c_i's are unknown

Note: f is symmetric about y_o

2. y_o = minimum of the sample data

3. b_i's are the values of the i^{th} variable in the sample data when $y=y_o$, that is, $x_i=b_i$ when $y=y_o$

method:

Take $f_1(x_1,x_2,\cdots,x_n) = f(x_1,x_2,\cdots,) - y_o$,

thus $f_1(x_1,x_2,\cdots,x_n) = a|x_1-b_1|^{c_1}|x_2-b_2|^{c_2}\cdots|x_n-b_n|^{c_n}$

Take g

$= l_n(f_1) = l_n(a) + c_1 l_n|x_1-b_1| + c_2 l_n|x_2-b_2| + \cdots + c_n l_n|x_n-b_n|$.

Then let $z_i = l_n|x_i-b_i|$ $c_o = l_n(a)$, $g = c_o + c_1z_1 + \cdots + c_n^2z_n$

and do a least squares regression for g with the z_i's as independent variables.

Advantage:

The method allows the data to be fitted to a polynomial even though there is no preconception of the polynominal form.

Disadvantages:

The fitted polynomial tends to lie below the data points. This is due to the fact that logarithms tend to give large (in absolute value) values to numbers between 0 and 1 and relatively smaller value to numbers greater than 1.

Shift Versus No Shift

A least squares regression with these transformed data creates a curve that necessarily goes through the origin. If the data are not shifted to bring the minimum to the origin, the fit cannot be expected to very good (in the sense of a large R^2) (Taylor, 1979).

When a correlation analysis is performed on the transformed data, the variables seem to behave in a more "realistic" manner. Most relationships between variables are similar to those found in the raw data correlation matrix, some are increased and a few change sign (Table 14).

Potential evapotranspiration and net solar radiation are now related to the other variables in an identical way. R values between potential evapotranspiration and the other variables tend to be higher (stronger tracking) than those associated with net solar radiation. This is a rudimentary argument for retaining the potential evapotranspiration variable over the net solar radiation variable, since each is highly correlated with the other. The only other significant correlation is between plant available water and slope. Since plant available water is inherently more related to conifer growth than slope, unless slope is limiting (which is a rareity in the study area), it is more likely to be retained for model building. Figures 18 through 23 show plots of the transformed variables.

To understand the data set structure to a greater degree, and to explore possibilities in the reduction of the number of variables used, a principal components analysis (PCA) was performed.

PCA is probably the best known ordination procedure, although not necessarily the most appropriate for all types of analyses. PCA operates on a p-dimensional (7 in this case) raw data matrix that consists of p variables each measured at a number of sample sites (35 in this case). The matrix may be either transformed or left in raw form depending on the nature of the data and the objective of the analysis. The initial step in most PCA algorithms is a movement of the origin of the p-dimensional coordinate system that describes the set (or cloud) of observations to its centroid. Subsequently, each one of the p principal component axes is calculated. Each axis is a best fit line accounting for a maximum amount of variance in each dimension, all of which are mutually orthogonal. Because of the independence or orthogonality between axes,

TABLE 14.- Transformed Potential Independent Variable Correlation Matrix

SOR	ET	ELEV	SLOP	SASP	CASP	PAW	
SOR	1.0000						
ET	0.7884	1.0000					
ELEV	0.1578	0.2919	1.0000				
SLOP	0.5421	0.6568	0.4487	1.0000			
SASP	-0.0369	-0.0277	0.0887	0.0042	1.0000		
CASP	-0.2279	-0.1367	-0.0210	-0.1653	0.6581	1.0000	
PAW	0.4851	0.6538	0.4048	0.9219	0.0163	-0.0279	1.0000

Figure 18.- Plot of Transformed Potential Evapotranspiration vs. Transformed Growth

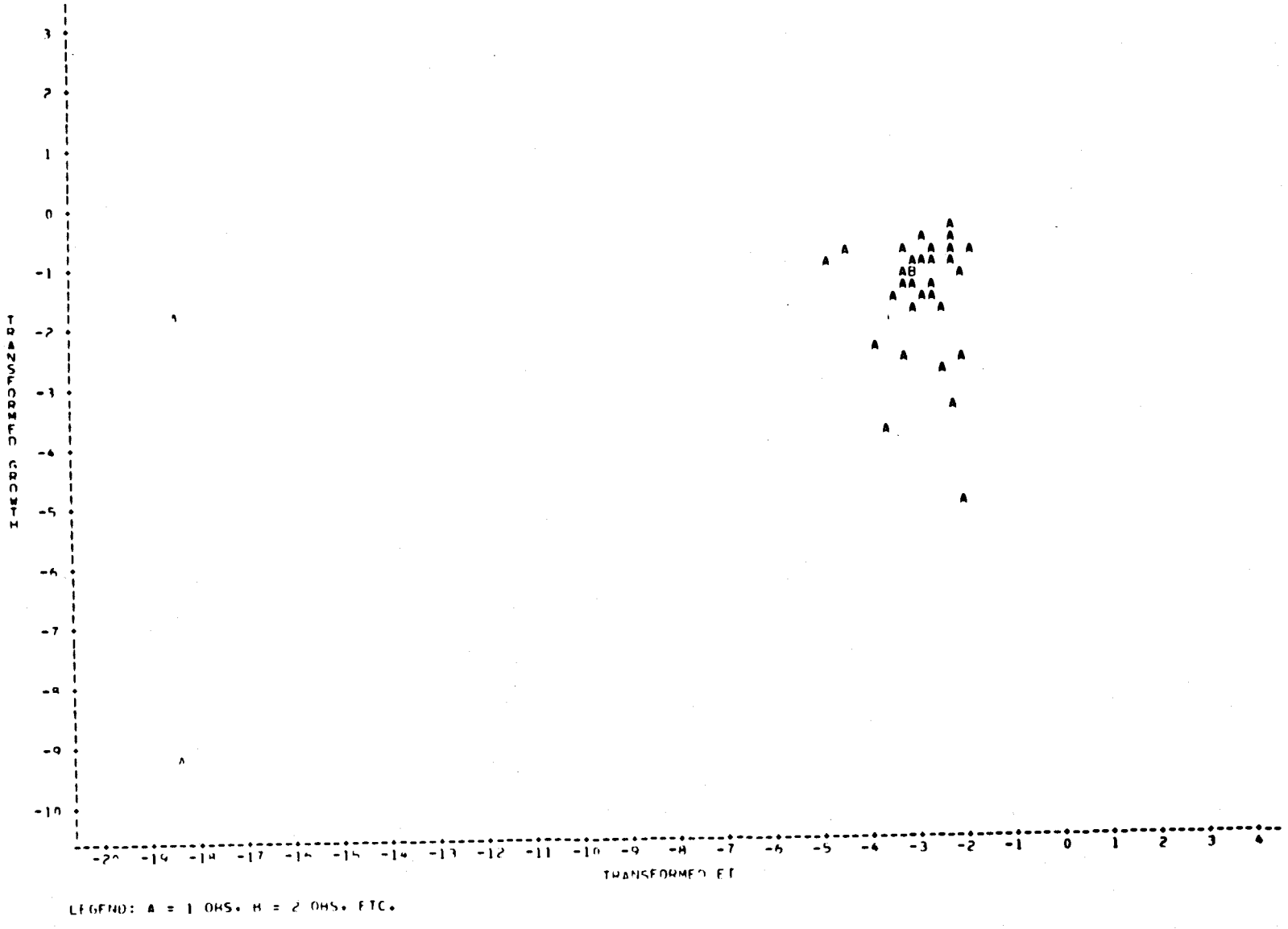

Figure 19.- Plot of Transformed Elevation vs. Transformed Growth

Figure 20.- Plot of Transformed Slope vs. Transformed Growth

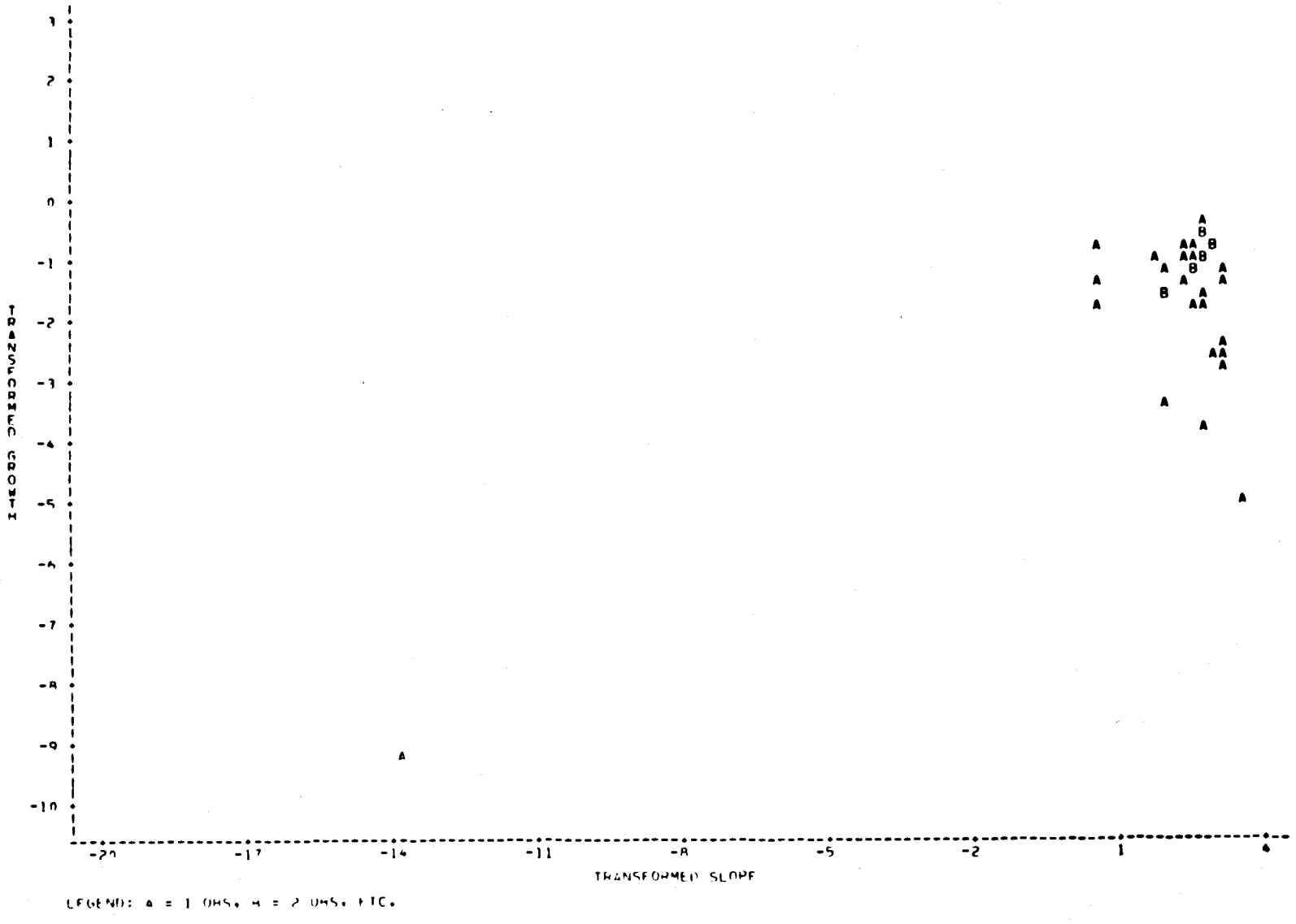

Figure 21.- Plot of Transformed Sine of Aspect vs. Transformed Growth

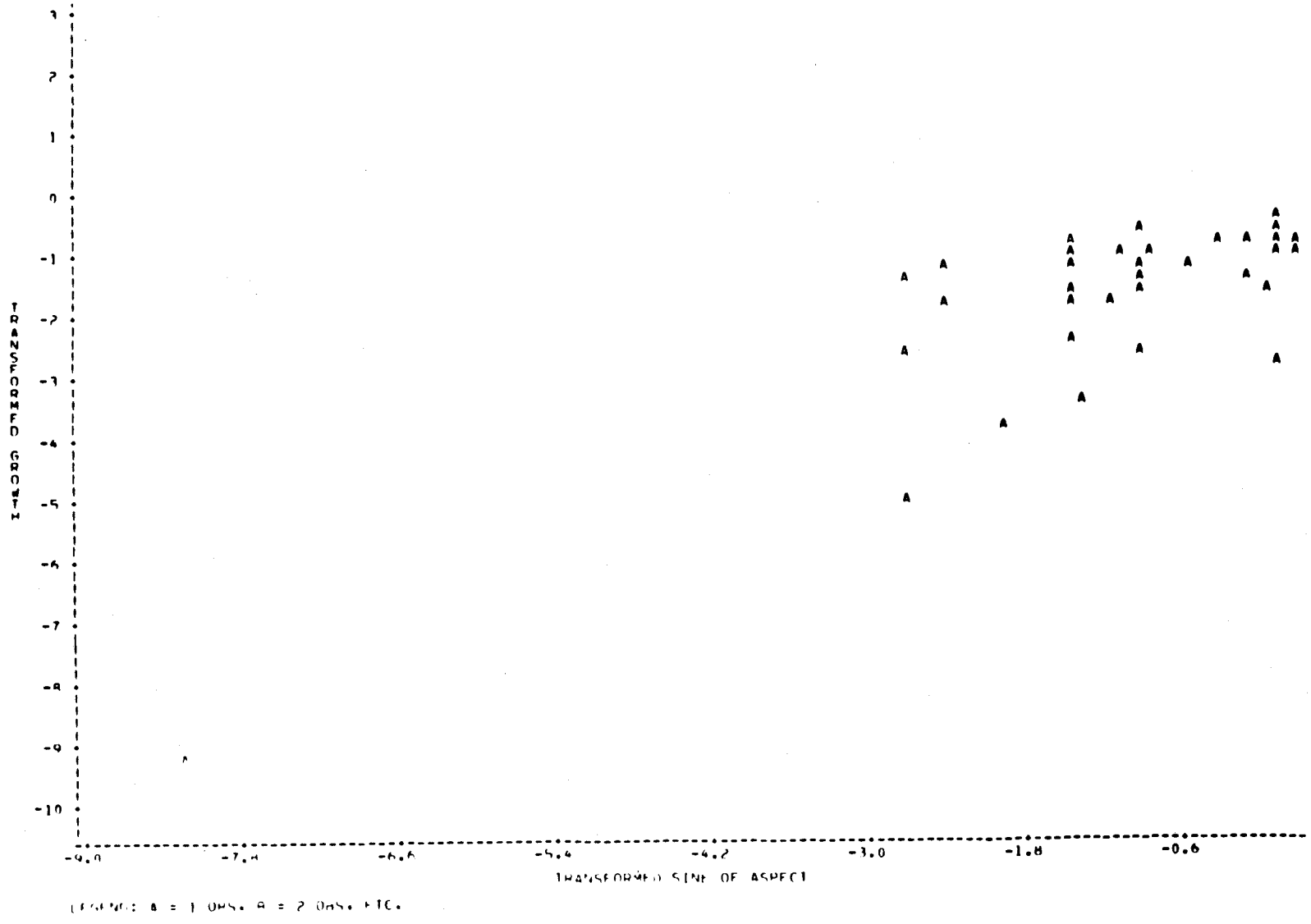

LEGEND: A = 1 OBS, B = 2 OBS, ETC.

Figure 22.- Plot of Transformed Cosine of Aspect vs. Transformed Growth

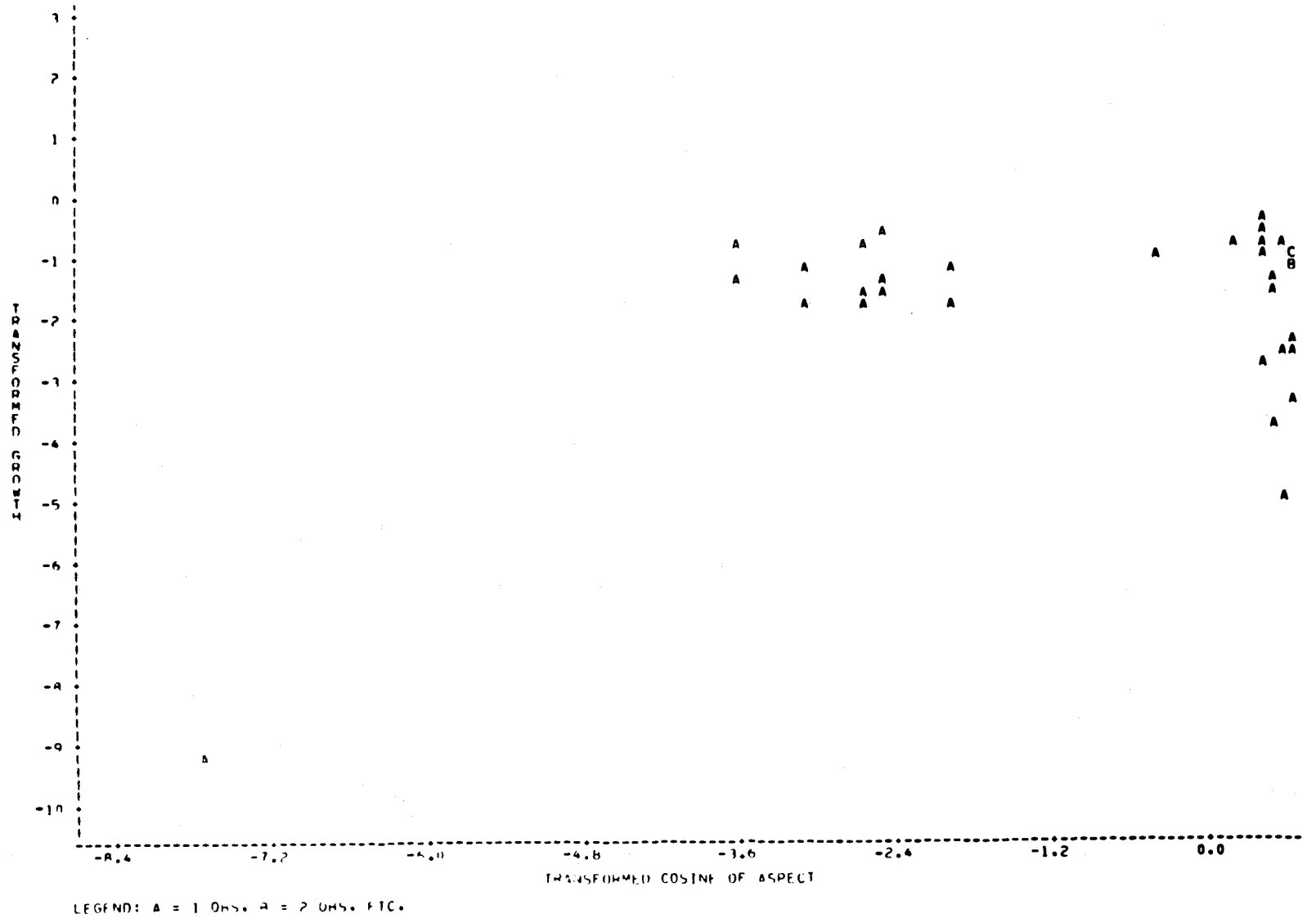

Figure 23.- Plot of Transformed Plant Available Water vs. Transformed Growth

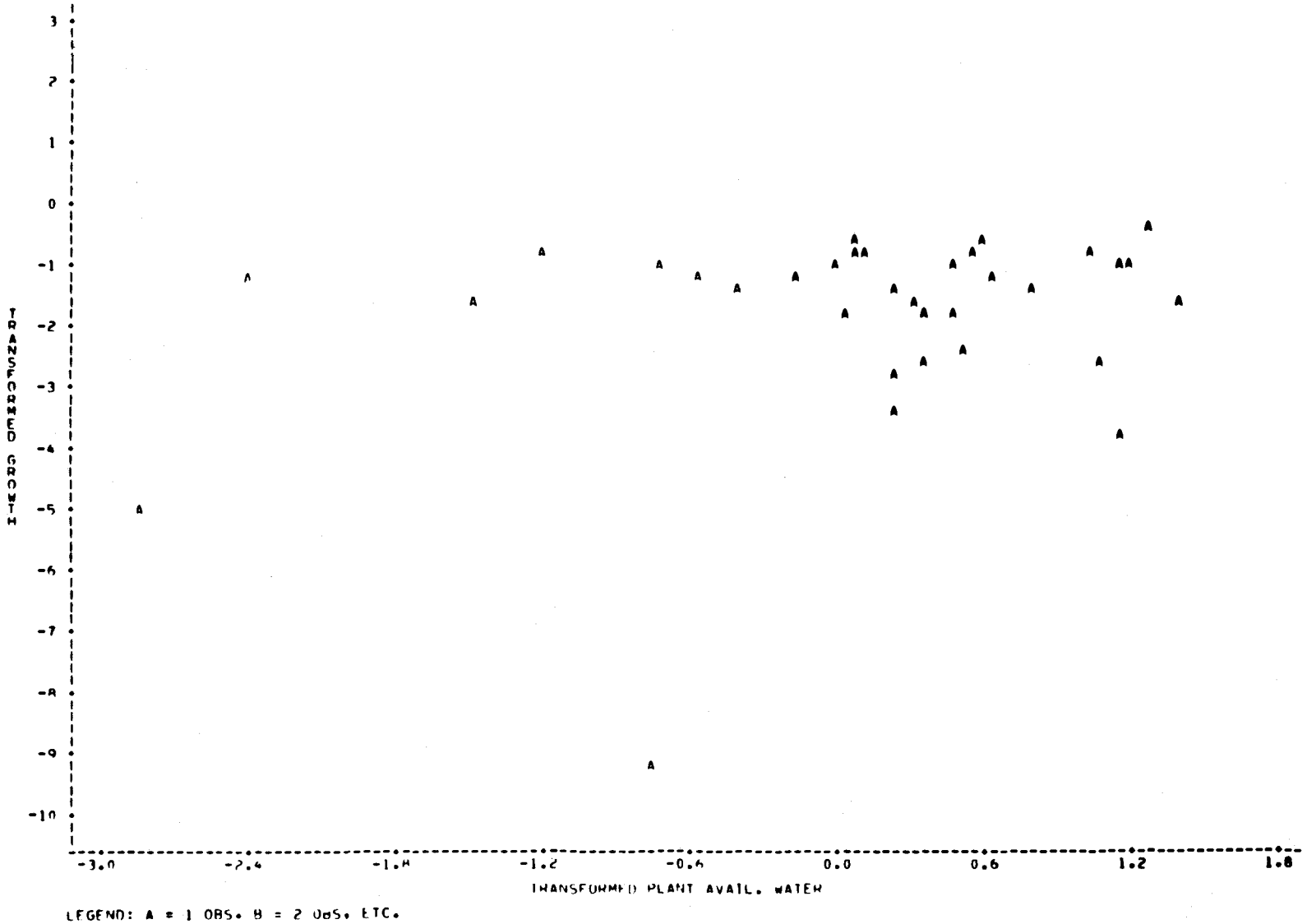

there is no covariance between components, only a variance for each dimension, which in fact describes the length of the respective principal components axes.

A PCA was performed on both the raw data and the shifted-log transformed data. An examination of each eignevalue listing shown in Table 15 shows that the relative importance of each variable in explaining variance in the total data set is not different between the raw and transformed data. A greater amount of variance is accounted for by the first three components (potential evapotranspiration, net solar radiation and elevation) in the transformed set than in the raw set. This is because of the tighter correlation structure of the transformed data set.

From the PCA's and correlation analyses candidate variables for retention in the data set were identified, in the case that a reduction in the number of variables was needed. An understanding of the data set structure was also derived from the analyses by determining the proportion of variability in the growth variable accounted for by each variable. The graphical displays of the raw and transformed data provided a way in which the correlation structure and sampling characteristics of the data could be illustrated.

The next step in the data analysis involved performing a series of multiple regressions using as the dependent variable the conifer growth at each sample site and all possible combinations (63) of the transformed independent variables. As would be expected the equation that used all independent variables represented a relationship which accounted for the greatest amount of variance in the transformed dependent variable.

For extension of the model over the entire study area, limitations in the sampling scheme and redundance in the data set must be confronted. First, since all of the sample sites were located in an elevation range of 1905m (6250 ft.) to 2304m (7560 ft.) and the study area ranges from approximately 1524m (5000 ft.) to 2590m (8500 ft.), it would not be appropriate to retain the elevation variable. Second, the variables of net solar radiation and potential evaportranspiration are highly correlated and represent redundancy in the data set. Based on the information used to calculate each variable in relation to conifer growth it was decided to retain potential evapotranspiration over net solar radiation. Finally, the slope variable is highly correlated with plant available

TABLE 15.- PCA Results for Raw and Shifted-Log Data

Raw Data

Variable	Eigenvalue	Percent of Variance	Cumulative Percent
SOR	1.8559	26.5	26.5
ET	1.7324	24.7	51.3
ELEV	1.1228	16.0	67.3
SLOP	0.9760	13.9	81.2
SASP	0.6227	8.9	90.1
CASP	0.5548	7.9	98.1
PAW	0.1354	1.9	100.0

Shifted-Log Data

SOR	3.2612	46.6	46.6
ET	1.6730	23.9	70.5
ELEV	0.9146	13.1	83.6
SLOP	0.5774	8.2	91.8
SASP	0.3423	4.9	96.7
CASP	0.1738	2.5	99.2
PAW	0.0578	0.8	100.0

water (R=.922) and like elevation is not well represented in the sampling scheme. The range of slopes sampled was approximtely 13 to 50 percent, while the actual range found in the study area was 0 to well over 100 percent. As a result, the slope variable was dropped from the data set, but its analog, plant available water, was retained.

The final set of independent variables included potential evapotranspiration, aspect (both sine and cosine) and plant available water.

A multiple regression procedure was performed on the adjusted data set giving the results shown in Table 16.

To predict actual growth rate, the transformation (shifted-log) must be "undone", giving the conifer growth rate equation the form shown in Table 17. Model and site measured transformed growth rates are also shown in Table 17.

Before this model can be utilized in any type of land capability estimation it must be first evaluated on a data set that is independent of the set from which it was developed. This is the subject of Chapter 6.

TABLE 16.- Model Variables and Their Coefficients

Variable*	Coefficient	Standard Error of Coefficient
ET	0.105	0.075
SASP	0.420	0.267
CASP	-0.254	0.189
PAW	0.828	0.094
Constant	-1.205	0.366

$$Growth^* = -1.205 + (0.105)ET^* + (0.42)SASP - (0.254)CASP + (0.828)PAW$$

Variable	F-Value to Enter or Remove	Significance	R^2	Change R^2
ET	1.948	0.173	0.464	0.460
PAW	77.213	0.000	0.840	0.376
CASP	1.813	0.819	0.849	0.009
SASP	2.477	0.126	0.858	0.009

*Transformed variables

TABLE 17.- Model and Site Measured Transformed Growth Rates

Site Number	Model Transformed Growth Rate	Ground Measured Transformed Growth Rate
1	-0.7157	-0.677
2	-1.1351	-0 915
3	-0.9936	-0.741
4	-2.8396	-0.868
5	-1.3751	-0.761
6	-1.2550	-0.813
7	-1.2163	-1.121
8	-1.2551	-1.008
9	-1.3105	-2.817
10	-1.4774	-1.445
11	-1.4706	-0.581
12	-0.4302	-0.462
13	-2.5410	-2.699
14	-1.5854	-3.747
15	-1.6413	-1.833
16	-1.7678	-1.129
17	-2.3736	-1.273
18	-2.7134	-1.075
19	-1.5095	-0.929
20	-0.9551	-0.934
21	0.1861	-0.746
22	-3.9376	-1.205
23	-0.4230	-1.586
24	-	-
25	-1.0707	-2.601
26	-2.0361	-1.478
27	-0.6477	-1.490
28	-2.7179	-1.668
29	-1.9677	-3.310
30	-1.9609	-2.340
31	-1.2412	-1.740
32	-5.2723	-9.210
33	-2.6155	-1.843
34	-5.0832	-4.962
35	-0.9987	-1.595

Growth Rate (ft./yr) =

$$\exp[-1.2053693 + 0.10484853\,(\text{Pot. Evapo.} - 0.31599999) + 0.42025284\,(\sin(\text{ASPECT}) + 0.40673665) - 0.2542485\,(\cos(\text{ASPECT}) - 0.91354) + 0.82808963\,(\text{Plant Avail. Water} - 4.4799999)] + 0.23579999$$

CHAPTER 6. MODEL VERIFICATION

An independent data set from which the conifer growth rate model could be evaluated was assembled from an intensive sampling effort during the Summer of 1979.

Sample site location was deliberate, but did not involve a statistically rigorous design. Each site location was determined in the field with the aid of aerial photography and a concerted effort placed on including a wide range of topographic conditions (i.e. elevation, slope and aspect) in the sites visited. To facilitate speed of the sampling procedure and ease of location of the sites, sampling followed the dense road network through the study area. Care was taken to allocate the sample sites in proportion to the areas of the two soil parent materials (granitic and volcanic) that make up the study area. Of the 42 sites visited, 24 were located on volcanic soils and the remaining 18 on the granitics. Figure 24 shows the sample site locations. The sample site locations were transferred to a 15 minute USGS topographic map base, and from transformation equations developed earlier in the study, study area data base coordinates were derived for each location. This was necessary so that the conifer growth rate model could be run for each site as part of the verification procedure.

Data collected at each sample site were less voluminous than during the initial (Summer of 1978) sampling effort. Only those measurements crucial to a comparison of model and actual conditions were made due to manpower and time constraints. The ages and heights of 3 dominant - codominant conifers were measured at each site along with each tree's diameter at breast height (dbh) and measures of topographic slope and aspect. From these data a representative conifer growth rate value was calculated for each site. This was done in the same way as with the initial sample sites where the mean tree age was divided by the mean tree height (See Appendix 2 for an example).

The conifer growth rate model was run for each sample site and compared to the measured values. The comparison was a correlation anlaysis that would serve to indicate how well model derived and actual conifer growth rates tracked each other. Rather than testing for similarity in magnitudes of the two numbers, similarity in relative trend

Figure 24.- Study Area Sample Site Location

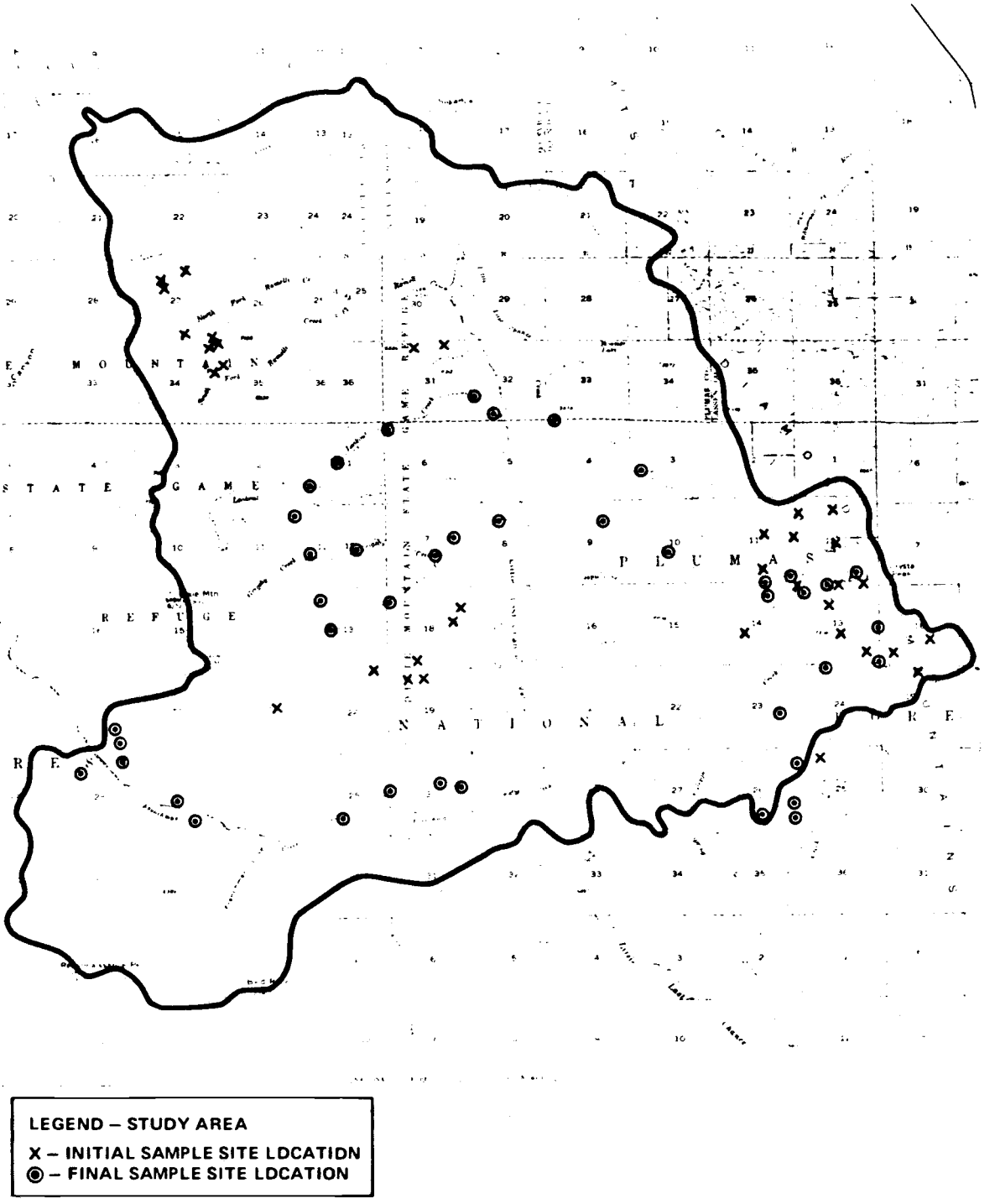

via the correlation procedure was investigated. This was deemed appropriate because of the eventual use of the model. The conifer growth rate model would be used to aid in judging land capability for conifer regeneration. If one area was shown to have a higher conifer growth rate in the past than another, this was considered evidence that it would be superior for conifer growth in the future. The precise magnitude of superority would not be taken from this model with a great deal of confidence. This is in part due to the initial and final sampling schemes, as well as to the way in which conifer growth was quantified. The correlation analysis showed that there is some instability associated with the ability of the model to provide consistent results (in terms of tracking) for the sites located on the volcanic soils. Results for sites on the granitics were encouraging (Table 18). This is evidence that the variables included in the model accounted for a good portion (30 percent) of the variability in conifer growth for those trees situated on granitic soils. Table 19 shows a series of significance tests for the three derived r-values. The low overall r, and also the r associated with sites on the volcanic soils, could be due to a number of factors including:

(1) An inadequate number of sample sites used in the development of the conifer growth rate model;

(2) the spatial distribution of the initial and final sample sites over the study area not including all variability of conditions (e.g. terrain and soil type) in the sample;

(3) additional, unaccounted for environmental factors affecting conifer growth on volcanic soils;

(4) the possibility that all variables included in the growth rate model were not limiting (or only marginally so) to conifer growth on volcanic soils;

(5) or error associated with the location of sample sites within the study area data base.

TABLE 18.- Conifer Growth Rate by Site

Site Number*	Actual Rate (ft./yr.)	Model Estimated Rate (ft./yr.)
1	0.77	4.20
2	0.74	3.21
3	0.89	3.77
4	1.07	1.26
5	1.00	3.47
6	OUT OF STUDY AREA	
7	0.54	0.29
8	0.60	0.61
9	0.86	3.83
10	0.90	4.10
11	0.87	5.18
12	0.80	3.96
13	1.03	4.27
14	0.78	0.29
15	0.61	2.12
16	0.82	0.28
17	0.55	2.54
18	0.66	0.29
19	0.49	1.73
20	0.72	1.26
21	1.08	0.29
22	1.03	3.87
23	0.61	0.65
24	0.90	3.18
25	0.53	0.29
26	0.68	0.26
27	0.53	0.29
28	0.71	0.29
29	0.63	0.63
30	0.30	0.37
31	0.45	0.35
32	0.46	0.39
33	0.24	0.42
34	0.46	0.36
35	0.47	0.37
36	0.54	0.47
37	0.35	0.45
38	0.73	0.42
39	0.46	0.30
40	1.25	1.52
41	0.83	0.87
42	0.54	0.29

*Sites 1-24 were located on volcanic parent material
Sites 25-42 were located on granite parent material

R-value (overall) = 0.54
R-value (volcanic parent material) = 0.38
R-value (granite parent material) = 0.77

TABLE 19.- Interval Estimates for Calculated R-Values

R-value (overall) = 0.54

$z' = 0.604$, from: $z' = 1/2\ [\log_e(1+r) - \log_e(1-r)]$

$$\sigma(z') = \frac{1}{n-3} = \frac{1}{41-3} = 0.162$$

$z(0.01) = 2.576$

$z(0.05) = 1.960$

$$z' - z(1-\alpha/2)\,\sigma(z') \leq z \leq z' + z\,(1-\alpha/2)\sigma(z')$$

$$0.604 - (2.576)(0.162) \leq z \leq 0.604 + (2.576)(0.162)$$

$$0.187 \leq z \leq 1.021$$

therefore, the 99 percent confidence interval estimate for ρ is:

$$0.185 \leq \rho \leq 0.770, \text{ from } r = \frac{(e^{2z}-1)}{(e^{2z}+1)}$$

and the 95 percent confidence interval estimate for ρ is:

$$0.604 - (0.96)(0.162) \leq z \leq 0.604 + (1.96)(0.162)$$

$$0.286 \leq z \leq 0.922$$

therefore, $0.278 \leq \rho \leq 0.727$

R-value (volcanic parent material) = 0.38

$z' = 0.400$

$\sigma(z)' = 0.224$

The 99 percent confidence interval estimate for ρ is:

$$0.400 - (2.576)(0.224) \leq z \leq 0.400 + (2.576)(0.224)$$

$$-0.177 \leq z \leq 0.977$$

$$-0.175 \leq \rho \leq 0.752$$

TABLE 19.- Concluded

The 95 percent confidence interval estimate for ρ is:

$$0.400 - (1.96)(0.224) \leq z \leq 0.400 + (1.96)(0.224)$$

$$-0.039 \leq z \leq 0.839$$

$$-0.039 \leq \rho \leq 0.685$$

R - value (granite parent material) = 0.77

$z' = 1.02$

$\sigma(z') = 0.224$

The 99 percent confidence interval estimte for ρ is:

$$1.02 - (2.576)(0.224) \leq z \leq 1.02 + (2.576)(0.224)$$

$$0.443 \leq z \leq 1.597$$

$$0.416 \leq \rho \leq 0.921$$

The 95 percent confidence interval estimate for ρ is:

$$1.02 - (1.96)(0.224) \leq z \leq 1.02 + (1.96)(0.224)$$

$$0.581 \leq z \leq 1.459$$

$$0.523 \leq \rho \leq 0.897$$

CHAPTER 7. CONCLUSIONS

The model for predicting conifer growth rate based on potential evapotranspiration, plant available water and topographic aspect developed in this study will be useful in the assessment of areas within the study area for conifer regeneration potential. Some improvements can be made to the model and its inputs that would improve subsequent studies and their results. A more complete record of earth surface temperature through the conifer growing season would have given a better indication of moisture stress. This could have been accomplished with ground based temperature measurements to calibrate and fill the gaps in the satellite derived data record. Higher quality digital terrain data currently available would have added precision to the model and improved the net solar radiation model output. In lieu of these improvements the model can be a useful tool in indicating land potential for conifer growth as long as all of the limitations are considered when interpreting predictions.

Future work following an approach similar to the one in this study above all should begin with a well designed sampling scheme. Such an approach would greatly enhance the validity and acceptability of the study's results as well as maximize efficiency in terms of time and cost for any type of field sampling effort.

In this study a large proportion of the initial field sampling effort was oriented toward soil sampling and mapping because of the lack of an acceptable inventory and mapping of existing soils. The selection of a study area with well mapped soils could significantly reduce costly soil sampling in the field. The sampling procedure could have been much abbreviated without the concern for soils. This would have allowed for a much more thorough evaluation of conifer growth over the study area and a greater number of sample sites over a larger area could have been visited. In this way the final model would have been considerably more accurate or stable.

The sensitivity and accuracy of the models used to predict potential evapotranspiration need to be evaluated to assess the contribution of each of the inputs and determine precisely how well they combine to predict potential conditions in the study area.

An alternative thermal data source should be considered. The availability of NOAA-5 digital radiometer data was at best unreliable. Due to the 90 day rotating archive NOAA maintains, research involving the use of these data for periods greater than 3 months past must be planned early or the data will not be in existence. Essential parameters such as instrument number, satellite attitude, etc. needed for data calibration are extremely hard to acquire. Subsequent NOAA series satellite programs seem to be working toward retaining and providing these data with more ease. Alternatives to NOAA-5 and the NOAA series may include data from the GOES satellites, HCMM or future Landsats that will collect thermal data.

Despite the above mentioned limitations, the conceptual framework of this study was perceived to be important and useful by personnel of the USFS as an input into their program of land capability evaluation and mapping. Forest Service personnel of the Plumas National Forest have indicated that they regard this study as being not only highly innovative but also particularly useful in relation to their need for selecting those areas having the greatest potential for timber production.

BIBLIOGRAPHY

Beck, Donald E. "Height-Growth Patterns and Site Index of White Pine in the Southern Appalachians", Forest Science, 17: June 1971.

Bender, Edward A. An Introduction to Mathematical Modeling. New York: John Wiley and sons, 1978.

Black, T. A. and McNaughton, K. G. "Average Bowen Ratio Methods of Calculating Evapotranspiration Applied to a Douglas Fir Forest", Boundary-Layer Meteorology 2: 1954.

California, Department of Water Resources, Division of Water Resources Report on Water Supply and Use of Water on Middle Fork of Feather River and Tributaries, Plumas and Sierra Counties, California, August 1937.

California, Department of Water Resources, Northeastern Sierra Groundwater Investigation, February 1963.

California, Department of Water Resources, Lake Davis Water Investigation, September 1971.

California, Department of Water Resources, Climate of the Sierra Valley Area, 30 October 1973.

California, Department of Water Resources, Land Resources of the Sierra Valley Area, 30 October 1973.

California, Department of Water Resources, Socio-Economic Resources of the Sierra Valley Area, 30 October 1978.

California, Department of Water Resources, Solar Radiation Measurements in California, 1974.

Christiansen, J. E. Estimating Pan Evaporation and Evaportranspiration from Climatic Data, Irrigation and Drainage Specialty Conference, American Society of Civil Engineers, Las Vegas, Nevada, 1966.

Curtis, Robert O., DeMars, Donald J. and Herman, Francis, R. "Which Dependent Variable in Site Index-Height-Age Regressions?", Forest Science, 20: March 1974.

Dym, Olive L. and Ivey, Elizabeth S. Principles of Mathematical Modeling. New York: Academic Press, 1980.

Ek, Alan R. and Monserud, Robert A. "Performance and Comparison of Stand Growth Models Based on Individual Tree and Diameter-Class Growth", Canadian Journal of Forest Research, 9: June 1979.

Faye, D. C. F. and MacDonald, G. B. "Growth and Development of Sugar Maple as Revealed by Stem Analysis", Canadian Journal of Forest Research, 7: September 1977.

Frank, C. E. and Lee, R. Potential Solar Beam Irradiation on Slopes, Rocky Mountain Forest and Range Experiment Station, 1966.

Geiger, Rudolf. The Climate Near the Ground. Cambridge: Harvard University Press, 1955.

Hatch, Charles R., Gerrard, Douglas J. and Tappener, John C. III. "Exposed Crown Surface Area: A Mathematical Index of Individual Tree Growth Potential", Canadian Journal of Forest Research, 5: June 1975.

Jensen, M. E. and Haise, R. E. "Estimating Evapotranspiration from Solar Radiation", Journal of the Irrigation and Drainage Division, American Society of Civil Engineers; 89: 1963.

Kemeny, John G., Snell, J. Laurie and Thompson, Gerald L. Introduction to Finite Mathematics. Englewood Cliffs: Prentice-Hall, 1957.

Khorram, Siamak and Smith, H. Gregory. "Topographic Analysis of a Wildland Area Based on Digital Terrain Data", Proceedings of the American Society of Photogrammetry-American Congress on Surveying and Mapping, 1979.

Linacre, E. T. "Climate and the Evaporation from Crops", Journal of the American Society of Civil Engineers, IR4: 1967.

Linacre, E. T. "Estimation of Net-Radiation Flux", Agricultural Meteorology, 5: 1968.

Maki, Daniel P. and Thompson, Maynard. Mathematical Models and Applications. Englewood Cliffs: Prentice-Hall, 1973.

Penman, H. L. "Natural Evaporation from Open Water, Bare Soil and Grass", Proceedings of the Royal Society, 193: 1948

Pimmentel, Richard A. Morphometrics - The Multivariate Analysis of Biological Data. Dubuque: Kendall/Hunt, 1979.

Pruitt, W. O. "Cyclic Relations Between Evapotranspiration and Radiation", Transactions of the American Society of Agricultural Engineers, 7: 1964.

Tanner, C. G. and Pelton, W. L. "Potential Evapotranspiration Estimates by the Approximate Energy Balance Method of Penman", Journal of Geophysical Research, 65: 1960.

Taylor, Derrick L. University of California, Berkeley, California. Interview. 15 July 1979.

Turc, L. "Estimating Irrigation Water Requirements and Potential Evapotranspiration", Annuals of Agronomy, 12: 1961.

U.S. Department of Agriculture. Soil Survey of Sierra Valley Area, California, Parts of Sierra, Plumes and Lassen Counties, October, 1975.

U.S. Department of Commerce. Bureau of the Census. United States Census of Population: 1950. Vol. 1, Characteristics of the Population, California.

U.S. Department of Commerce: Bureau of the Census. United States Census of Population: 1960. Vol 1, Characteristics of the Population, California.

U.S. Department of Commerce. Bureau of the Census. United States Census of Population: 1970. Vol. 1, Characteristics of the Population, California.

U.S. Department of Commerce. Bureau of the Census. United States Census of Population: 1980. Vol. 1, Characteristics of the Population, California.

U.S. Department of the Interior. National Cartographic Information Center. Digital Terrain Tapes User Guide, 1978.

U.S. Department of the Interior. Landsat Data User's Handbook, 1976.

University of California. Remote Sensing Research Program. Information Note 74-3 Revision 3, 1974.

Yang, R. C., Kozak, A. and Smith, J. H. G. "The Potential of Weibull - Type Functions as Flexible Growth Curves", Canadian Journal of Forest Research, 8: 1978.

APPENDICES

APPENDIX I

Dominant/Codominant Conifer Growth Measurements

Site No.	Tree No.	Height (ft.)	Age (yrs.)
1	1	104	127
	2	92	130
	3	112	157
2	1	42	60
	2	48	55
	3	57	116
3	1	130	185
	2	91	114
	3	91	139
4	1	92	140
	2	106	165
	3	93	139
5	1	85	115
	2	88	120
	3	73	115
6	1	114	180
	2	95	140
	3	86	138
	4	114	144
7	1	59	129
	2	62	105
	3	106	170
8	1	94	195
	2	50	66
	3	65	87
9	1	40	149
	2	34	114
	3	33	99
10	1	28	55
	2	37	66
	3	26	72
11	1	87	115
	2	87	111
	3	94	111
12	1	-	-
	2	66	76
	3	50	58

Site No.	Tree No.	Height (ft.)	Age (yrs.)
13	1	67	228
	2	74	255
	3	63	190
14	1	83	269
	2	53	276
	3	65	239
15	1	119	325
	2	125	300
	3	122	300
16	1	88	165
	2	40	68
	3	33	55
17	1	53	76
	2	83	132
	3	126	300
18	1	77	159
	2	78	126
	3	81	124
19	1	73	110
	2	67	101
	3	53	95
20	1	61	105
	2	83	133
	3	61	88
21	1	80	120
	2	80	115
	3	82	110
22	1	79	140
	2	87	210
	3	82	150
	4	100	150
23	1	70	122
	2	89	260
	3	56	106
24	Outside of the Study Area		
25	1	57	210
	2	27	61

Site No.	Tree No.	Height (ft.)	Age (yrs.)
26	1	60	130
	2	93	215
	3	68	137
	4	75	156
27	1	98	200
	2	128	280
	3	106	240
28	1	96	170
	2	70	230
	3	60	137
	4	86	198
29	1	68	300
	2	98	340
	3	90	300
30	1	67	153
	2	54	145
	3	61	250
31	1	82	210
	2	92	250
	3	81	160
32	1	78	350
	2	87	350
33	1	87	210
	2	94	230
	3	93	255
34	1	84	500
	2	34	78
	3	49	110
35	1	110	210
	2	113	240
	3	106	300

Site 1 Description

Date - 7/18/78 By - JCM Photo# - 14-12 Stop# - 1
Soil Series - Millich Area - Frenchman Reservoir Forest - Plumas
Ranger District - Milford State - CA County - Plumas
Location - Sec 18 T24 R16
Parent Rock - Andesite Tuff Breccia
Formation Name - Bonita
Landofrm - Mtn. Mid-Slope
Slope-42%
Aspect - S50°E
Elevation - 6200 ft.
Erosion - None

Horizon	Depth (cm)	Color		Texture	Stone/Rock % Volume
		Dry/moist	Mottling		
A11	0-4	10 YR 5/2 10 YR 3/2		loam +	30/10
A12	4-18	10 YR 3/2		loam +	30/10
B2+	18-69	7.5 YR 4/1		c/+	

Moderately Weathered (Fractolithic) - cracks 4" apart

Soil Sample Laboratory Analysis - Site I

Sample Depth (cm)	Sand <1.0 >0.5 mm	Silt <0.05 >0.002 mm	Clay <0.002 >0.001 mm	% Coarse Fragments	Bulk Density Clod	Bulk Density Rock	Soil Moisture 1/3 Bar	Soil Moisture 5 Bar	Soil Moisture 15 Bar	AWC
0-18	46.0	32.0	22.0		0.85		27.3		15.8	12.5
18-69	34.0	33.0	34.0		1.00		28.5		18.6	9.9

Sample Depth (cm)	P.A.W.	
0-18	2.42	
		→ at 60 cm P.A.W. = 6.58
18-69	4.95	

APPENDIX II

Model Verification Sample Site Data

Site No.	Tree	Age (yrs.)	Height (ft.)	Dia. Breast Ht. (in.)	
	1	135	100	28.3	Slope (%) = 28
1	2	120	80	28.7	Aspect (°) = N60°E
	3	89	84	20.8	Mean Growth Rate (ft/yr) = 0.77
	1	90	69	18.3	Slope (%) = 15
2	2	91	66	20.0	Aspect (°) = N8°W
	3	81	60	23.5	Mean Growth Rate (ft/yr) = 0.74
	1	67	68	18.4	Slope (%) = 16
3	2	68	54	16.1	Aspect (°) = N5°W
	3	90	79	21.5	Mean Growth Rate (ft/yr) = 0.89
	1	75	90	28.4	Slope (%) = 3
4	2	90	85	28.8	Aspect (°) = S
	3	76	82	26.2	Mean Growth Rate (ft/yr) = 1.07
	1	82	76	20.5	Slope (%) = 14
5	2	47	65	20.6	Aspect (°) = S22°E
	3	92	81	22.0	Mean Growth Rate (ft/yr) = 1.00
	1	103	72	21.3	Slope (%) = 25
6	2	140	94	30.8	Aspect (°) = S72°E
	3	121	93	24.8	Mean Growth Rate (ft/yr) = 0.71
	1	144	82	26.0	Slope (%) = 48
7	2	149	83	19.2	Aspect (°) = N78°E
	3	158	79	18.2	Mean Growth Rate (ft/yr) = 0.54
	1	185	85	22.3	Slope (%) = 32
8	2	92	84	16.5	Aspect (°) = E
	3	95	54	14.3	Mean Growth Rate (ft/yr) = 0.60
	1	127	103	26.5	Slope (%) = 12
9	2	94	74	20.0	Aspect (°) = S22°W
	3	95	94	30.1	Mean Growth Rate (ft/yr) = 0.86
	1	69	50	14.0	Slope (%) = 22
10	2	103	85	18.4	Aspect (°) = S48°E
	3	69	81	20.0	Mean Growth Rate (ft/yr) = 0.90
	1	65	57	17.6	Slope (%) = 18
11	2	68	61	23.4	Aspect (°) = N25°E
	3	76	63	18.4	Mean Growth Rate (ft/yr) = 0.87
	1	92	69	18.5	Slope (%) = 33
12	2	82	73	17.6	Aspect (°) = N
	3	94	73	20.3	Mean Growth Rate (ft/yr) = 0.80

Site No.	Tree	Age (yrs.)	Height (ft.)	Dia. Breast Ht. (in.)	
	1	91	93	27.8	Slope (%) = 0
13	2	57	74	19.0	Aspect (°) = S30°E
	3	90	78	23.0	Mean Growth Rate (ft/yr) = 1.03
	1	57	36	15.5	Slope (%) = 15
14	2	48	42	16.2	Aspect (°) = S62°E
	3	61	51	16.0	Mean Growth Rate (ft/yr) = 0.78
	1	120	70	20.0	Slope (%) = 34
15	2	111	70	17.2	Aspect (°) = E
	3	106	64	18.3	Mean Growth Rate (ft/yr) = 0.61
	1	68	58	16.9	Slope (%) = 28
16	2	49	42	13.1	Aspect (°) = S40°E
	3	56	41	15.5	Mean Growth Rate (ft/yr) = 0.82
	1	135	65	18.3	Slope (%) = 27
17	2	118	72	21.0	Aspect (°) = N38°E
	3	151	85	23.9	Mean Growth Rate (ft/yr) = 0.55
	1	135	73	26.4	Slope (%) = 14
18	2	80	66	21.2	Aspect (°) = N30°E
	3	47	34	12.0	Mean Growth Rate (ft/yr) = 0.66
	1	185	86	28.0	Slope (%) = 22
19	2	150	79	25.0	Aspect (°) = N42°W
	3	-	-	-	Mean Growth Rate (ft/yr) = 0.49
	1	91	57	16.0	Slope (%) = 10
20	2	90	69	19.2	Aspect (°) = N
	3	87	67	19.4	Mean Growth Rate (ft/yr) = 0.72
	1	37	53	12.1	Slope (%) = 0
21	2	50	40	14.4	Aspect (°) = Undefined
	3	56	55	20.5	Mean Growth Rate (ft/yr) = 1.08
	1	75	74	20.5	Slope (%) = 22
22	2	64	60	16.7	Aspect (°) = N22°W
	3	62	73	15.0	Mean Growth Rate (ft/yr) = 1.03
	1	75	42	12.1	Slope (%) = 25
23	2	73	43	13.4	Aspect (°) = N20°W
	3	74	51	15.1	Mean Growth Rate (ft/yr) = 0.61
	1	77	55	18.6	Slope (%) = 10
24	2	55	55	21.0	Aspect (°) = S60°E
	3	55	59	15.8	Mean Growth Rate (ft/yr) = 0.90
	1	137	55	24.5	Slope (%) = 25
25	2	102	67	20.2	Aspect (°) = S32°W
	3	106	60	18.4	Mean Growth Rate (ft/yr) = 0.53

Site No.	Tree	Age (yrs.)	Height (ft.)	Dia. Breast Ht. (in.)	
	1	93	53	17.5	Slope (%) = 45
26	2	89	66	16.9	Aspect (°) = N80°W
	3	74	56	13.6	Mean Growth Rate (ft/yr) = 0.68
	1	87	45	17.8	Slope (%) = 30
27	2	69	35	15.6	Aspect (°) = W
	3	74	41	10.9	Mean Growth Rate (ft/yr) = 0.53
	1	76	42	13.5	Slope (%) = 28
28	2	62	56	16.7	Aspect (°) = S40°E
	3	67	50	13.4	Mean Growth Rate (ft/yr) = 0.71
	1	78	49	14.1	Slope (%) = 32
29	2	78	46	14.6	Aspect (°) = N60°W
	3	71	49	14.0	Mean Growth Rate (ft/yr) = 0.63
	1	265	84	24.1	Slope (%) = 42
30	2	239	68	21.9	Aspect (°) = N52°W
	3	245	74	18.9	Mean Growth Rate (ft/yr) = 0.30
	1	90	36	11.2	Slope (%) = 10
31	2	85	45	14.6	Aspect (°) = S
	3	83	34	11.6	Mean Growth Rate (ft/yr) = 0.45
	1	145	59	22.5	Slope (%) = 15
32	2	110	42	19.2	Aspect (°) = S22°W
	3	32	31	9.2	Mean Growth Rate (ft/yr) = 0.46
	1	321	71	24.4	Slope (%) = 28
33	2	307	72	24.7	Aspect (°) = S10°W
	3	325	85	27.5	Mean Growth Rate (ft/yr) = 0.24
	1	108	65	19.0	Slope (%) = 18
34	2	80	42	14.9	Aspect (°) = S32°W
	3	103	27	12.8	Mean Growth Rate (ft/yr) = 0.46
	1	271	115	26.2	Slope (%) = 2
35	2	224	102	16.9	Aspect (°) = N68°E
	3	39	33	9.4	Mean Growth Rate (ft/yr) = 0.47
	1	87	44	14.4	Slope (%) = 32
36	2	49	31	10.4	Aspect (°) = S32°W
	3	68	36	10.3	Mean Growth Rate (ft/yr) = 0.54
	1	90	27	14.6	Slope (%) = 26
37	2	68	33	13.4	Aspect (°) = S68°E
	3	88	26	15.5	Mean Growth Rate (ft/yr) = 0.35
	1	92	63	12.2	Slope (%) = 23
38	2	85	73	14.4	Aspect (°) = N65°W
	3	82	54	10.7	Mean Growth Rate (ft/yr) = 0.73

Site No.	Tree	Age (yrs.)	Height (ft.)	Dia. Breast Ht. (in.)	
	1	111	83	23.5	Slope (%) = 18
39	2	165	73	21.9	Aspect (°) = N40°W
	3	190	59	18.9	Mean Growth Rate (ft/yr) = 0.46
	1	141	65	21.2	Slope (%) = 12
40	2	159	56	23.7	Aspect (°) = E
	3	136	61	19.7	Mean Growth Rate (ft/yr) = 1.25
	1	85	69	13.8	Slope (%) = 48
41	2	87	76	15.6	Aspect (°) = N30°E
	3	87	70	13.0	Mean Growth Rate (ft/yr) = 0.83
	1	105	60	15.9	Slope (%) =
42	2	95	59	12.8	Aspect (°) =
	3	112	48	12.2	Mean Growth Rate (ft/yr) = 0.54